Development and Applications of Self-learning Simulation in Finite Element Analysis

Submitted by Ali Dahham Nassr
to the University of Exeter as a thesis for the degree of
Doctor of Philosophy in Engineering
In December 2018

I certify that all material in this thesis which is not my own work has been identified and that no material has previously been submitted and approved for the award of a degree by this or any other University.

Signature: ……

To my parents, lovely wife and sons whom I owe my whole life.

AKNOWLEDGEMENTS

First of all, I should thank my mighty God for many blessings and for giving me health and strength to finish this research.

I would like to thank my supervisor, Professor Akbar Javadi, who guided me and supported me throughout my PhD study at University of Exeter. He is very generous, kind and knowledgeable. His patience and encouragement gave me the confidence during the hard time of the study which I will never forget.

I would like to extend thanks to the Ministry of Higher Education of Iraq for the financial support and encouragements, and the Iraqi Cultural Attaché in London for their kind help and guidance during my study which is hugely appreciated.

I wish to express my thankfulness to my mother and father for their love, prayers, encouragement and support, they have been greatest inspiration of my life; to my lovely sisters for their prayers, trust and support.

I would like to thank all staff members in the College of Engineering, Mathematics and Physical Sciences and all my friends for their invaluable friendship.

My deepest thanks to my Lovely wife whose love, help and encouragement made this work possible. She is always believing in me and understanding my situation. Special mention goes to my lovely Sons, Mohammed and Ibrahim whom bring my life with brightness and happiness.

ABSTRACT

Numerical analysis such as the finite element analysis (FEA) have been widely used to solve many engineering problems. Constitutive modelling is an important component of any numerical analysis and is used to describe the material behaviour. The accuracy and reliability of numerical analysis is greatly reliant on the constitutive model that is integrated in the finite element code. In recent years, data mining techniques such as artificial neural network (ANN), genetic programming (GP) and evolutionary polynomial regression (EPR) have been employed as alternative approach to the conventional constitutive modelling. In particular, EPR offers great advantages over other data mining techniques. However, these techniques require a large database to learn and extract the material behaviour. On the other hand, the link between laboratory or field tests and numerical analysis is still weak and more investigation is needed to improve the way that they matched each other. Training a data mining technique within the self-learning simulation framework is currently considered as one of the solutions that can be utilised to accurately represent the actual material behaviour. In this thesis an EPR based machine learning technique is utilised in the heart of the self-learning framework with an automation process which is coded in MATLAB environment. The methodology is applied to simulate different material behaviour in a number of structural and geotechnical applications. Two training strategies are used to train the EPR in the developed framework, total stress-strain and incremental stress-strain strategies. The results show that integrating EPR based models in the framework allows to learn the material response during the self-learning process and provide accurate predictions to the actual behaviour. Moreover, for the first time, the behaviour of a complex material, frozen soil, is modelled based on the EPR approach. The results of the EPR model predictions are compared with the actual data and it is shown that the proposed model can capture and reproduce the behaviour of the frozen soil with a very high accuracy.

The developed EPR based self-learning methodology presents a unified approach to material modelling that can also help the user to gain a deeper insight into the behaviour of the materials. The methodology is generic and can be extended to modelling different engineering materials.

List of Publications from This Research

Journal papers

- **Nassr, A**., Javadi, A., Faramarzi, A., 2018. Developing constitutive models from EPR-based self-learning finite element analysis. Int. J. Numer. Anal. Methods Geomech. 42, 401–417. doi:10.1002/nag.2747.

- **Nassr, A**., Esmaeili-falak, M., Katebi, H., Javadi, A., 2018. A new approach to modelling the behaviour of frozen soils. Eng. Geol. 246, 82–90. doi:10.1016/j.enggeo.2018.09.018

Conference papers

- **Nassr, A.,** Javadi, A., Faramarzi, A., (2016). Self-learning finite element method and engineering applications. Proceedings of the 24th Annual Conference of the Association of Computational Mechanics in Engineering (ACME), 31 Mar – 01 April, University of Cardiff, Cardiff, UK, pp: 14-17.

- **Nassr, A.,** Javadi, A.A., (2017). Analysis of a plate using EPR-based self-learning finite element method. Proceedings of the 25th Annual Conference of the Association of Computational Mechanics (UKACM), 11 –13 April, University of Birmingham, Birmingham, UK, pp: 22-25.

Table of Contents

List of Figures

List of Tables

List of Abbreviations

AGF: Artificial Ground Freezing

ANFIS: Adaptive Neuro-Fuzzy Inference System

ANN: Artificial Neural Network

BBC: Boston Blue Clay

CD: Consolidated Drained

CoD: Coefficient of Determination

DC: Duncan Chang

DSS: Direct Shear Test

EA: Evolutionary Algorithm

EPR: Evolutionary Polynomial Regression

FE: Finite Element

FEA: Finite Elemet Analysis

FEM: Finite Element Method

GA: Genetic Algorithm

GFRP: Glass Fibre-Reinforced Polymer

GP: Genetic Programming

HP: Hypoplastic

JGLF: Jet Grouting Laboratory Formulation

LGP: Linear Genetic Programing

LMA: Levenberg-Marquardt Algorithm

LS: Least Square

MC: Mohr-Coulomb

MCC: Modified Cam Clay

CSL: Critical State Line

MLP: Multi-Layer Perceptron

MLR: Multi-Linear Regression

MOGA : Multi-Objective Genetic Algorithm

MR: Multiple Regression

MRA: Multiple Regression Analysis

NANN: Nasted Adaptive Neural Network

NN: Neural Network

NNCM: Neural Network Based Constitutive Model

PCS : Penalisation of Complex Structures

PSSP: Plane-Strain Strain Probe

RAC: Recycled Aggregate Concrete

SDI: Slake Durability Index

Self-Sim: Self-learning Simulation

SOGA: Single Objective Genetic Algorithm

SSE: Sum of Squared Errors

SVD: Singular Valuable Decomposition

SVM: Support Vector Machine

TTSP: True Triaxial Strain Probe

UCS: Uniaxial Compression Strength

UMAT: User Material Subrotine

UU: Unconsolidated Undrained

VUMAT: Vectorlized User Material Subroutine

WLA: Wildlife Liquefaction Array

List of Symbols

σ	Vector of stress
ε	Vector of strain
E	Youngs' modulus
E_i	Initial elastic modulus
E_{ur}	Elastic modulus of unloading and reloading
E_{50}	Primary elastic modulus
μ	Poisson's' ratio
$\emptyset$	Angle of shearing resistance
ψ	Dilatancy angle
C	Apparent cohesion
P_c	Pre consolidation pressure
M	Slope of the CSL
q	Deviator stress
p'	Mean effective stress
D_{50}	Median particle size
C_C	Coefficient of curvature
C_u	Coefficient of uniformity
h	Hardness of material
n_s	Shape factor
e	Void ratio
$\sigma_3^{'}$	Effective confining pressure
σ_d^i	Deviator stress
ε_v^i	Volumetric strain
$\Delta\varepsilon_v^i$	Incremental volumetric strain
i	Load increment
n	Porosity
t	Age of mixture
C_{iv}^d	Volumetric content of cement
w/c	Water cement ratio
S	Coefficient of cement type

$C\%$	Cement content
$S\%$	Sand content
$ML\%$	Silt content
$CL\%$	Clay content
$OM\%$	Organic content
SDI	Slake durability index
d	Density
V_P	Ultrasonic P-wave velocity
d_p	Bar diameter
L_d/d_p	Ratio of embedment length to bar diameter
c/d_p	Ratio of concrete cover to bar diameter
T_b	Bond strength
D	Stiffness matrix
D^e	Elastic Stiffness matrix
D^p	Plastic stiffness matrix
J	Jacobian matrix
D_{NN}	Neural network stiffness matrix
ε_x	Strain in x-direction
ε_y	Strain in y-direction
ε_z	Strain in z-direction
γ_{xy}	Shear strain in x-y plane
γ_{yz}	Shear strain in y-z plane
γ_{xz}	Shear strain in x-z plane
σ_x	Stress in x-direction
σ_y	Stress in y-direction
σ_z	Stress in z-direction
τ_{xy}	Shear stress in x-y plane
τ_{yz}	Shear stress in y-z plane
τ_{xz}	Shear stress in x-z plane
ε_{11}	Strain in axial direction
σ_{11}	Stress in axial direction

S22	Stress in vertical direction
E22	Strain in vertical direction
U_1	Displacement in horizontal direction
U_2	Displacement in vertical direction
M	Moment
Θ	Rotation
n	Time step
k_{con}	Algorithmic tangent stiffness
S_a	Surface response spectra
T	Temperature
∇T	Temperature gradient
J_{EPR}	Jacobian matrix of EPR
G	Shear modulus
K	Bulk modulus
λ	Lame's first parameter
M	P-wave modulus
σ_1	Major principal stress
σ_3	Minor principle stress
G_s	Specific gravity of soil
$\dot{\varepsilon}$	Strain rate
ε_q	Distortional strain
$\Delta\varepsilon_y$	Incremental axial strain

CHAPTER 1

Introduction

1.1 General Background

The finite element method (FEM) is a very powerful technique which has been used over several decades. The method is utilised to solve very complex engineering problems of different disciplines including structural analysis, fluid mechanics, thermal analysis, and electromagnetics, among others. One of the essential components of the FEM is the constitutive model which is used to represent the behaviour of materials at the point or element level. In their basic formulation, constitutive models describe the stress-strain relationship (Hashash et al., 2004b). The successful application of finite element simulations in engineering problems is largely dependent on the choice of an appropriate constitutive model that represents the material behaviour. Constitutive models have been developed for various materials such as concrete, soil, rock, polymer, etc. These models range from simple elastic to more complex nonlinear elastic, elastoplastic, hyperelastic, etc. Despite the large number of constitutive models developed with different degrees of complexity, it has been indicated that none of these models can entirely capture the real material behaviour under different loading conditions. Furthermore, implementation of such complex models into finite element code could be very challenging, consequently delimiting their functionality in engineering applications (Shin and Pande, 2000). The high demand for developing accurate and robust constitutive models for different materials encourages many researchers to work in this field. Recently, with the significant developments in computational software and hardware, the field of constitutive modelling has been extended beyond the classical constitutive modelling theories, to computer-aided pattern recognition approaches which have been introduced as an alternative approach for modelling of a wide range of engineering applications.

A number of data-driven techniques such as an artificial neural network (ANN), genetic programming (GP) and evolutionary polynomial regression (EPR) have been used for modelling of different material behaviour (e.g. Ahangar-Asr et al., 2011; Ghaboussi et al., 1991; Javadi and Rezania, 2009; Rezania, 2008).

The main purpose of developing a constitutive model is to be implemented in numerical analysis such as FEM. The implementation of constitutive models based on data mining techniques such as ANN and EPR in FEA has been presented in different ways by a number of researchers (e.g. Hashash et al., 2004b; Rezania; et al., 2008).

ANN-based constitutive modelling has been successfully incorporated in finite element code through an interesting and comprehensive training procedure called autoprogressive or self-learning algorithm. This work was first presented by Ghaboussi et al. (1998) and (Shin and Pande, 2000) and then extended to a full framework, named self-learning simulation, by (Hashash et al., 2006a). The results from these works revealed that ANN models trained in this way, could learn and capture the embedded information in non-homogenous structural tests and provide better predictions of material behaviour compared with traditional constitutive models.

Although there has been some valuable research on the development of the self-learning FEM based on ANN and the demonstration of the advantages that ANN offers in constitutive modelling, however, to date, the algorithm has been applied to simulate relatively limited aspects of engineering problems. More importantly, it is well known that ANNs have some drawbacks. For instance, when using ANNs, the number of neurons, number of hidden layers, transfer function, etc. must be determined a priori, requiring a time-consuming trial and error procedure. Moreover, the black box nature, the large complexity of the network structure, the lack of interpretability of the relationship between input and output have prevented the ANNs from achieving their full potential (Ahangar-Asr, 2012; Faramarzi, 2011; Rezania; et al., 2008; Rezania, 2008). On the other hand, using the EPR in constitutive modelling has been presented as an alternative approach that avoids some of the shortcomings of ANN in material modelling. EPR employs a combination of a genetic algorithm (GA) and the least square method (LS) to search for mathematical formula to represent the behaviour of a system (Giustolisi and Savic, 2006).

EPR was first used for environmental modelling by (Giustolisi and Savic, 2006). Recently, the application of EPR for material modelling and the implementation of EPR-based constitutive models in FEM have been presented as an effective alternative approach for simulation of different boundary value problems (Faramarzi, 2011; Faramarzi et al., 2012; Javadi and Rezania, 2009; Rezania, 2008). This thesis presents the application of EPR for constitutive modelling of materials in the framework of self-learning simulation. An automated process of EPR based self-learning finite element simulation is developed and coded in MATLAB environment. The application of the EPR based self-learning finite element simulation is illustrated through analysis of a number of civil engineering problems in the areas of structural engineering and geotechnics.

1.2 Objectives

In this thesis, the effectiveness and capabilities of EPR in representing the constitutive behaviour of materials in a transparent and explicit form, has been the inspiration to use this technique in the heart of the self-learning algorithm to build a robust constitutive model. The main objectives of this work are as follows:

- Review and present the recently developed approaches in constitutive modelling of different engineering materials and their implementation in FEA.
- Develop and demonstrate a new methodology of incorporating the data mining technique, EPR, into finite element code (ABAQUS) through an automated process coded in MATLAB environment.
- Take advantage of using EPR in constitutive modelling in the framework of self-learning simulation and reduce the gap between laboratory or field tests and numerical modelling.
- Develop and introduce constitutive models using experimental (laboratory) and hypothetical (simulated) data by using the EPR based self-learning technique.
- Develop and demonstrate constitutive models within EPR-based self-learning simulation model using different training strategies.
- Simplify the way of training EPR within the self-learning simulation algorithm.

- Verify the capability of the proposed algorithm using some structural and geotechnical problems.
- Develop an EPR-based constitutive model for frozen soils using experimental data.

1.3 Contribution to the knowledge

Developing a self-learning simulation algorithm based on a robust data mining technique is very important in accurate prediction of behaviour of engineering systems and representation of the material behaviour. Using the advantages that EPR offers over other data mining techniques, especially in terms of the transparent form of its equations, can significantly simplify the incorporation of data mining technique in finite element analysis. The main contribution of this work is the development of a unified framework, based on the self-learning simulation methodology to model the response of various materials (linear elastic, nonlinear elastic, elastoplastic, etc.) under different loading conditions. Also, for the first time, a robust constitutive model is presented to describe the complex behaviour of frozen soils using EPR approach.

1.4 Layout and structure of the thesis

This thesis is divided into seven chapters. The main description of each chapter content is briefly summarised in the following paragraphs.

Chapter one (current chapter) provides a general introduction and objectives of the thesis. It presents the contribution of the thesis and illustrates how the thesis is organised.

Chapter two presents a general background to constitutive modelling of materials. The chapter begins with a historical review of using conventional constitutive material modelling and then illustrates the importance and purpose of their implementation in numerical analysis, mainly the FEM.

Chapter three presents the use of data mining-based constitutive modelling. In particular, the use of the ANN, GP and EPR in material modelling is introduced in detail. The main advantages of EPR over other data mining techniques are highlighted in this chapter.

Chapter four describes the methodology of the self-learning simulation based on ANN. Some applications of ANN-based self-learning simulation are presented. The main advantages of the self-learning simulation are highlighted. This chapter also illustrates the developed algorithm for using EPR-based self-learning simulation in detail. Furthermore, it introduces different strategies which are followed to train the EPR-based constitutive models within the self-learning framework.

In chapter five, some applications of the developed EPR-based self-learning simulation are presented. These include modelling the behaviour of structural boundary value problems including truss and an aluminium plate considering linear elastic, nonlinear elastic and elastic-plastic behaviour. The results from these applications are used to verify the developed algorithm.

In chapter six the modelling of the very complex behaviour of frozen soils is introduced to verify the capability of the EPR as a unified approach to constitutive modelling of materials. Furthermore, EPR-based self-learning algorithm is applied to simulate a geotechnical application. This include simulation of consolidated drained triaxial test using experimental data.

Chapter seven includes the main conclusions of the thesis and provides some suggestions for further research.

CHAPTER 2

Constitutive Modelling of Materials

2.1 Introduction

The fundamental aim of a successful engineering project is to reduce the time and cost which are very important factors in the design and construction of many civil engineering structures. As cost considerations are vital at initial design stages, determinations of loading capacity and durability of structures, numerical simulations during construction can avoid or minimise the possibility of expensive and time-consuming in later stages of project (Basan, 2016). Selection of an appropriate material, together with the knowledge of its behaviour is one of the main decisions to be made in the early design stages of any engineering application. Every single operating condition, especially the severe ones such as higher mechanical loadings or changes in temperature, influence the engineering material in use and causes deterioration of material properties, due to, usually concurrent processes of deformation and damage. These can cause failure of an engineering component, or the whole structure could collapse. To avoid unexpected events such as building damage, an earthquake, etc., simulations and engineering analysis must be performed in advance, to predict a safe design life for components and structures. Most of the practical methods for predicting the design life of engineering structures are based on empiricism. Therefore, a significant amount of experimental and field data are required to have realistic predictions. Durability calculations are performed in early design stages when experimental/field data are rarely available (due to demanding, expensive and long-lasting experiments). It would therefore be useful to predict material response under applied loading condition, and typically this is the task of constitutive modelling (Basan, 2016).

Constitutive model can be defined as a set of simplified mathematical equations that connect the state of stresses and strains (stress-strain history, strain rate, and other field quantities) and predict the response of given material under applied load, displacement, temperature, etc. Generally, constitutive models can be very different for different materials used in engineering applications, such as steel, concrete, soil, rock, polymer, etc. Despite the variety of material behaviour responses, the primary principles and concepts are mostly the same in establishing and developing the constitutive models for different materials. The mathematical formulation of a constitutive model depends not only on the material properties itself but also on its purpose and degree of accuracy required. There are some criteria to choose the best model, and these are highly reliant on the experience and judgment of the engineer whose task is to select a model that (Basan, 2016):

- describes the physical phenomena representing the system,
- is able to predict the behaviour of the material accurately, and
- can be incorporated into a robust numerical algorithm such finite element method (FEM).

2.2 Material behaviour models

In material modelling, a mathematical form is firstly postulated according to the understanding of the phenomena. In the next step, some experimental measurements are taken from the material being tested and the behaviour of the material is extracted to define the variables of the proposed model. Selecting an appropriate model to describe material behaviour is very important, hence choosing inappropriate model could lead to entirely wrong prediction (Bower, 2010).

Whatever the type of material and the physical mechanism that appears when the material is under loading condition, the response and real behaviour of a material can be within the following categories: rigid, elastic, viscous, plastic and perfectly plastic (Lemaitre and Chaboche, 2000). The classification of materials behaviour according to the above criteria is shown in Table (2-1). There are many models developed to represent the stress-strain behaviour and failure of different

materials, all of which have advantages and shortcomings depending on their applications.

Chen (1985) introduced some fundamental criteria for model validation. The models should consider the theoretical assumption concerning the continuum mechanics principles such as the requirements of continuity, stability, uniqueness, etc. The developed models also need to fit the experimental data created from a number of available standardised tests, and their parameters should be easily determined from these tests. Furthermore, assessing the ease with which they can be implemented in numerical models such as FEM is also vital.

Table 2-1: Material behaviour classification (Lemaitre and Chaboche, 2000).

Type of solid	Material behaviour	Rate dependency
Elastic	Perfectly elastic solid	Independent
	Viscoelastic solid	Dependent
Plastic	Rigid-perfectly plastic solid	Independent
	Elastic perfectly plastic solid	
	Elastoplastic hardening solid	
Viscoplastic	Perfectly viscoplastic solid	Dependent
	Elastic perfectly viscoplastic solid	
	Elastic viscoplastic hardening solid	

2.3 Classical constitutive models

Various types of traditional constitutive models of different engineering materials have been widely developed over the last decades. Constitutive models can be classified according to the degree of complexity from simple linear elastic to more advanced elastic-plastic models. Some materials (including geomaterials, e.g., soils and rocks) exhibit very complex behaviour when subjected to different conditions. Therefore, it would be useful to briefly present some of the commonly used constitutive models in geotechnical applications.

The earliest model was introduced by (Hooke, 1675) to represent the stress-strain relationship of linear elastic material behaviour. The general form of Hooke's law is:

$$\sigma = E\,\varepsilon \tag{2-1}$$

where E is Young's modulus and $\sigma,\ \varepsilon$ are stress and strain respectively. However, the simple linear isotropic elastic model is unable to simulate the main important soil responses (e.g. change in stiffness). At the end of 19th century, material modelling using the plasticity theory was introduced. The concept of this model was developed by Mohr. The combination and generalization of Hooke's law and Coulomb's law was gathered in a plasticity framework which is known as Mohr-Coulomb model (MC). This model is an elastic perfectly plastic constitutive model which is wieldy used in engineering practice. In the field of geotechnical engineering, this model is defined by two elastic parameters based on Hooke's law (Young's modulus *E*, and Poisson's ratio μ) to define the elastic behaviour, strength parameters (apparent cohesion c, angle of shearing resistance ϕ) to define the plastic behaviour and dilatancy angle (*ψ)* to define the irreversible volume change due to shearing.

Although the model has been commonly used to analyse different geotechnical engineering applications such as stability of slopes, dams, shallow foundation, etc., it does not consider hardening or softening behaviour of soils. It also does not consider the effects of volume change on shear behaviour and vice versa. Duncan and Chang, (1970) developed a model (called Duncan Chang model) based on stress-strain relationship in the drained triaxial test. In this model, the deviator stress-axial strain curve can be approximated by a hyperbolic model as shown in Figure (2-1) (Ti et al., 2009).

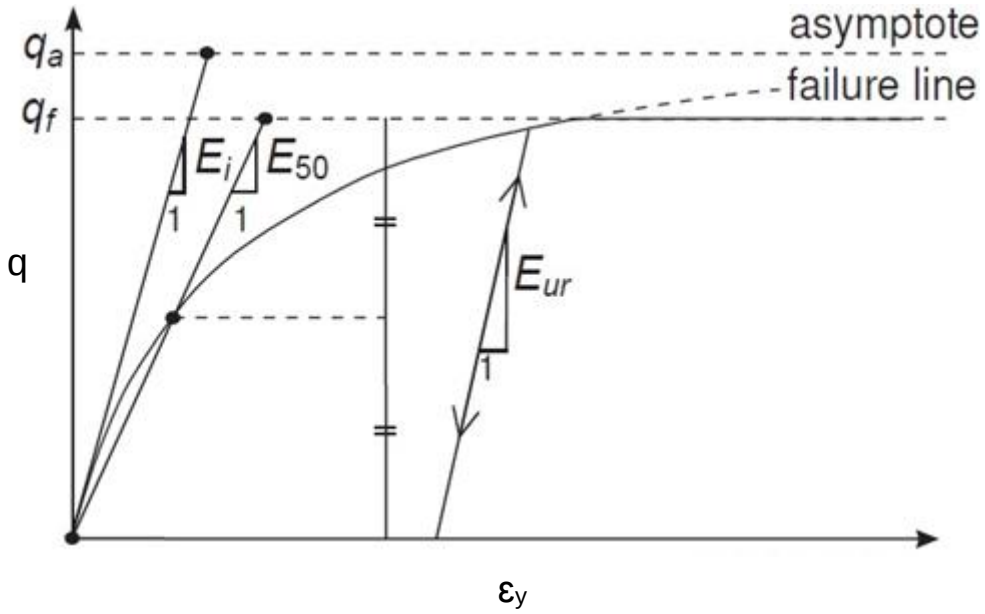

Figure 2-1: Hyperbolic stress-strain curve; q is deviator stress, ε_y is axial strain, E_i is initial elastic modulus, E_{ur} is the elastic modulus of unloading and reloading, E_{50} is primary elastic modulus.

In the Duncan Chang model, the failure behaviour follows the MC failure criterion. The main advantages of this model are its ability to define the non-linearity, stress dependency and inelastic response of soils. The model parameters can be determined directly from standard triaxial tests. Therefore, this model has been applied to analyse different geotechnical applications. However, this model has some shortcomings; for example, differentiation between loading and unloading is not clear. Also, the model cannot represent the behaviour of soils under entirely plastic range (Ti et al., 2009).

The geotechnical group at Cambridge University developed the Cam Clay model, which is a more advanced and realistic model based on the critical state theory. This model is an elastic-plastic strain hardening model where the hardening plasticity is applied to model the nonlinear behaviour of soils (Roscoe and Schofield, 1963). Later, many modifications have been made to improve the capability of the model to meet the requirements of more complex conditions (i.e. Modified Cam Clay Model, MCC) (Roscoe and Burland, 1968).

The MCC is a well-known constitutive model for soils and is widely used in analysing different geotechnical applications. The yield surface of MCC model can be shown in Figure (2-2). However, this model also has some limitations. Yu (1998) noted that this model is unable to provide reasonable predictions of the undrained condition of loose sand and normally consolidated clay due to the assumption of associated flow rule. Further, (Munda et al., 2014) reviewed the effectiveness of MCC model for fine-grained soil by comparing the results of MCC model with experimental data of different samples. They showed that the model provided resealable agreement with the experimental data in drained condition while there were apparent discrepancies of the results under undrained condition. The generalisation of MCC model to be used for different types of soil and conditions is the main limitation of this model (Ti et al., 2009).

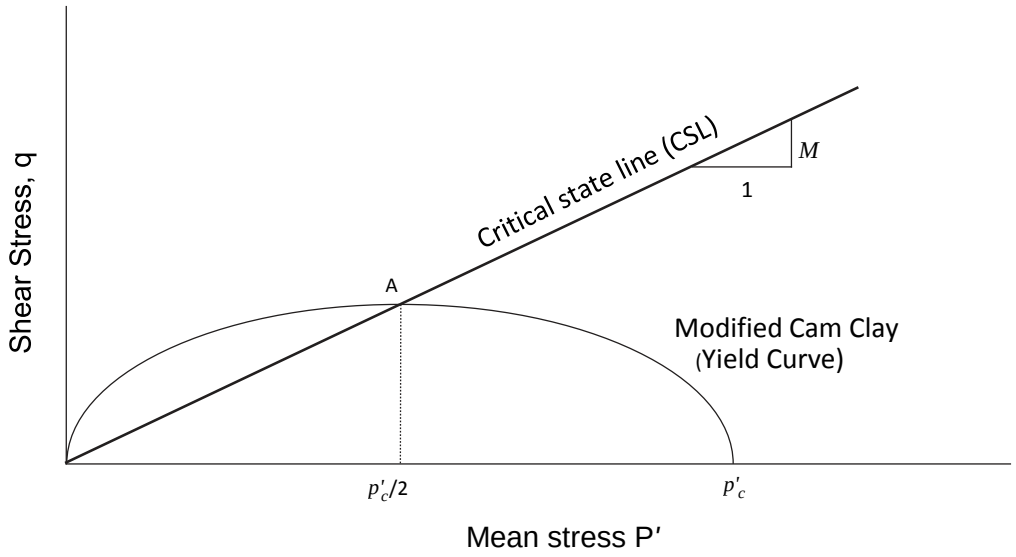

Figure 2-2: Yield surface of MCC Model in the q - p' plane; *M* is the slope of the CSL in the p-q space, p_c is pre consolidation pressure.

2.4 Applications of conventional constitutive models

Constitutive modelling of different engineering materials has been the theme of research over several decades. A large number of books, papers, reports, etc. deal with the developments in constitutive modelling to represent the material response subjected to certain conditions. Most of the classical constitutive models have been subjected to several modifications to minimise their limitations and enhance their performance in representing material behaviour.

2.4.1 Constitutive models in numerical analysis

High accuracy predictions of material behaviour are very essential to reduce the cost, time and risk of failure. Numerical simulation and analysis of an engineering problem is formulated within an advanced computational system (a numerical model). Numerical methods such as the FEM play an important role in solving different boundary value problems. The successful application of finite element simulations in engineering applications is greatly dependent on the selection of an appropriate model that is able to describe the material behaviour (e.g. stress-strain curve). The field of constitutive modelling in numerical analysis has been significantly developed with time with the development of more advanced and sophisticated models to extract the real behaviours of materials (Figure 2-3).

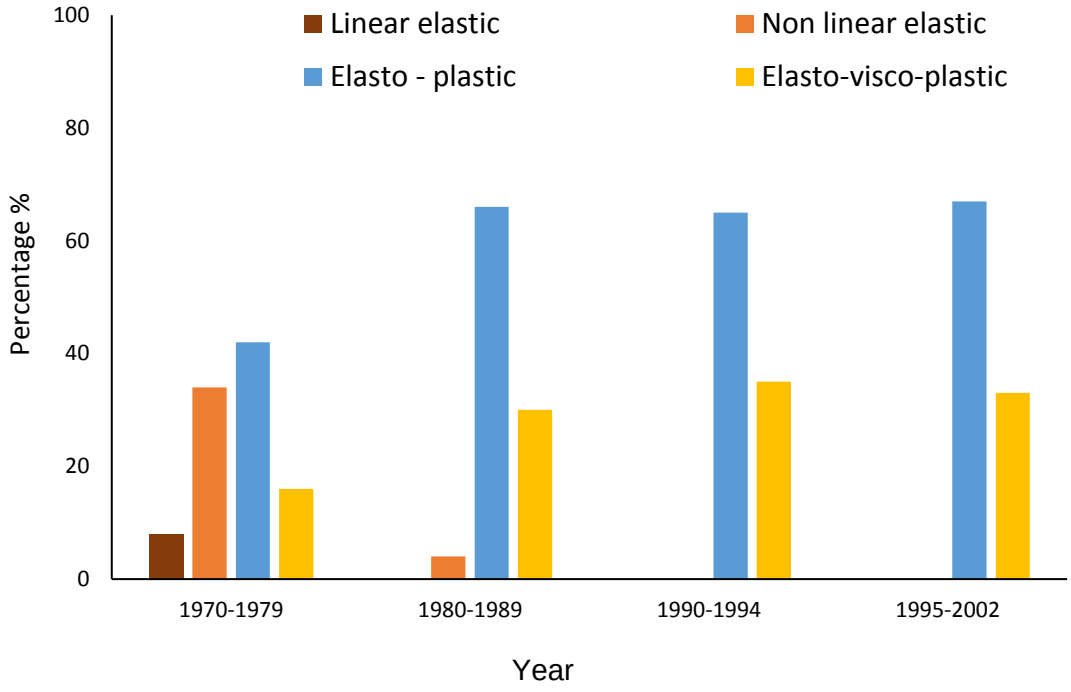

Figure 2-3: Evolution of different types of constitutive model used in numerical analysis of soft soils between 1970 to 2002 (Mestat et al., 2017)

A large number of constitutive models have been developed to analyse different engineering applications including static and dynamic analyses. For instance, in the field of geotechnical engineering, significant amount of research has been conducted to develop and implement these models in numerical (especially finite element analysis) to solve various problems such as shallow foundations, tunnels, deep excavations, slope stability, as well as problems involving more complex material behaviour such as frozen soils. Therefore, it would be useful to review some typical works done in the literature, in particular, the recent ones, on constitutive models with their modifications in the analysis of different boundary value problems.

Loukidis and Salgado, (2009) performed a numerical study using FEM, based on the Mohr-Coulomb model to evaluate the bearing capacity of the strip and circular footings designed on sandy soil. They investigated the possible effect of dilatancy angle (ψ) on the bearing capacity of foundations with and without associated flow rule. The results showed good agreement between FEA and rigorous analytical methods.

In this work some assumptions were made without considering their effects on the results. Also, the analysis applied only on sandy soil, and the possibility to be applied on different types of soil was not indicated.

Modified cam clay (MCC) model was used to perform coupled numerical analysis using FEM to study the compression and uplift capacity of a shallow foundation under undrained and partially undrained conditions (Li et al., 2015). This paper emphasised the failure mechanism and responses of pore pressure within the soil. The compression and uplift of the foundation were modelled based on the simulation of triaxial compression and tension tests in order to gain a clear understanding of the soil behaviour. The soil was assumed as homogenous, and the yield surface of MCC was considered as isotropic. This study could be considered as a validation of using MCC in the coupled analysis.

Wang et al., (2016) investigated the effect of seepage on the effective stresses of a slope using the Duncan Chang model. Triaxial compression experiments and numerical simulation, both including the seepage effects, were performed. In this work, the Duncan Chang model was modified by applying the concept of equivalent confining pressure, and the modified model was verified through comparison between the experimental and finite element simulation results. Also, a case study of slope stability analysis under seepage effects confirmed the reliability of the Duncan Chang model for estimation of factor of safety for slope considering the seepage effects. However, the study included some modifications to the Duncan Chang model assuming seepage does not affect the internal angle of effective shearing resistance, which may not be applicable in some other conditions.

Ng et al., (2015) studied the capability of three different constitutive models to simulate the response of an existing tunnel to stress relief during a basement excavation. The results computed from the implementation of Mohr-Coulomb (MC), Duncan Chang (DC) and Hypoplastic (HP) models in finite element analysis were compared with a three-dimensional centrifuge model test. It was shown that, in this case, the ability of HP model in predicting soil heave due to stress relief of all excavation stages is better than other models and that the changes in soil stiffness with strain and stress paths were captured well by the HP model, even with small strains.

They also showed that none of the three models could estimate the changes in tunnel size and maximum tensile bending strain in the transverse direction. To address this problem, the authors may need to consider the actual soil stiffness around the tunnel. Thus, the accuracy of these models are contingent on being consistant with field conditions.

2.4.2 Constitutive models of frozen soils

Frozen soil is a complex multiphase material including soil particles, frozen water, unfrozen water and air (Lackner et al., 2005; Pimentel et al., 2012; Xue-lei et al., 2013). Recently, some attempts have been made to develop constitutive models to represent the complex behaviour of frozen soils.

Lai et al. (2016) introduced a constitutive model for frozen saline sandy soil based on series of triaxial compression tests. The developed model involved the effect of salt content on mechanical properties of frozen ground. They showed that the proposed model could simulate the mechanical properties of materials with both straight critical state line and curved critical state line as well as predicting the deformation regularity of such soil. The proposed model was able to introduce the influence of different parameters on the frozen soil behaviour such as salt content and anisotropy.

Rotta Loria et al., (2017) presented an elasto-plastic constitutive model, based on associated flow rule, which is able to simulate the non-linear mechanical behaviour of frozen silt. The model was verified against triaxial test results available in the literature, and it was shown that it could predict the non-linear mechanical response of frozen silt subject to both low and high confinement. However, this model has parameters that need to be calibrated based on experimental tests. The main issue is that some of the parameters, such as variation in temperature, need to be implicitly considered. This could limit the capability of the model in capturing the frozen soil behaviour under different environmental field conditions.

Xu et al. (2017) introduced an elasto-plastic model, including the effects of temperature and strain rate on the mechanical behaviour of frozen Helin Loess. Based on the experimental results, the stress-strain curves of saturated frozen Helin loess exhibited strain-softening behaviour under different temperatures and strain rates.

The model parameters were identified by fitting the experimental data. Comparing the experimental and simulated results showed a good agreement, and it was shown that the constitutive model could predict the behaviour of frozen Helin loess with reasonable accuracy.

It should be mentioned that, although these models showed good agreement with experimental results, they include many assumptions and the presented equations are highly complex. Therefore, implementation of these models in numerical analysis could be very challenging. Furthermore, the developed models have not been used in a case study to show their ability in solving a boundary value problem.

2.5 Summary

The field of constitutive modelling has been considerably developed with time, especially with the significant developments in the advanced computational algorithms. Each constitutive model has its own limitations and shortcomings. Although there has been considerable amount of research on the development of a wide range of constitutive models based on empirical data and theoretical assumptions with high complexities, none of these models is able to extract the exact behaviour of the material under different loading conditions. Moreover, most of these models have (material) parameters with little or no physical meaning (Shin and Pande, 2000). Recently with developments in computational techniques, the area of material modelling has been extended beyond the conventional theories, to computer-aided pattern recognition algorithms which have been reintroduced for modelling of a wide range of engineering applications. Some data-driven techniques such as an ANN, GP, EPR, etc have been utilised successfully to model the behaviour of various materials. In the next chapter, the description and application of the main types of data mining techniques will be presented in detail.

CHAPTER 3

Data Mining Approach in Constitutive Modelling

3.1 Introduction

The field of constitutive modelling has been progressed in parallel with the rapid development of computational algorithms and user-friendly software packages. The existing codes and software packages enable researchers to solve very complex problems in different areas of engineering including structural and geotechnical engineering, biomedical engineering, aerospace and many others. Numerical analysis, such as FEA, has been widely used to simulate very challenging problems. The accuracy of such analysis is highly reliant on the appropriate constitutive model that is able to represent material behaviour under different conditions.

To address the difficulties of classical constitutive models mentioned previously, many researchers have exploited the use of artificial intelligence and data mining techniques (i.e. ANN,GP, and EPR) to extract the real behaviour of different complex materials (e.g. soils, rocks, concrete, polymers, etc).

In this chapter, these types of data mining techniques are firstly discussed in detail, reviewing their main contributions in representing the behaviour of materials (in general and soils in particular) in numerical analysis. Towards the end of this chapter, the focus will be on the successful applications of EPR-based constitutive modelling and its advantages over other methods.

3.2 Artificial neural network (ANN)

Artificial neural networks (ANNs) are pattern recognition techniques that have been inspired by the human brain and nervous system. ANNs have been successfully employed in data modelling in different science and engineering applications. The main features of ANN are its capability to learn and be fault tolerant (i.e. noise data). Thus ANNs have excellent interpolative capabilities, and their performance depends on the information provided to them during training. ANNs can be deployed in most situations, for instance when an uncertain model with a purely analytical basis is required in engineering applications (Millar, 2008). The main advantage of using ANNs over classical models is that ANNs can learn from samples of data and generate models that can describe the behaviour of engineering systems without any assumption on the relationships between the input and output parameters of the system (Shahin et al., 2008).

ANN is the most widely used data mining technique in constitutive modelling of materials. Ghaboussi et al., (1991) were the first to introduce ANN-based constitutive modelling to describe the behaviour of concrete. The work on neural network-based constitutive modelling was then extended to more complex non-linear material behaviour, including geomaterials (Ellis et al., 1995, 1992). The results of these and many other works have indicated that ANN-based constitutive models can represent the highly non-linear behaviour of a wide range of engineering materials with a reasonable accuracy. ANNs have the capability to work with large quantities of data and learn the complex response of materials by training with an appropriate set of input and output variables.

In general, ANN consists of some artificial neurons, also known as nodes, which are arranged in layers. Usually there is an input layer, an output layer and one or more intermediate layers, named hidden layers. Each neuron in a layer is fully linked to every neuron in the next layer through weighted connections as shown in Figure (3-1).

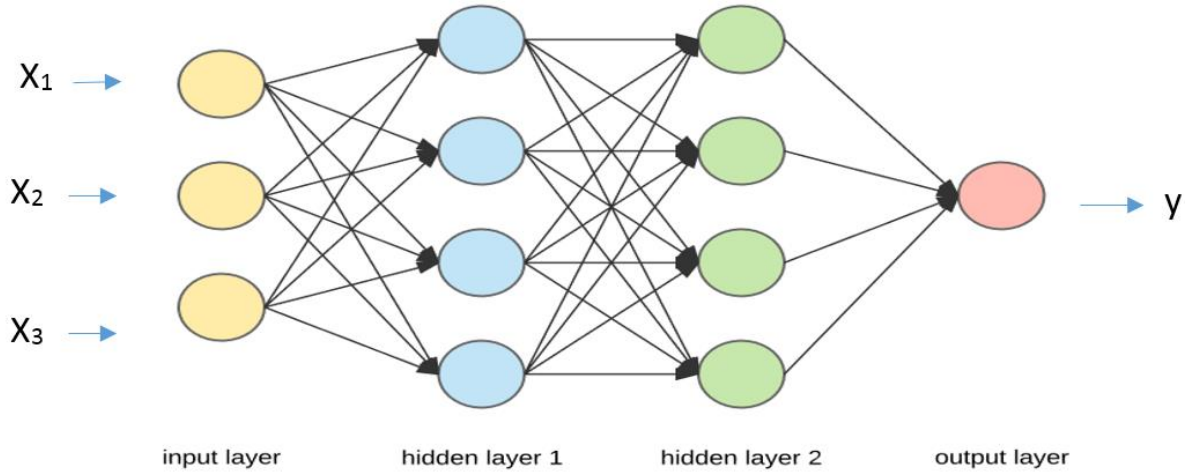

Figure 3-1: Typical neural network form; X_1, X_2 ,X_3 are the input variables, y is the output variable.

ANN modelling is rather similar to some traditional statistical models in that both try to extract the relationship between a set of input variables and the corresponding output variables. The weighted connections represent the information stored in the process of the network. The model is trained by updating its connection weights via the training process. This process is continued until the predicted output variable(s) are satisfactorily agreed with the target values of the training data. The algorithm of training of a neural network in such a way is called back-propagation in the sense that the observed error in the predicted output variable is used to update the connection weights. The back-propagation is one of the most widely used training approaches for multi-layered feedforward networks (Shin, 2001).

An important key point in developing ANN-based models is to choose the right input parameters that have the most significant influnce on the model prediction (Faraway and Chatfield, 1998). Among different types of ANN, multi-layer feedforward network has been the main type of neural network used in material constitutive modelling (e.g. Hashash et al., 2004b).

3.2.1 Applications of ANN in material modelling

Ghaboussi and Sidarta (1998) suggested nested adaptive neural network (NANN) to model the behaviour of geomaterials. They used NANN to construct models for the drained and undrained behaviour of sands in triaxial tests. NANN takes advantage of the nested structure of the material test data and represents it in the architecture of the neural network. Penumadu and Zhao (1999) presented the use of ANN to model the mechanical behaviour of sand and gravel. They used an excessive amount of experimental data from about 250 triaxial compression tests under drained condition. The ANN structure consisted of three hidden layers with 15 neurons in each layer, 11 neurons in the input layer and two outputs. This optimum structure was developed through a trial and error procedure. The input and output variables for the developed model were as follows:

Input variables $\longrightarrow$ $D_{50}, C_c, C_u, h, n_s, e, \varepsilon^i, \Delta\varepsilon^i, \sigma_3', \sigma_d^i, \varepsilon_v^i$

Output variables $\longrightarrow$ σ_d^{i+1}, ε_v^{i+1}

where D_{50}, C_c, C_u are parameters of particle size distribution curve, h is hardness of material, n_s and e are shape factor and void ratio respectively and σ_3' is the effective confining pressure. The current state of stress and strain was introduced in terms of deviator stress σ_d^i and volumetric strain ε_v^i. Providing the state of stress and strain, the proposed model was aimed to predict two output variables, deviator stress (σ_d^{i+1}) and volumetric strain (ε_v^{i+1}) for the next stress-strain state corresponding to an incremental axial strain ($\Delta\varepsilon^i$). The results revealed that the proposed model was able to represent the non-linear stress-strain and volume change behaviour of the soil with an acceptable level of accuracy. However, the model trained on such vast amount of experimental data has not been implemented in numerical analysis such as FEA.

Banimahd et al., (2005) modelled the stress-strain behaviour of sandy soils using ANN based on results from an extensive set of undrained triaxial tests. They developed a model using multi-layer perceptron (MLP), which is a class of feedforward ANN, to predict the undrained behaviour of in situ sandy soils. An incremental training procedure was utilised to train the MLP neural network. Verification of the model capability was performed through a sensitivity analysis.

However, the MLP neural network required significant effort and a complex procedure to identify the key parameters that influence the behaviour of the soil. Millar, (2008) demonstrated that using an ANN can provide new capabilities over a broad range of problem areas in rock mechanics and rock engineering.

Correia et al., (2013) investigated the applications of data mining in transportation geotechnics. The research included the use of ANN, support vector machine (SVM) and evolutionary computation techniques such as multiple regression (MR). The analysis involved the compaction management, mechanical behaviour of jet grouting material and pavement evaluation. In the case of compaction, they used collection tables based on fieldwork and experiments in France as database. The evaluation process aimed to model the compaction control parameters and provide understanding of the relationship between parameters that contribute to the compaction work of an embankment layer. The results showed that ANN and SVM present better accuracy than the traditional multiple regression method. They also showed the capability of data mining techniques in predicting the mechanical behaviour of improved soils (i.e. from jet grouting technology). In this analysis, modelling the uniaxial compressive strength (UCS) and elastic (Young's) modulus at small strains (E_o) were predicted using ANN and SVM. The analysis used the following variables:

$(^{n}/_{C_{iv}^{d}})$ the ratio between the mixture porosity and volumetric content of cement, (t) the age of the mixture, (W/C) water cement ratio, (s) coefficient of cement type, (C%) cement content, and (S%, ML%, CL%, OM%) the percentage of sand, silt, clay and organic matter respectively. The results illustrated that SVM produces a higher accuracy compared with ANN (Figure 3-2). The authors mentioned that although ANN can be considered as an advanced computational tool to extract implicit information from the available data space, however, it is a black box system and suffers from slow convergence speed, low generalisation performance and overfitting problems.

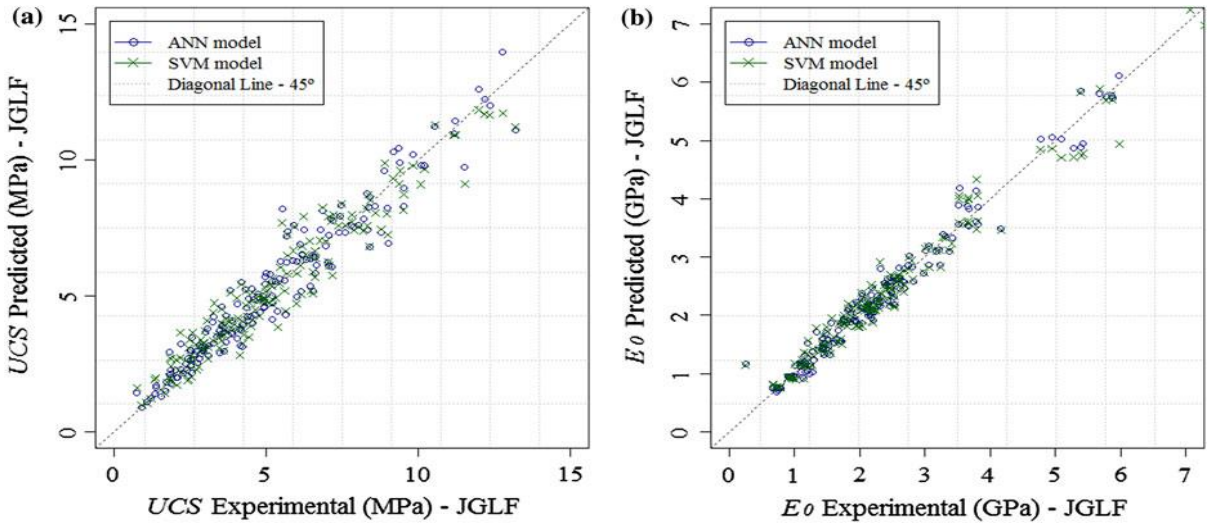

Figure 3-2: Comparison between experimental results and prediction of ANN and SVM for a) UCS b) E_o (Correia et al., 2013).

Khademi et al., (2016) introduced a comparative study to deal with the modelling of 28 day compressive strength of recycled aggregate concrete (RAC) using three different data-driven techniques, ANN, adaptive neuro-fuzzy inference system (ANFIS) and multiple linear regression (MR). They included 14 input (dimensional and non-dimensional) parameters in the training process. It was noticed that all the data-driven models used performed better when the non-dimensional parameters were used. The results also revealed that ANN and ANFIS predicted better than MR. However, the study declared that including some non-dimensional parameters would cause increase or decrease in the accuracy of the prediction of the compressive strength of concrete. This can be noted as one of the drawbacks of such data-driven techniques.

Sharma et al., (2017) presented a comparative modelling study to evaluate the unconfined compressive strength (UCS) of rocks by utilising three different data mining techniques ANN, MR and ANFIS. Rock collected from five geological regions in India were used in this study. Extensive laboratory tests were used to develop the models and they were all trained using three input variables which were density (d), slake durability index (SDI) and ultrasonic P-wave velocity (V_P) while the only output was UCS. The neural network structure used is shown in Figure (3-3). The results of the predicted UCS using the developed models versus the observed UCS are presented in Figure (3-4).

The authors intended from this work to minimise the uncertainty and inconsistency that come from using statistical models such as MR and ANN and highlighted the performance of using ANFIS among others. However, the results have not shown a clear difference between the performance of ANN and ANFIS. Also, the study did not consider other possible variables that might be affected during the analysis such as type of material filling and grain size distribution.

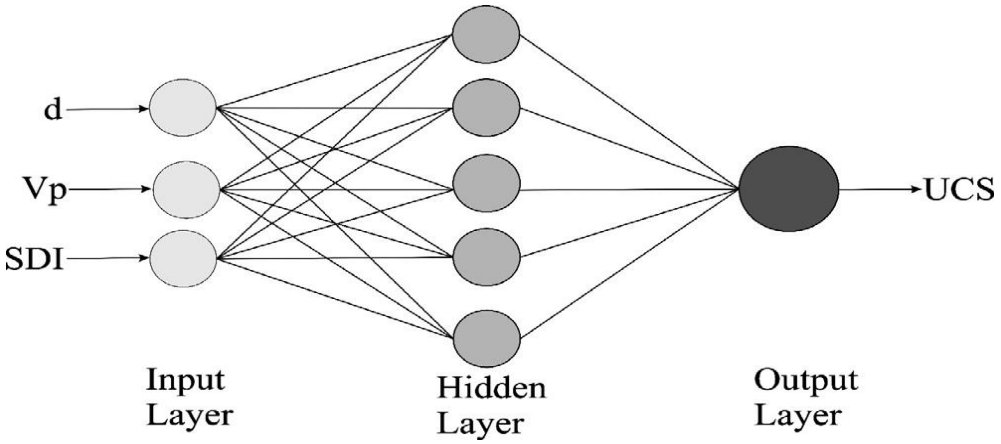

Figure 3-3: A schematic structure of ANN (Sharma et al., 2017).

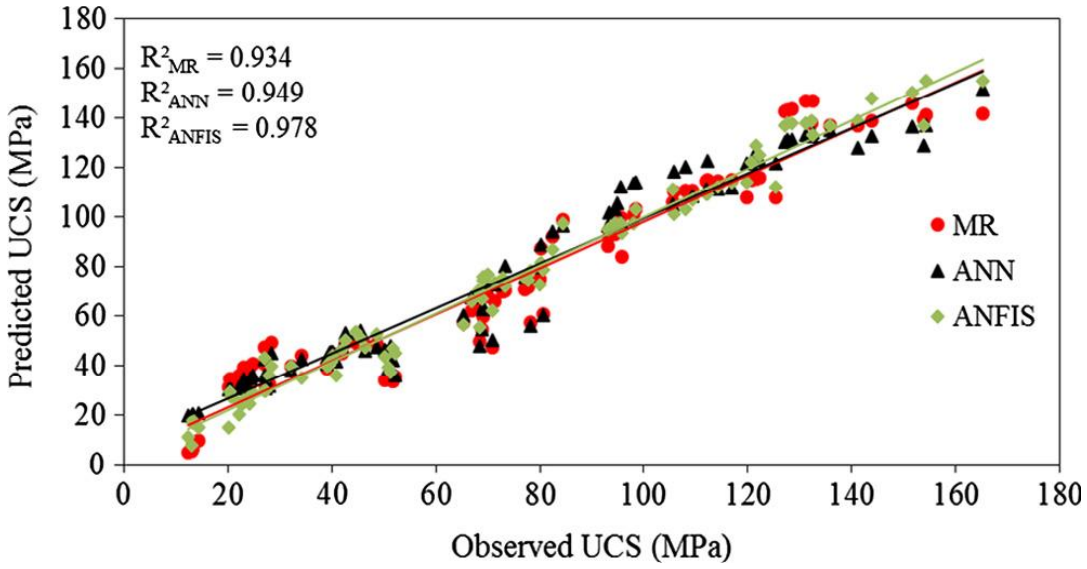

Figure 3-4: Comparison between measured and predicted UCS using MR, ANN and ANFIS models (Sharma et al., 2017).

Yan et al., (2017) proposed a new algorithm to improve the capabilities of ANN by combining the approximation ability of ANN with the global search ability of GA for modelling the bonding behaviour of glass fibre-reinforced polymer (GFRP) bar to concrete. In this approach, the ANN was used to map the relationship between the bond strength and the contributing parameters while GA was used to optimise the connection weights and biases of ANN. Data available from 157 beam-test specimens from the literature were utilised for training, including seven input parameters (bar surface, bar position, bar diameter (d_p), ratio of concrete cover to bar diameter (c/d_p), ratio of embedment length to bar diameter (L_d/d_p) and one output parameter, the bond strength (τ_b). The effectiveness of the developed ANN-GA model was evaluated by comparison with the original ANN model and a mulit-nonlinear regression model MNLR. The results revealed that the developed model predicts the bond strength more accurately in comparison with other conventional models and also better matches with the experimental data. However, the ANN-GA modelling strategy has its own limitations. For instance, the selection of variables including in the algorithm, size and quality of data plays an important role in providing accurate predictions.

3.2.2 Incorporation of ANN-based material models in FEM

The use of ANNs as constitutive models in numerical methods, particularly the FEM, has increased over the past few decades. Javadi and his co-workers introduced the use of ANN in constitutive modelling to represent the response of complex materials including soils. They developed an intelligent finite element code based on the incorporation of a back-propagation neural network in FEA. The method was applied to some engineering applications and it was indicated that ANNs could be efficient in extracting and representing the constitutive behaviour of complex materials (Javadi et al., 2003).

Furukawa and Hoffman (2004) presented an algorithm to implement ANN into FEA to describe monotonic and cyclic plastic deformation. They used two ANNs to learn the kinematic hardening and isotropic hardening behaviour of materials. The structure of their proposed neural networks and the corresponding inputs and outputs are presented in Figure (3-5). In this figure, Y and R show the kinematic and isotropic hardenings respectively and ε^p is the plastic strain.

The subscripts k, k-1 and k-2 refer to the current and previous states of every parameter. After training, the developed model was implemented in a commercial finite element (FE) code, MARC, via its user subroutine utility for material models.

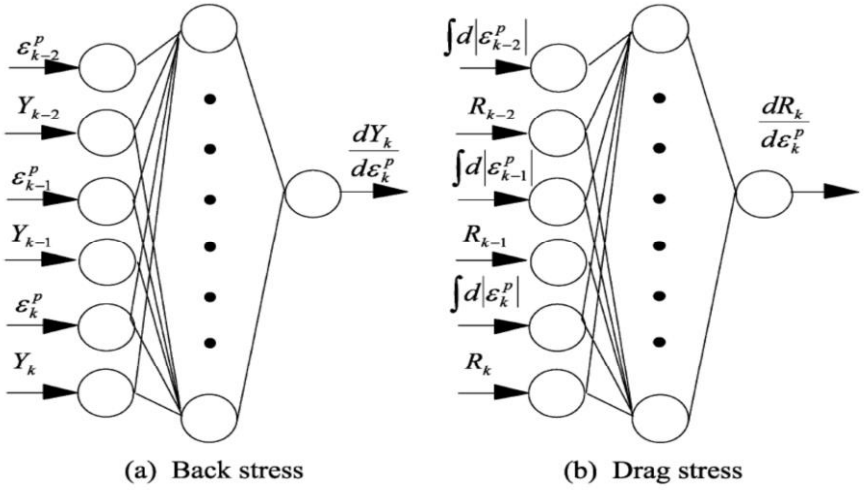

Figure 3-5: Neural network material models for back and drag stresses (Furukawa and Hoffman, 2004).

The stress-strain relation was presented through the stiffness matrix (D) defined as:

$$\boldsymbol{\sigma = D\,\varepsilon} \tag{3-1}$$

where D was given by the sum of the elastic matrix D^e and the plastic matrix D^p

$$\mathbf{D = D^e + D^p} \tag{3-2}$$

The Young's modulus *E* and Poisson's ratio μ were used to derive the elastic matrix while the plastic matrix was continuously updated using the trained ANN model. The validation of the model performance was presented in which two material models similar to Figure (3-5) were generated using real data with monotonic plastic deformation. The non-linear kinematic hardening model (Chaboche model) and also laboratory data were used to validate the proposed approach. The results showed acceptable agreement by following the same procedure for the cyclic plastic deformation.

Finally, the developed ANN models were implemented in the finite element engine (MARC) utilising the introduced technique to represent the behaviour of the central part of a tensile specimen under cyclic loading. The results are presented in Figure (3-6).

It can be noted from this figure that, although the proposed ANN-based finite element analysis shows divergence from the experimental data at higher number of cycles, it shows better prediction compared with the Chaboche model.

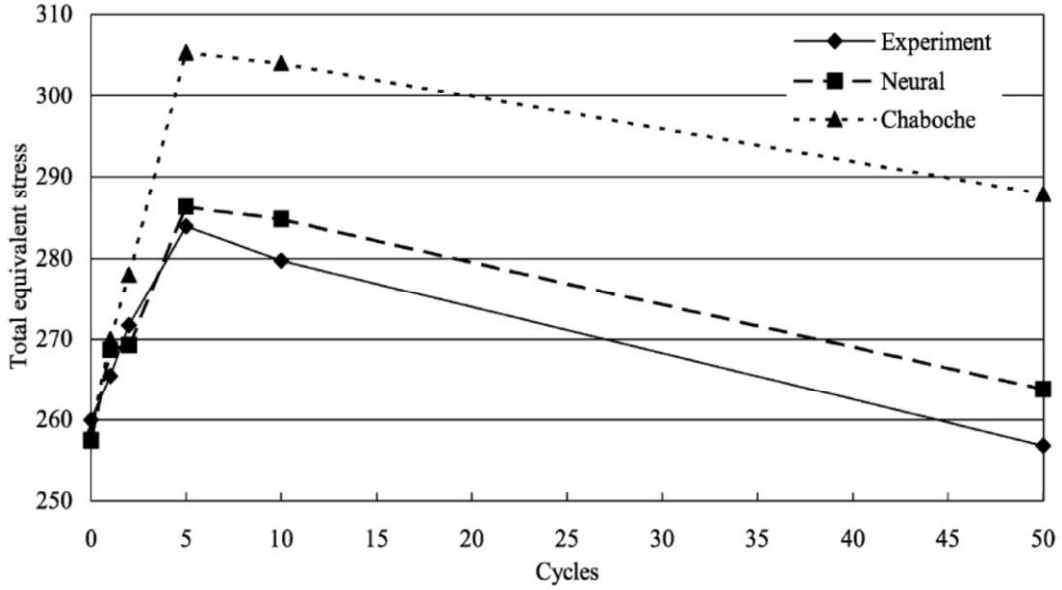

Figure 3-6: Comparison of experimental data, ANN-based FEM and Chaboche model in terms of total equivalent stress against cycles (Furukawa and Hoffman, 2004).

Hashash et al., (2004b) addressed some of the issues related to the use of ANN based constitutive models in FEA with a number of numerical examples. They defined the material stiffness matrix, required in incremental FEA procedure, as:

$$\frac{\partial^{n+1}\Delta\sigma_i}{\partial^{n+1}\Delta\varepsilon_j} = \frac{\partial(n+1_{\sigma_i} - n_{\sigma_i})}{\partial^{n+1}\Delta\varepsilon_j} = \frac{\partial^{n+1}\sigma_i}{\partial^{n+1}\Delta\varepsilon_j} \quad (3\text{-}3)$$

In the above equation n+1 refers to the next state of stresses and strains. The differentiation of the above equation can lead to calculation the material stiffness (Jacobian) matrix which can provide efficient convergence of the global solution. However, the incorporation of an ANN based constitutive model in equation (3-3) could result in a set of equations with complex mathematical structure that would not provide the user with a meaningful relationship between the input and output parameters of the material model.

Kessler et al., (2007) implemented an ANN-based constitutive model in FEA for prediction of the rheological behaviour of Aluminium. They compared the performance of an ANN model trained based on experimental tests of 6061 aluminium under compression at various temperatures (found in literature) with two conventional constitutive models (power law and tabular data).

The incorporation of the developed ANN model in the finite element code (ABAQUS) was via its user-defined subroutine VUMAT while the other two conventional models were analysed using the built-in models in ABAQUS.

The data extracted from the actual stress-strain curves were used to train the ANN by applying a set of networks with different number of neurons and different neural network structures. The analysis included four variables (stress, strain, strain rate and temperature). The results shown in Figure (3-7) demonstrate the predictions of the ANN and the conventional models versus the experimental results at 450 °C. These results indicate that the ANN-based finite element model has a better performance than the conventional constitutive models to mirror the experimental data. It can also be seen from this figure that the power law model captures the behaviour only with high strain level and the model based on tabular data provides a reasonable prediction.

However, the values of some input variables needed to be estimated a priori. Moreover, the model based on tabulated data underestimates the stresses when tested with different temperatures.

In this paper, the advantage of using ANN over the classical modelling approach was highlighted, however, the description of the way the proposed ANN model was implemented in finite element code has not been clarified.

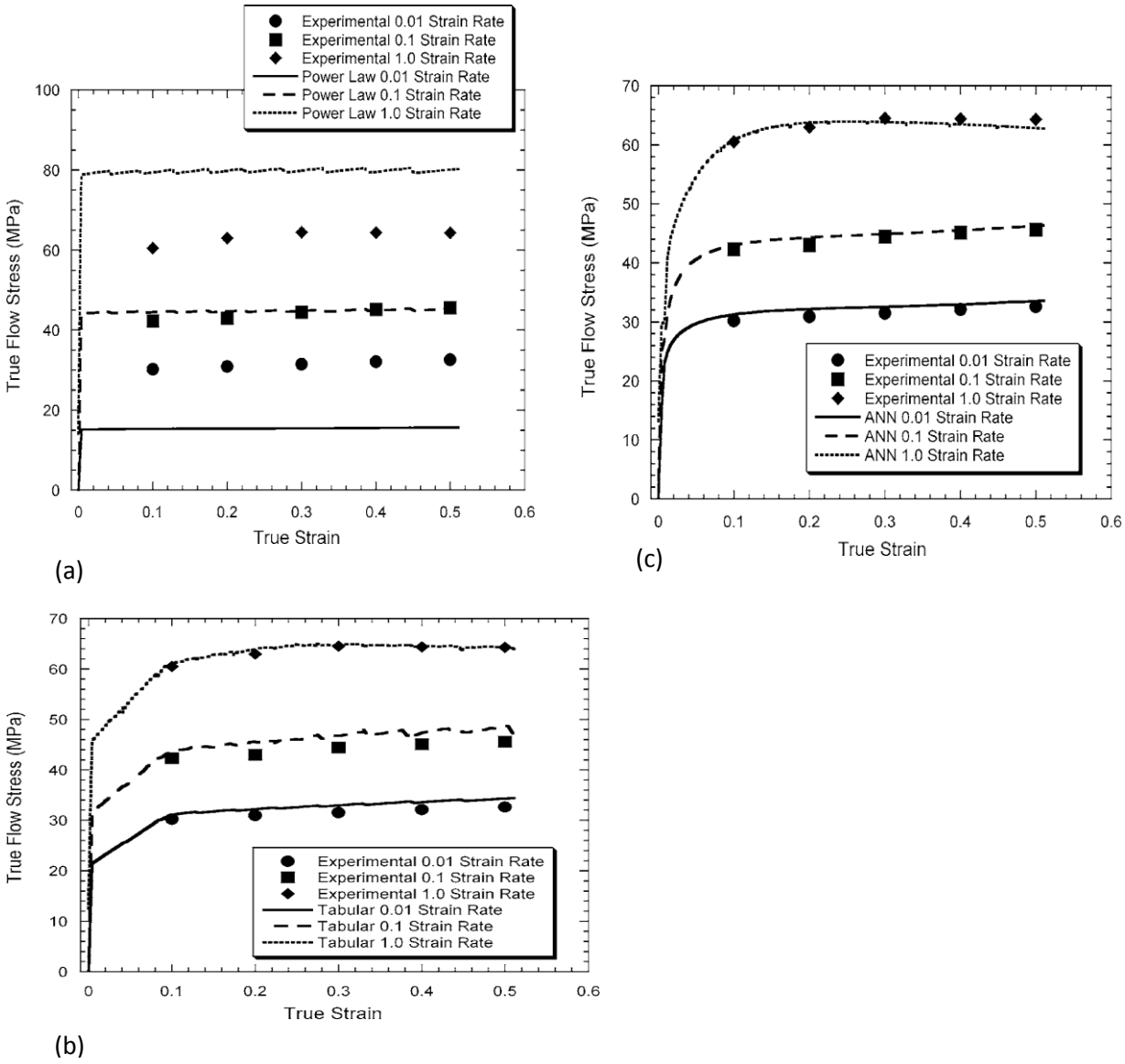

Figure 3-7: A comparison of experimental data and finite element model results using (a) power law model, (b) tabular data and (c) ANN model, presenting the real stress-strain relationships at 450 ˚C (Kessler et al., 2007).

Some researchers also introduced the ANN approach for modelling of the cyclic behaviour of materials and their implementation in FEA (e.g., Kim et al., 2010; Yun et al., 2008a, 2008b).

3.3 Genetic programming (GP)

Evolutionary algorithms (EAs) are search strategies inspired by biological evolution in nature (such as selection, crossover, and mutation) in which computer implementation of such evolutionary mechanisms is utilised to solve a function identification problem. The primary aim of this function identification problem is to search for a function in a symbolic structure that matches a set of experimental or field data (Rezania, 2008).

The major types of evolutionary algorithms are genetic algorithm GA and genetic programming GP. The GA is mainly used in parameter optimisation to generate the best values for model parameters by using a string of numbers to represent the solution.

Koza, (1992) extended the GA to an evolutionary computing method as a domain-independent problem-solving approach (called genetic programming GP). In GP, a series of computer programs made of functions and terminals are evolved to generate a transparent and structured model representing the system being analysed. GP has recently become more popular as an optimisation and learning technique. This technique generates mathematical equations to fit a set of data to represent the behaviour of a system (or a material).

The GP modelling process is first initialised by generating an initial population of computer models. This population involves a set of functions and terminals which are randomly chosen and defined by the user for a particular problem. They are arranged in a tree structure to make up a computer model. The model consists of nodes which are elements from the terminal set (e.g. constants = 3, variables x_1, x_2, x_3, and functional set (e.g. mathematical operators ±, x^y).

A typical GP tree structure, representing the algebraic expression of $[(3 + x_1)/(x_2 - x_3)]^2$ is illustrated in Figure (3-8).

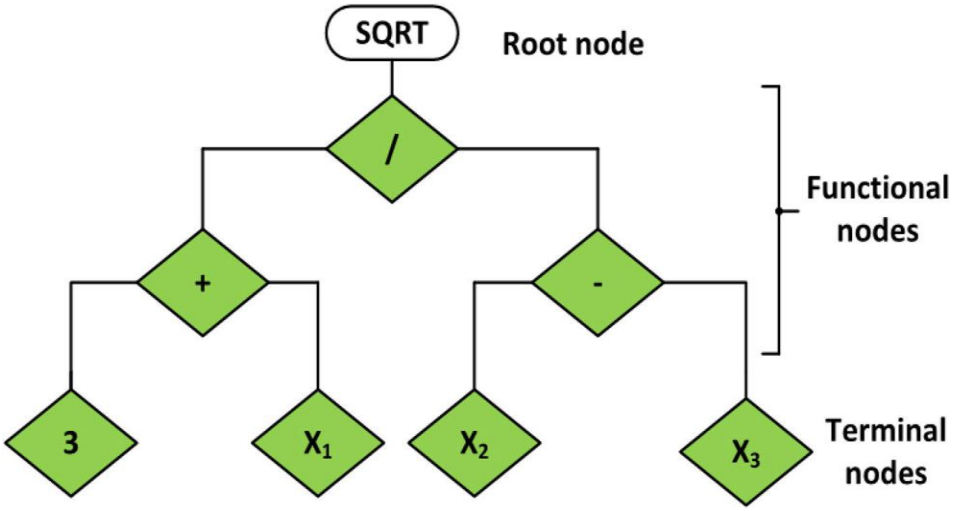

Figure 3-8: A typical GP tree structure for function $[(3 + x_1)/(x_2 - x_3)]^2$ (Fatehnia and Amirinia, 2018).

GP begins with finding a set of functions that correspond to the nature of the problem. Every single element in the population gets a measure of its fitness in the current generation. The fitness criteria are determined by the objective function (i.e. how fit the individual is within the population). Through the process of reproduction, cross-over, and mutation, a new population is evolved representing a certain proportion of the computer models. Reproduction is achieved by copying a computer model from the current population into the next generation without any change. This is usually done based on the fitness of each tree structure. The mutation process is the exchange of a randomly chosen functional or terminal node with others from the same function or terminal set.

Eventually, to improve the fitness of the population, the tree structures undergoes cross-over which is the genetic recombination of randomly selected portions of two computer models. A typical cross-over operation in GP is shown in Figure (3-9). (Fatehnia and Amirinia, 2018).

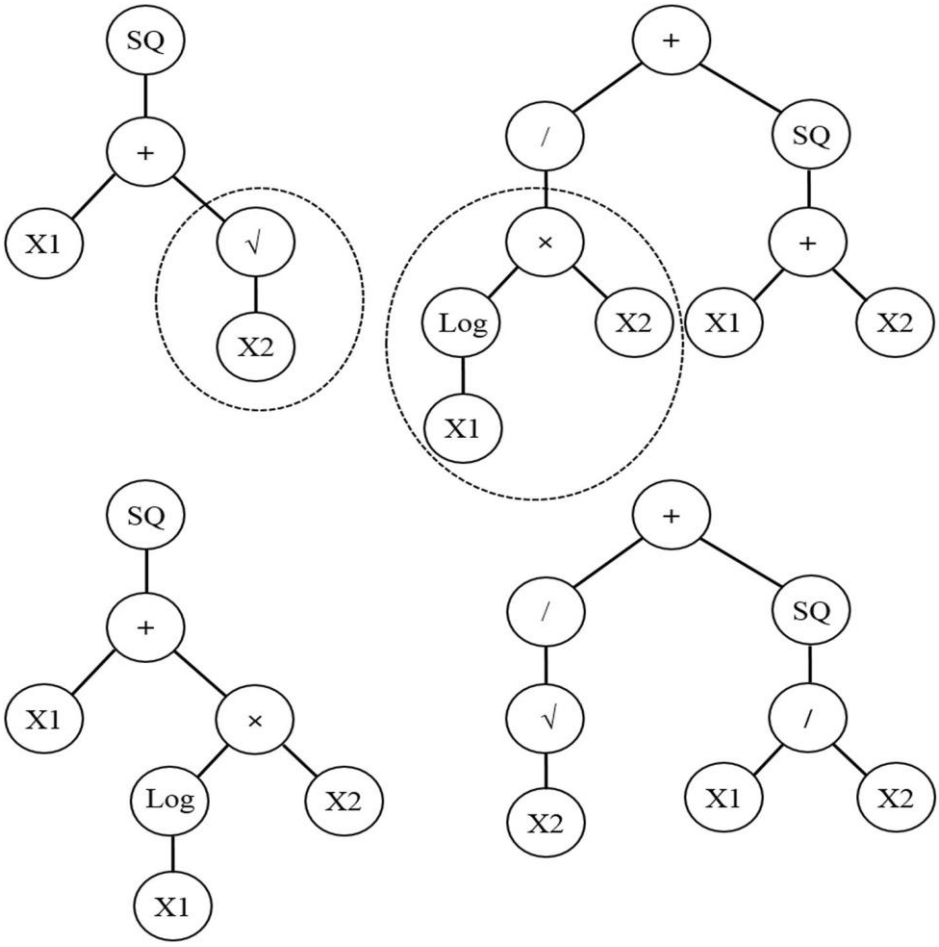

Figure 3-9: Typical cross-over operation in GP.

The new population will then replace the current population. The evolutionary process of GP is stopped when the termination criteria are fulfilled which is either the maximum number of generations or a specific tolerance. Finally, the best computer model is created by GP according to the fitness function chosen (Fatehnia and Amirinia, 2018).

3.3.1 Applications of GP in material modelling

GP, as one of the most general evolutionary computation algorithms, has been recently used in material modelling of the field of civil engineering. In particular, the capabilities of GP in the field of geotechnics have been investigated by some researchers (Javadi et al., 2006; Javadi and Rezania, 2006; Rezania and Javadi, 2007).

Javadi et al., (2006) introduced GP for estimation of the lateral displacements of soil due to liquefaction during earthquake. The prediction of lateral displacements during liquefaction is a complex problem due to the large number of parameters involved, including the parameters related to the earthquake intensity, soil properties and geology of the site. The results of this work showed that the GP model outperforms the multilinear regression model in prediction of lateral displacements.

Following this work, Rezania and Javadi (2007) proposed a new GP-based model to estimate the settlement of shallow foundations resting on cohesionless soils. They discussed the possible errors that may occur in predicting the settlement of foundations using the traditional methods. The results showed that the GP model provides a more accurate prediction compared with the conventional methods and also ANN in determining the settlement of shallow foundations.

Although GP generally outperforms ANN, provides global interpretations and gives the user a clear insight into the relation between contributing input and output parameters, it also has some shortcomings. It has been shown that GP is not a robust tool in determining constants of a model, and it produces functions which grow in length over time (Giustolisi and Savic, 2006).

3.4 Evolutionary polynomial regression (EPR)

3.4.1 General overview

As mentioned above, ANN and GP have been successfully used in material modelling and their applications in various engineering problems (including constitutive modelling) have gained increasing attention. ANN and GP are powerful non-linear modelling techniques that are able to represent the complex behaviour of various materials. However, these methods have their own limitations. For instance, when using ANNs, the number of hidden layers, number of neurons, transfer functions, etc. must be initially determined, using a time-demanding trial-and-error procedure. Moreover, the black box nature, the high complexity of the network structure, and the lack of interpretability have the main obstacles in using the ANNs in material modelling (Faramarzi, 2011; Javadi and Rezania, 2009a; Rezania, 2008).

On the other hand, GP has problem in finding the constants of the mathematical expressions generated during the training process. Also, in GP the number of terms in the model can exceed and the evolutionary search can be prolonged (Giustolisi and Savic, 2006). To address the limitations of ANN and GP, another data mining technique named EPR, has been developed. EPR is a combination of genetic algorithm GA and least square LS introduced by Giustolisi and Savic, (2006).

3.4.2 EPR based models

To understand the differences between mathematical modelling algorithms, usually, colours are used to specify their level of required information. In this classification, white box, grey box, and black box models are considered. The definition of each model can be illustrated as in the following points (Giustolisi and Savic,2006):

- White box model is referred to a model with known variables, parameters and underlaying physical laws. It declares the relationship of the system in form of set or single equation.
- Grey box model is considered as a conceptual model which its mathematical structure can be derived from conceptualisation of physical aspect or via a set of differential equations representing a physical phenomenon. EPR is considered as a symbolic grey box model.
- Black box model is referred to a system with no prior information about the relationship between variables. ANN is an example of a black box model.

EPR is a new hybrid approach based on evolutionary computing, aimed to search for polynomial structures representing the behaviour of a system (Giustolisi and Savic, 2006). EPR implements numerical and symbolic regression to perform evolutionary polynomial structure. The main idea of the EPR is to use evolutionary search for exponents of polynomial expressions by means of a genetic algorithm (GA). GA allows an efficient search for explicit equations that represent the behaviour of a system and offers more control over the complexity of the structures generated (Giustolisi and Savic, 2009). A typical formulation of EPR expression can be written as (Giustolisi and Savic, 2009, 2006):

$$Y = \sum_{j=1}^{m} F(\mathbf{X}, f(\mathbf{X}), a_j) + a_0 \quad (3\text{-}4)$$

where Y is the estimated vector of output of the system; a_j is a constant; F is a function constructed by the process; X is the matrix of input variables; f is a function defined by the user and m is the number of terms of expression excluding the bias term (a_0) (Giustolisi and Savic, 2006). Genetic algorithm is utilised to select the useful input vectors from X to be integrated together. The building blocks of the structure of F can be defined by the user based on an understanding of the physical process. While the selection of feasible structures is done during an evolutionary process, the parameters a_j are determined by the least square method. The first step in the identification of the model structure is to convert equation (3-4) to the following vector form (Giustolisi and Savic, 2009).

$$Y_{Nx1}(\Theta, Z) = [\, I_{Nx1} \;\; Z^j_{Nxm}] \times [\, a_0 \;\; a_1 \;\; \ldots\ldots \;\; a_m]^T = Z_{Nxd} \times \Theta^T_{dx1} \quad (3\text{-}5)$$

Where $Y_{Nx1}(\Theta, Z)$ is the least squares estimate vector of the N target values; Θ_{dx1} is the vector of d= m+1 parameters a_j and a_0 (Θ^T is the transposed vector); Z_{Nxd} is a matrix generated by I (unitary vector) for bias a_0, and m vectors of variables Z^j. For a fixed j variables Z^j is a product of the independent predictor vectors of inputs, $X = \langle X_1 \; X_2 \ldots . \; X_k \rangle$.

Generally, EPR follows a two-step process for constructing a mathematical model. In the first step, it searches for the best form of the function structure and in the second step, it uses the least squares method to find the adjustable parameters of the symbolic structures. In this way, EPR algorithm searches for the best set of input combinations and related exponents simultaneously. The matrix of input parameters X is given as (Giustolisi and Savic, 2006):

$$X = \begin{bmatrix} X_{11} & X_{12} & X_{1k} \\ X_{21} & X_{22} & X_{2k} \\ \ldots & \ldots & \ldots \\ X_{N1} & X_{N2} & X_{NK} \end{bmatrix} = [\, X_1 \quad X_2 \; \ldots\ldots\ldots \; X_k \,] \quad (3\text{-}6)$$

where the k^{th} column of X refers to the candidate variables for the j^{th} term of Equation (3-5). The j^{th} term of Equation (3-5) can be written as:

$$Z^{j}_{Nx1} = [\ (X_1)^{ES(j,1)} .\ (X_1)^{ES(j,2)} \ldots\ldots (X_k)^{ES(j,k)}\ ] \quad (3\text{-}7)$$

where Zj is the j^{th} column vector whose elements are products of candidate-independent inputs and ES is a matrix of exponents. Therefore, the problem is to find the matrix ES_{kxm} of exponents the values of which can be within user-defined bounds. For example, if a vector of candidate exponents for variables (inputs) in X is selected to be EX [0, 2, 3] and m (the number of terms without bias) is 4, and k (the number of candidate-independent variables/inputs) is 3, then polynomial regression problem is to find a matrix of exponents ES_{4x3} (Giustolisi and Savic, 2006). An example of such a matrix is given here:

$$ES = \begin{bmatrix} 0 & 2 & 3 \\ 0 & 2 & 2 \\ 2 & 3 & 0 \\ 2 & 2 & 0 \end{bmatrix} \quad (3\text{-}8)$$

Each exponent in ES matrix corresponds to a value from the user-defined vector EX. Also, each row in the ES matrix determines the exponents of the candidate variables of the j^{th} term in equations (3-4) and (3-5). This would allow the transformation of the symbolic regression problem into one of choosing the best ES matrix. In this way, the best structure of the EPR model can be generated. If the above matrix is substituted into Equation (3-7) the following terms can be formed:

$Z_1 = (X_1)^0 . (X_2)^2 . (X_3)^3 = X_2^2 . X_3^3$

$Z_2 = (X_1)^0 . (X_2)^2 . (X_3)^2 = X_2^2 . X_3^2$

$Z_3 = (X_1)^2 . (X_2)^3 . (X_3)^0 = X_1^2 . X_2^3$

$Z_4 = (X_1)^2 . (X_2)^2 . (X_3)^0 = X_1^2 . X_2^2$

Equation (3-5) it can be written as:

$$Y = a_\circ + a_1 . \mathbf{Z}_1 + a_2 . \mathbf{Z}_2 + a_3 . \mathbf{Z}_3 + a_4 . \mathbf{Z}_4 = a_\circ + a_1 . \mathbf{X}_2^2 . \mathbf{X}_3^3 + a_2 . \mathbf{X}_2^2 . \mathbf{X}_3^2 + a_3 . \mathbf{X}_1^2 . \mathbf{X}_2^3 + a_4 . \mathbf{X}_1^2 . \mathbf{X}_2^2 \quad (3\text{-}9)$$

The adjustable parameters (a_j) can be estimated by using the LS method based on minimisation of the sum of square errors (SSE) which is used to map the search toward the best fit model and can be presented as:

$$SSE = \frac{\sum_{i=1}^{N}(y_{a-}\ y_b)^2}{N} \tag{3-10}$$

where y_a are the target values in the training data and y_b are the model predictions computed by EPR. The presence of zero in the exponent matrix ensures the ability to exclude some of the inputs from the regression model. The modelling procedure of EPR starts from a constant mean of output values. By increasing the number of evolutions, it gradually picks up the different parameters to construct equations representing the system.

The best structure of the EPR model is identified using a GA search over the values in the user-defined vector of particular exponents. Detailed description of the GA procedure and its role in EPR can be found in (Giustolisi and Savic, 2006).

The EPR process is stopped when the termination criteria are satisfied, which could be either the maximum number of generations, the maximum number of terms in the EPR equation or a specified tolerance. The general flowchart of the EPR procedure is shown in Figure (3-10).

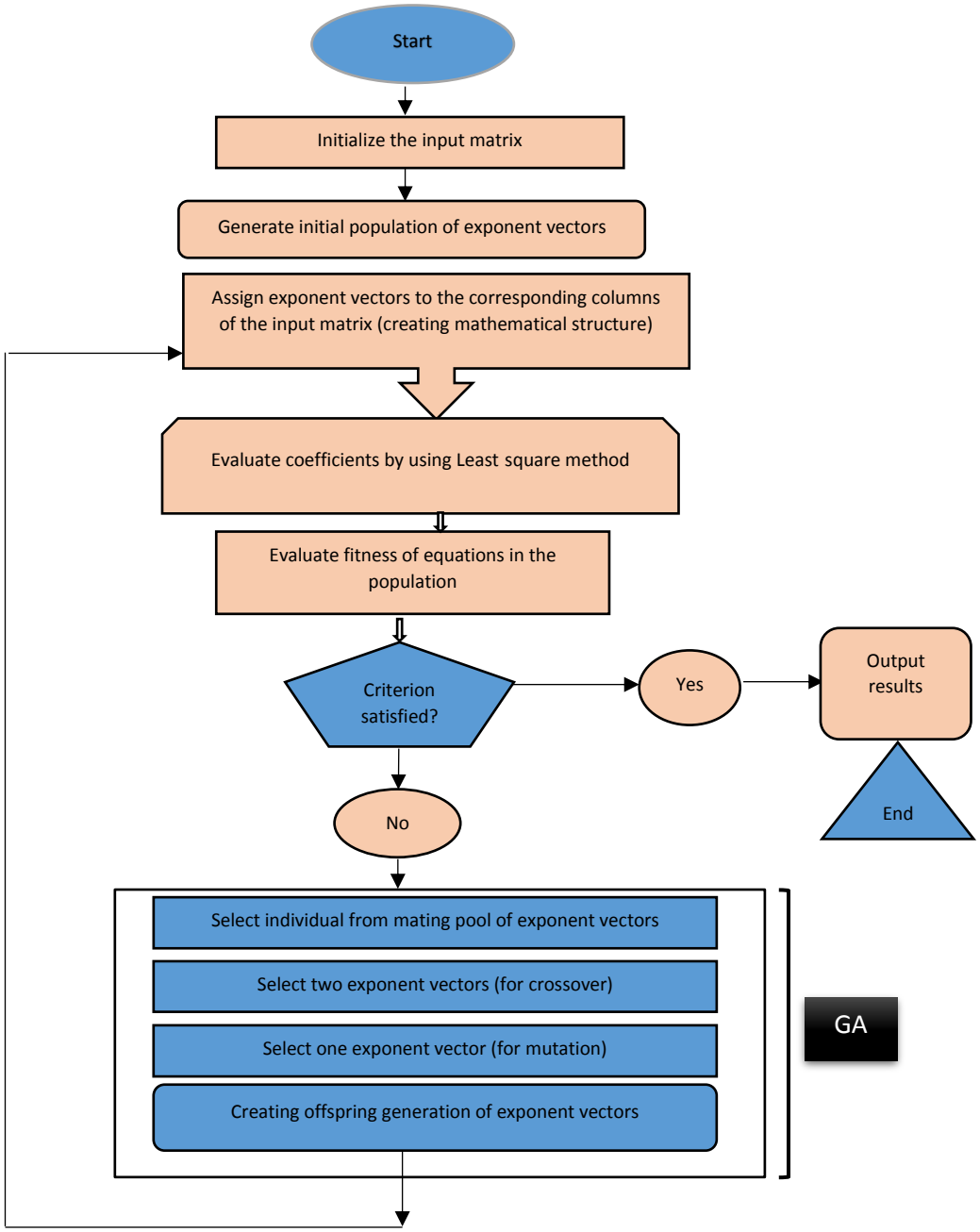

Figure 3-10: Flowchart of the EPR procedure (Doglioni A., 2004).

3.4.2.1 Least square technique

Determination of a_j in equation 3-9 is defined as an inverse problem of solving an overdetermined linear system based on the least squares method. This problem is usually solved by the Gaussian elimination method. Instead, an evolutionary search approach could generate candidate solutions such as combinations of exponents of X variable that are related to an ill-conditioned inverse problem.

The rectangular matrix ($Z_{N\times d}$) shown below could not be of full rank (Giustolisi and Savic, 2006).

$$Z = [\, I_{N\times 1} \;\; Z^1_{N\times 1} \;\; Z^2_{N\times 1} \;\; Z^3_{N\times 1} \;\; \ldots\ldots Z^m_{N\times 1} \;\;]_{N\times(m+1)N\times d} \qquad (3\text{-}11)$$

Particularly if the solution has a column of zeros or the columns Z^j are linearly dependent. In this case, significant issues are raised to the Gaussian elimination approach and consequently a more rigorous method is required. In the EPR procedure, Singular Value Decomposition (SVD) is utilised to estimate the parameters a_j of the matrix Z. This technique enhances the process of finding the solution to the least square problem (Faramarzi, 2011; Rezania, 2008).

3.4.3 Objective functions used in EPR

EPR optimisation can be achieved by using different objective functions in order to have the best characteristic equation(s) representing the phenomena being studied. Either single or multi-objective configuration can be used in the framework of EPR. Figure (3-11) illustrates the main objective functions available in EPR. In general, EPR provides a different approach to model selection through a detailed analysis of complexity (i.e. a number of terms, number of exponents, number of inputs) and model fitness.

Usually, the best modelling technique is also the simplest model that adequately matches the purpose of the system being analysed. The principle of parsimony points out that for a set of equivalent models representing a single phenomenon, the user needs to select the simplest model to represent a set of available data. Consequently, the fitness in a regression procedure should also include the trade-off between the complexity and fitness of the model. To achieve this, the following techniques can be considered (Doglioni, 2004).

i) ***Single objective function***: an objective function is utilised to represent the fitness without having models with unnecessary complexities.

ii) ***Multi-objective functions:*** at least two objective functions are involved; one function controls the fitness of the models, while another one can manage the model complexity. The main advantage of this approach is that it returns a set of non-dominated models each one introducing fitness

and complexity features. In this case, there is no need for prior assumption made by the user of the number of building blocks. However, the user needs to set the maximum number of terms, whereas the control on the complexity will let the number of blocks vary according to the model's fitness (Doglioni, 2004; Giustolisi and Savic, 2006).

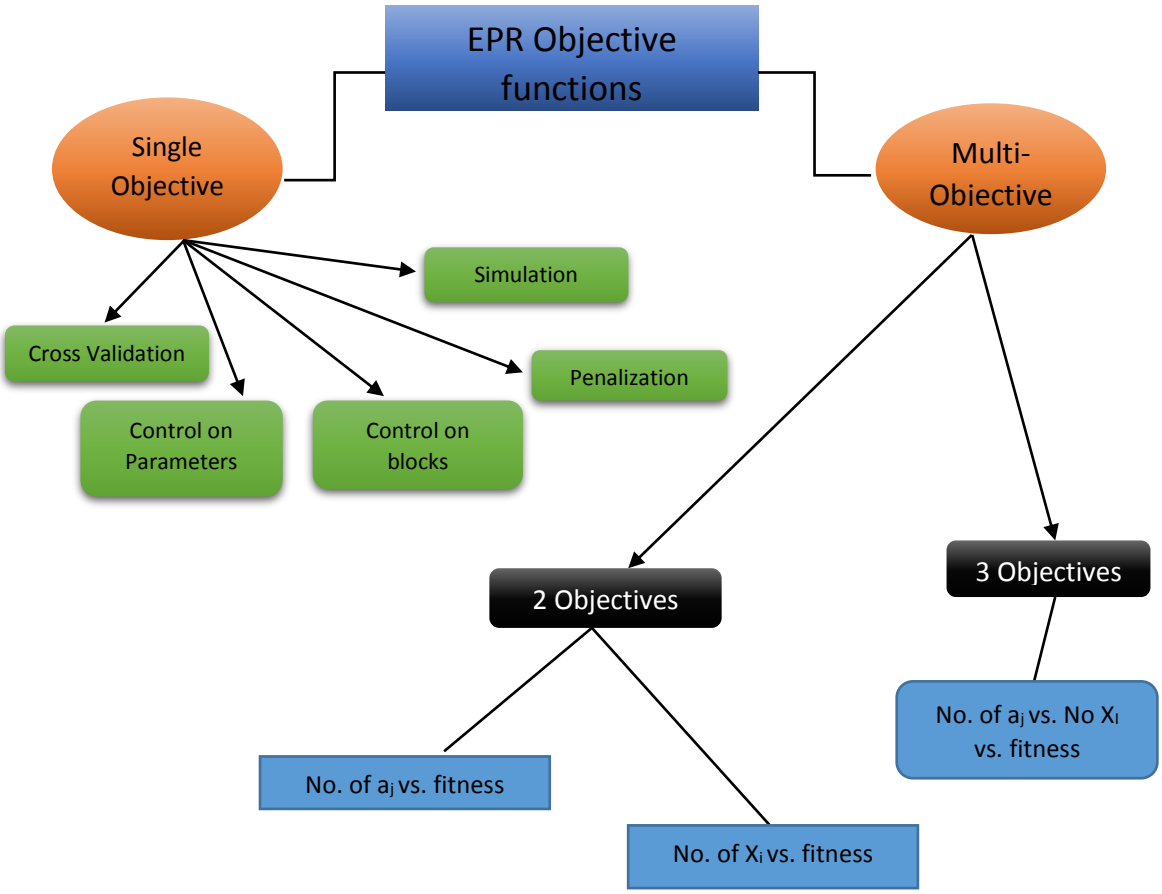

Figure 3-11: Overview of main objective functions in EPR (Doglioni, 2004).

3.4.3.1 Single Objective technique

In EPR, to represent a set of experimental or field data, a regression-based technique is used. To model a particular application, EPR needs to search among several potential models to find an optimum model. In EPR, the search process for the possible models is done through changing the exponents for the models (columns of matrix ($\boldsymbol{X}$)) and searching for the best fit set of parameters ($\boldsymbol{\Theta}$). Therefore, an objective function is required to avoid complexity and introduce the

best fit model. The 'complexity' here means including extra terms into the model or combinations of inputs parameters that provide noise to the raw data rather than representing the real behaviour of the entire system. In order to tackle the problem of overfitting, the following approaches are considered (Giustolisi and Savic, 2006).

i) Reduce the number of terms by penalising the complexity.
ii) Control the variance of a_j constants
iii) Control the variance of a_j. $\boldsymbol{Z_j}$ terms concerning the variation of residuals.
iv) Cross-validation of the models.
v) Optimisation of the sum of squared errors (SSE) evaluated on the simulation (off-line prediction) of the system being studied performed by the models.

Further details of these approaches can be found in (Doglioni, 2004)

3.4.3.2 Multi-objective technique

The previous versions of EPR used single objective genetic algorithm (SOGA) strategy to explore the search space. In this strategy, the maximum number of terms in the polynomial expressions can be assumed as in equation (3-5), then sequentially exploring the formula space with different number of terms. The SOGA strategy has a number of drawbacks as follows (Giustolisi and Savic, 2006):

a) When the number of polynomial terms increases, the performance of the SOGA decreases exponentially; hence more terms would lead to more GA runs.
b) The final results of SOGA strategy are usually difficult to be explained. The set of models can either be graded based on their fitness to available data or considering their structural complexity.
c) It is known that grading models based on structural complexity would need some subjective judgments. Therefore this process can be biased by the user's experience instead of being chosen according to some mathematical criteria.

d) The results do not include the entire formulas (the formulas with few terms are not presented). However, these formulas may have a better accuracy among others with more terms (Giustolisi and Savic, 2009).

To avoid the above drawbacks and limitations, a multi-objective genetic algorithm strategy (MOGA) has been added to EPR . This strategy aims to find the best model structures that respond to the fitness and minimise the structural complexity. The multi-objective modelling in hybrid evolutionary computing offers a number of advantages: It:

i) provides a set of appropriate symbolic models,
ii) makes a robust option to select the model, and
iii) provides a set of models with variable parsimony levels in efficient computational time.

MOGA based EPR aims to find the set of symbolic structures which perform well considering multiple criteria simultaneously. The objective functions used in the framework of EPR are:

i) Maximizing the fitness.
ii) Minimizing the total number of input variables selected by the modelling strategy.
iii) Decreasing the number of terms in the model structure.

The developed models are ranked according to Pareto dominance criterion.

MOGA based EPR decreases the computational time needed by the multiple runs of EPR.

The models that dominate others in the population of solutions are introduced to the user based on MOGA strategy (Giustolisi and Savic, 2009; Laucelli and Giustolisi, 2011). The most commonly used objective functions to measure the fitness of the symbolic structures are based on the SSE or the Penalisation of Complex Structures (PCS).

The result of SOGA based EPR optimisation includes a set of equally good models. It could be easier to rank them according to their SSE value than structural complexity. Arranging the models according to their structural complexity can be a difficult task (Giustolisi and Savic, 2009). The multi-objective technique generally improves both the post-processing aspect and the modelling framework of EPR. The developed EPR models are ranked according to the coefficient of determination (*CoD*) and also their structural complexity. There are

several objective functions implemented in the MOGA based EPR including (Giustolisi and Savic, 2009):

i)

$$CoD = 1 - \frac{N-1}{N} \frac{\sum_N [(Y_p - Y_a)^2]}{\sum_N [(Y_{a-} \frac{1}{N} \sum_N Y_a)^2]} = 1 - k \,.\, SSE \qquad (3\text{-}12)$$

$$k = \frac{2\,(N-1)}{\sum_N [(Y_a - \frac{1}{N} \sum_N Y_a)^2]}$$

where N is the number of data points on which the *CoD* is calculated, Y_a and Y_p are the vectors of actual and predicted data respectively.

ii) The number of constant values a_j

iii) The total number of inputs included in the symbolic structure (% of X_i).

It should be mentioned that the total number of inputs variables corresponds to the number of times that each input is included in the symbolic expression.

The EPR user must fix the maximum number of constants values, which sets an upper limit on the maximum number of the symbolic expression inputs. MOGA based EPR searches for the best non-dominated models considering both fitness on the models and structural complexity (placed on the best Pareto front surface) (Giustolisi and Savic, 2009; Laucelli and Giustolisi, 2011).

Furthermore, MOGA based EPR applies additional pressure to gain structural parsimony. The objective functions can be used either in double objective or all together as follows (Doglioni, 2004):

1) The coefficient of Determination (*CoD*) Vs. % of $\mathbf{X_i}$.
2) The coefficient of Determination (*CoD*) Vs. % of $\mathbf{a_j}$.
3) The Coefficient of Determination (*CoD*) Vs. ((% of $\mathbf{X_i}$) and (% of $\mathbf{a_j}$)).

If Pareto dominance criteria are chosen, the Multi-objective strategy provides the following advantages (Doglioni, 2004):

i) It requires less time: It should be faster for few objective functions compared with multiple single-objective runs.

ii) It deals simultaneously with multiple solutions.

iii) It provides a uniformly distributed range of Pareto solutions.

3.4.4 EPR user interface

EPR has been coded using MATLAB environment by Professor Giustolisi at Bari University, Italy and Professor Savic at Exeter University, UK (Giustolisi and Savic, 2006). EPR is provided with a user-friendly interface and works in an Excel add-in file. EPR has been updated several times with new versions adding new features. In particular, for the work of this project a new bespoke model has been provided with Multi-objective function (MOGA) to be easily integrated with other software used during the development of the EPR based self-learning framework. The new user interface of EPR is as shown in Figure (3-12). From this user interface, the user can set up the modelling phase according to the phenomena being studied and can also enter the number of generations and size of the population in the GA parameters box. There is an option for bias which looks for a symbolic structure having the constant $\mathbf{a_0}$. If the bias option is off, EPR will exclude all models containing $\mathbf{a_0}$. Otherwise, bias option is on by default and EPR will search for models with and without the term $\mathbf{a_0}$ (Doglioni, 2004). Also, EPR gives the user the ability to scale the data (scale input, scale output). Finally, the results of the EPR are directly written in a MATLAB file after completing the training process.

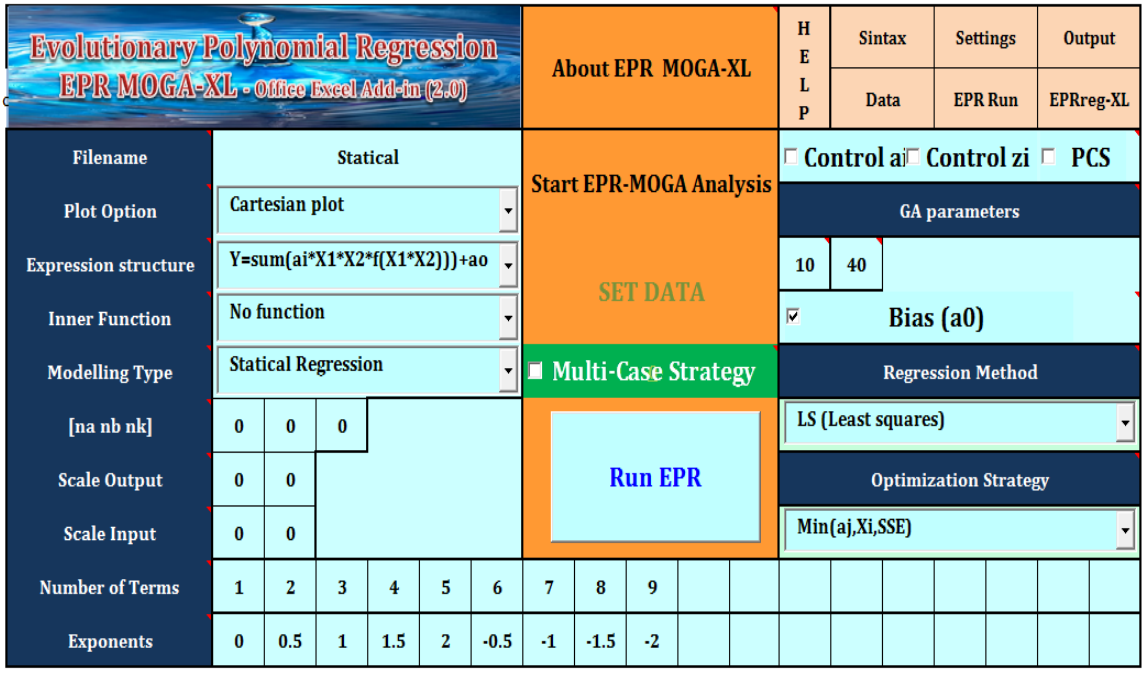

Figure 3-12: EPR User Interface.

3.4.5 EPR based material modelling

EPR has been proposed as an effective and alternative to other types of data mining techniques such as ANN and GP. An EPR based model provides a unified approach to material modelling. It has many advantages in introducing the behaviour of complex materials. EPR based model can learn and extract the material behaviour directly from experimental data. Consequently, it is the shortest route from experiments to numerical modelling (Faramarzi, 2011; Rezania, 2008). Models developed by EPR are concise and explicit mathematical equations that give the user an understanding of the effect of input variables on the predicted output. Another interesting feature in EPR is that in the training process, it can discard from EPR equations the parameters that have no effect on the material behaviour by including zero in the predefined exponents range. EPR was initially used for environmental and hydrological modelling (Berardi et al., 2008; Doglioni et al., 2010, 2008; Giustolisi et al., 2007; Giustolisi and Savic, 2006). In parallel, because of its outstanding performance in modelling of engineering systems, EPR was also successfully used for modelling of different civil engineering materials.

For instance, Rezania; et al., (2008) introduced the use of EPR for modelling of the nonlinear interaction between different parameters in civil engineering applications and compared it with the traditional and ANN based models. The EPR methodology was applied to some civil engineering applications including determination of the uplift capacity of suction caissons and shear strength of reinforced deep concrete beams. This study showed that EPR models perform well and overcome the issues related to traditional and ANN-based models.

Ahangar-Asr et al., (2011) used EPR to predict the mechanical behaviour of rubber concrete. They used extensive experimental data on rubber concrete and developed three models. The developed models predicted the compressive strength, tensile strength and elastic modulus of rubber concrete. Each model has eight input parameters that are known to affect the behaviour of rubber concrete. The results of the developed models were compared with the experimental data and also with linear regression, GP, and ANN models. The results revealed that EPR models were able to provide very accurate predictions for strength parameters of rubber concrete.

EPR was also utilised to model the behaviour of saturated and unsaturated soils. Comparison of results with experimental data showed a very close agreement. Results from some comparative studies have shown that the EPR models outperform the ANNs (Ahangar-Asr et al., 2012). EPR was also used to study the dynamic response of engineering materials. Faramarzi et al., (2011) utilised EPR to model the behaviour of steel plate shear walls under cyclic loading. They used experimental tests on steel plate structures to develop EPR models.

Rezania et al., (2011) used EPR for assessment of liquefaction potential and lateral displacement caused by earthquakes using data from real field case histories. The predictions of the developed EPR models were compared with those obtained from ANN and Multi-Linear Regression (MLR) models (Figure 3-13). The results showed that EPR could represent the liquefaction behaviour of soils accurately and outperform the existing ANN-based model. One of the key advantages of EPR over ANN is that EPR provides an explicit relationship between the contributing inputs and output variables.

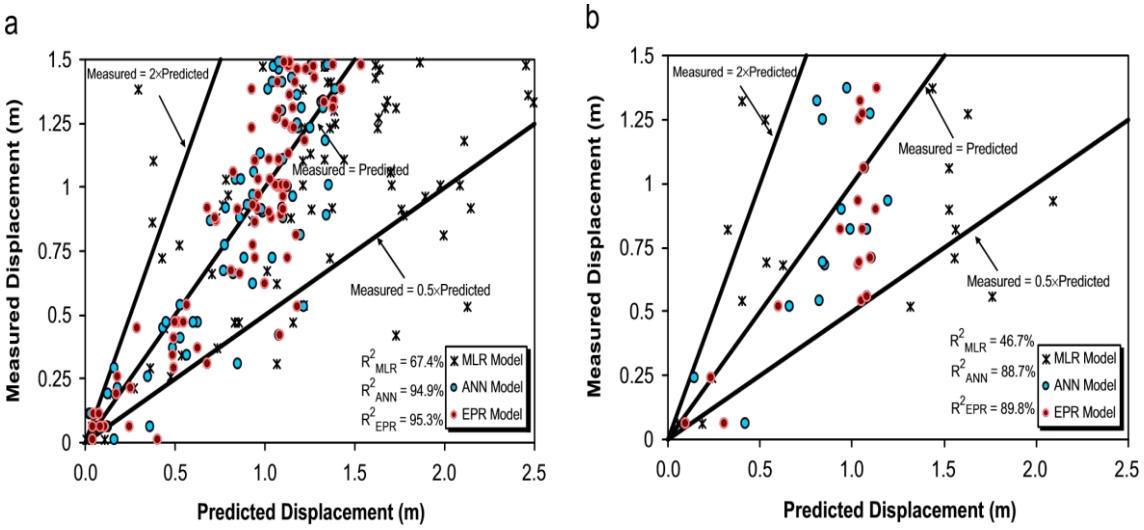

Figure 3-13: Results of EPR, MLR and ANN models for cases moderate displacement (a) training data (b) validation data (After Rezania et al., 2011).

Doglioni and Simeone, (2014) investigated the dynamic response of the deep karst aquifer of central Apulia, Italy using multi-objective EPR model. Four EPR models were developed to help understand the response of variations of groundwater level with symbolic equations.

3.4.6 Incorporation of EPR in finite element analysis

The methodology of incorporating EPR in FEA was first introduced in the work of Javadi and Rezania (Javadi and Rezania, 2009b; Rezania, 2008). They showed that a properly trained EPR-based constitutive model (trained on experimental data) could be readily implemented in a finite element model. Like neural network-based models, an EPR-based constitutive model does not require complex yield function, plastic potential, failure function, flow rule, etc. There is no need to check yielding, calculate the gradients of the plastic potential function and update the yield surface, etc. Figure (3-14) shows the procedures of both the conventional and EPR based FEM. The EPR-based FE methodology was applied to a number of boundary value problems, and the results were compared to those obtained from FE analyses using conventional and ANN-based constitutive models.

Rezania, (2008) introduced the implementation of EPR into FEM through a FEM procedure coded in Fortran to model some engineering problems. The methodology was initially tested through simple structural applications including linear and nonlinear elastic behaviour.

Then data from a series of triaxial tests were used to train the EPR models representing the soil behaviour. These models were then implemented into a FE code to analyse different geotechnical applications such as embankment, tunnel, and footing. Furthermore, a coupled analysis was carried out using data from simulated consolidated undrained triaxial tests. The data were generated by numerical simulation of the tests (using Modified Cam Clay model) under different confining pressures. Two different EPR models were developed including effective stress and permeability. A comparison between the predictions of the standard FEM using MCC model and the EPR-based finite element model showed excellent agreement. This encouraged the EPR based FEM to be applied to more complex applications (Rezania, 2008).

Faramarzi, (2011) and Faramarzi et al., (2012) and Javadi et al., (2012) presented the implementation of trained EPR models in FEA using ABAQUS (as the finite element engine) through its user-defined material module (UMAT). UMAT was used to update the stresses and provides the Jacobian matrix (J) for every increment in every integration point. The methodology of incorporation EPR into ABAQUS showed that it is possible to construct the material stiffness (Jacobian) matrix using partial derivatives of the trained EPR models.

The EPR based Jacobian matrix was integrated into finite element code, and the EPR-based FEM was applied to some boundary value problems including two and three dimensions, and cyclic loading analyses. The results from these analyses were compared with those obtained from conventional finite element method using Cam-Clay and Mohr-Coulomb models among others. The results showed that an EPR-based constitutive model (EPRCM) can be implemented in a finite element model in the same manner as a conventional constitutive model, with several advantages. This work is an essential step towards the incorporation of EPR based model into a commercial FE code.

Javadi et al., (2012) presented a new approach for modelling the behaviour of soils under cyclic loading. They developed an EPR model by generating data from numerical simulation (using MCC model) of triaxial tests under cyclic loading. The EPR model was then incorporated in a FE model and was used to simulate the cyclic loading tests. The results illustrated that EPR based finite element model was able to accurately predict and learn the complex behaviour of soils under cyclic loading considering the loading history of the soil. Although the work was primarily focused on soils, the methodology could be applied to other materials that have complex constitutive behaviours.

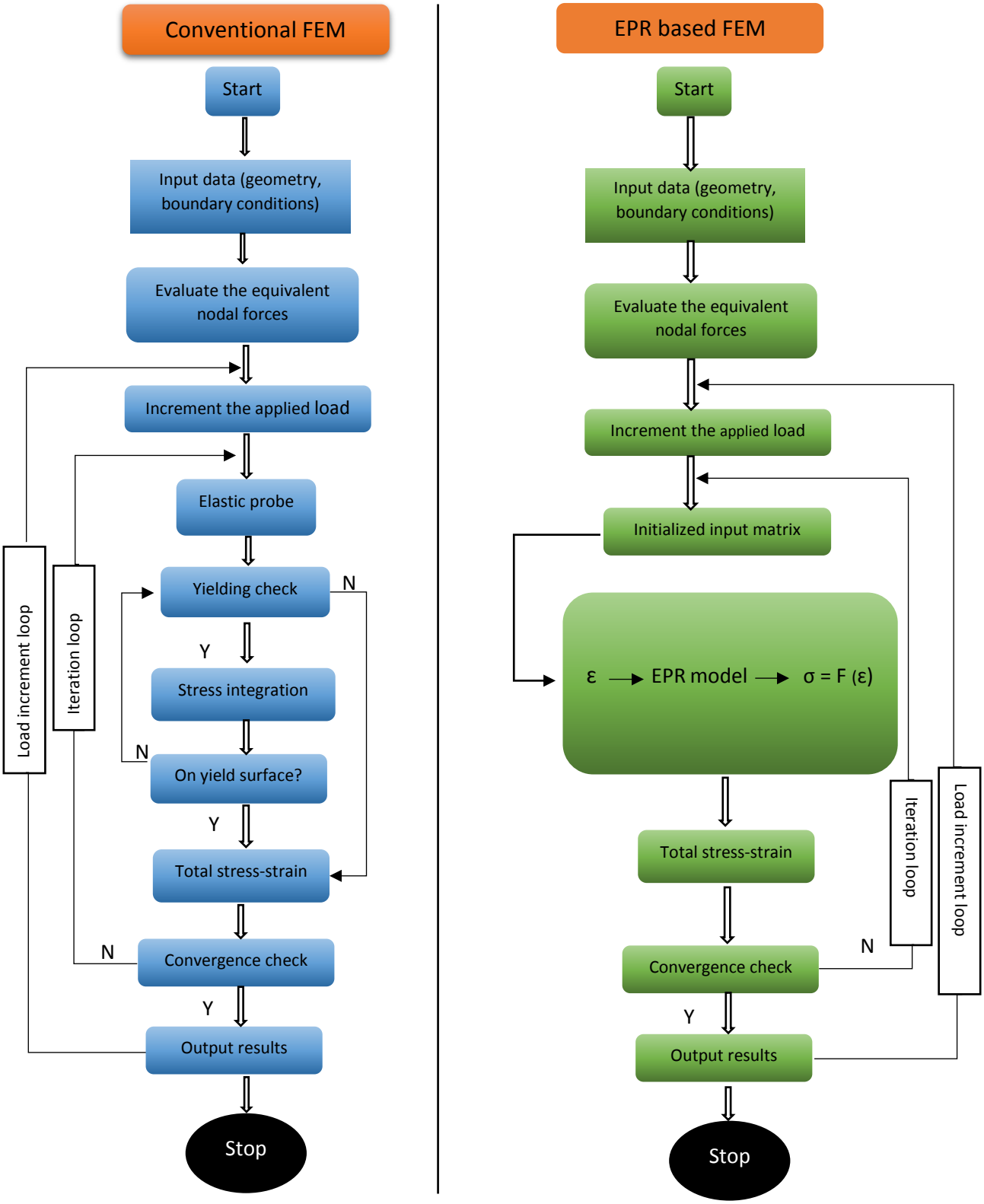

Figure 3-14: Comparison of Conventional FEM and EPR based FEM (After Rezania, 2008).

3.5 Summary

Data mining techniques have been widely used as a robust tool to represent the behaviour of various materials in different engineering disciplines. The main feature of these data-driven models is their ability to learn the material behaviour directly from experimental or field data. This approach to modelling can be considered as the shortest way from experimental (or field) data to numerical modelling. More importantly, they can be implemented in the numerical analysis, particularly FEM. This is a significant step forward in FE modelling of complex engineering problems. Although ANN based finite element modelling has been successfully applied to a number of engineering problems, however, it is well known that ANN suffers from some limitations and shortcomings. EPR was recently considered as an effective alternative tool that generates explicit equations and simplifies the way of incorporation in finite element method.

It should be mentioned that training of any type of data mining-based model requires a significant amount of data that would, in some cases, raise other challenges in material modelling. Consequently, another procedure called self-learning FEM was recently considered to train ANN and EPR models.

CHAPTER 4

Self-learning Approach to Constitutive Modelling

4.1 Introduction

The use of artificial intelligence techniques, especially ANNs and EPR, in material constitutive modelling has recently gained considerable attention among researchers. The implementation of such techniques has been proven as a robust procedure to represent various aspects of material behaviour for different engineering applications. However, the key to the successful use of these techniques is their implementation in numerical analysis (particularly FEM). Although valuable work has been done on developing constitutive models based on ANN and EPR and their implementation in FEA, it is generally known that ANNs and EPR require considerable amount of data in order to extract and learn the material behaviour. In other words, few laboratory tests would not be enough to develop an ANN- or EPR-based model. Generally, having a large amount of data from a single test on one sample is not possible. This problem was successfully addressed for ANN training through an innovative training procedure called auto-progressive algorithm originally presented by Ghaboussi and his co-workers (Ghaboussi et al., 1998). After that, the algorithm was extended and modified into a full framework by Hashash et al., (2003). It should be mentioned that although the way of training and learning capability of ANN was improved significantly in the auto-progressive algorithm, the mentioned previously drawbacks of ANN still prevail. Consequently, by exploiting the advantages that EPR can offer in representing material response in a simple and explicit model would be extremely useful to be used as a learning engine in the heart of the self-learning methodology. This chapter covers the applications of ANN-based self-learning algorithm and presents the new framework of EPR-based self-learning FEM.

Two different training strategies are presented. The advantages of employing EPR in the framework of self-learning FEM are highlighted.

4.2 Auto-progressive training algorithm

Ghaboussi et al. (1998) introduced a different approach to train ANN, named the auto-progressive algorithm. The concept of this algorithm is to use the information from a global load-displacement response of a structural test to train ANN-based models. The auto-progressive approach is used to extract the rich stress-strain data embedded in non-homogenous structural tests, to train the ANN models. The material model developed in this approach is extracted from an iterative non-linear FEA of the test sample and gradually improves the stress-strain data for training the ANN model. This allows to train ANN models from a limited number of structural tests in which one of the major limitations of ANN in material modelling can be avoided.

Sidarta and Ghaboussi, (1998) applied the auto-progressive algorithm using a series of non-uniform experimental tests (triaxial compression tests with end friction) on a sandy soil with different densities. The trained ANNs models were used in forward analysis of the triaxial tests with end friction and the developed models were used to predict the behaviour of the soil in a hypothetical test without end friction. The results revealed that the trained models could effectively learn the behaviour of sand very well in case of end frication and provide reasonable predictions for the tests without end friction. This has been one of the earliest works in this field.

4.2.1 Self-learning finite element algorithm

The methodology of auto-progressive training was extended to self-learning finite element algorithm. Shin and Pande, (2000) developed a strategy for training neural network based constitutive model (NNCM) by using data of stresses and strains at certain calibration points of structural tests in which stress-strain relations are not homogenous. They illustrated the proposed strategy by analysis of two engineering applications. The first application was a two-bar structure including two cases using different material behaviour.

In the first case, one bar was made from an elastic ideally plastic material while other one was made from a linear elastic material. In the second case, the structure included one bar with an elastic softening and the other bar with linear elastic behaviour.

The data from only one monitoring point was collected in both cases to train the ANN in the self-learning finite element code. The ANN model consisted of three inputs and three output variables (i.e. $\varepsilon_x, \varepsilon_y, \tau_{xy}$ and $\sigma_x, \sigma_y, \gamma_{xy}$ for input and output variables respectively).The results showed that the stress-strain relation matched well the original data after seven cycles of self-learning FEA. This could be related to the amount of data used for training ANN. The second problem was a panel of linear elastic material under plane stress condition subjected to a concentrated load on the top surface. Unlike the first problem, in this problem several monitoring points were used to provide input data for the self-learning FE model. It was found that the locations selected for the monitoring points may affect the training program and hence the convergence of the NNCM towards the standard solution. The application of the self-learning methodology was illustrated on a two relatively simple applications.

Shin and Pande, (2001) proposed another strategy to construct the tangential stiffness matrix using partial derivatives of ANN based model. They trained ANN via total stress-strain strategy and implemented the computed stiffness matrix in the self-learning FE code. The verification of the proposed approach was done by analysing a rock sample with fixed ends subjected to uniaxial cylindrical compression. Further applications of ANN with the self-learning finite element code were also implemented to identify anisotropic elastic material parameters from a single numerical test (Shin and Pande, 2003). The methodology consisted of two steps: in the first step a number of monitoring points of structural test were used to obtain data to train the NNCM embedded in FE code whereas in the next step the elastic constants were calculated. The first derivative of the NNCM leads to so called tangential stiffness matrix to obtain the elastic constants for a material at a specific value of current strain (ε_i):

$$D_{NN} = DNN_{ik}(\varepsilon_i, \sigma_k) = \frac{\partial \sigma_k}{\partial \sigma_i} \quad (4\text{-}1)$$

The structure of the ANN used in this methodology contained six nodes with each input and output layer having the following variables:

$\varepsilon_x, \varepsilon_y, \varepsilon_z, \gamma_{xy}, \gamma_{yz}, \gamma_{xz}$ as input, and $\sigma_x, \sigma_y, \sigma_z, \tau_{xy}, \tau_{yz}, \tau_{xz}$ as output.

To verify the capabilities of the proposed methodology, a plane stress panel with a circular cavity in its centre was used. The measurements of displacements at 66 nodes on the panel surface at 5 load increments of the FE simulation were used to train the NNCM. The material behaviour was linear elastic and after three cycles of self-learning FEA the discrepancy between the predicted and the actual data was reduced to an allowable value. The constitutive matrix based NN model was compared to the conventional orthotropic elastic matrix to obtain nine elastic constants. It should be mentioned that although the methodology was only applied to a simple boundary value problem it required too many monitoring points for a simple linear elastic behaviour. This means more complexity could be faced with more complex material and geometry.

4.2.2 Self-learning simulation (Self-Sim)

The self-learning FEM has proven to be a robust tool for extracting the real and complex material behaviour. This inverse analysis technique overcomes the limitations of the traditional constitutive modelling approach that requires pre-defined material models. Consequently, more improvements on the auto-progressive approach have been implemented to enhance the performance of this approach. Hashash et al, (2003) introduced the use of field measurements of excavation response to extract the constitute behaviour of soil. The methodology of auto-progressive training was extended in this work (second version) to construct a constitutive soil model using field observations of lateral wall deflections and surface settlement from several stages of a braced excavation. After that, the third version of the auto-progressive training procedure was developed by (Hashash et al., 2006a). They introduced a new framework to implement and extend the auto-progressive methodology in a software analysis procedure called self-learning simulation (Self-Sim). The methodology mainly followed the same procedure presented in the work of Ghaboussi et al. (1998) and Hashash et al., (2003).

The Self-Sim framework generally consists of two steps (Hashash et al., 2006a). In step 1, a laboratory experiment with boundary conditions and load is carried out and boundary forces and displacement are measured for each loading increment. Step 2 is achieved by developing a FE model to represent the geometry and corresponding measurements.

A neural network model is used as stress-strain relationship and trained at the beginning with linear elastic behaviour (within a small strain range). Two finite element analyses are run with the initial ANN model in parallel; finite element A (FE-A) simulates the behaviour of the structure under applied forces and determines stresses and strains at each integration point.

It is assumed that, since the applied boundary forces are accurate, and the equilibrium condition is satisfied, the computed stresses will be acceptable approximation of the actual stresses that are experienced throughout the test. However, the computed strains form this analysis could be a poor approximation of the actual strains, due to the difference between the computed and measured displacements.

In parallel, finite element B (FE-B) analyses the structure using the same initial ANN model whereby the measured boundary displacements are imposed. The strains obtained from this analysis are assumed to be accurate approximation of the actual strains, whereas the stresses may be a poor approximation of the actual stresses due to the difference between the computed and measured boundary forces. The stresses obtained from FE-A and the strains obtained from FE-B are collected to form stress-strain pairs of data and used to retrain the ANN model. The analyses of the finite element models A, B and subsequent training of the ANN model form the Self-Sim learning cycle. The procedure of analyses of finite elements A and B is repeated using a new ANN model which is updated at each iteration. Convergence is considered to be achieved when the results of both analyses (FE-A and FE-B) are matched. Each cycle of Self-Sim that accomplishes the applied load is called a pass. Several Self-Sim learning passes may be needed to extract accurate material behaviour.

Finally, the developed model can be utilised in the analysis of new boundary value problems. Figure (4-1) illustrates the Self-Sim algorithm applied to extract soil behaviour in a deep excavation problem. The self-learning simulation methodology has been applied to different material modelling problems for instance, soil behaviour, rate dependent materials and cyclic or dynamic response of material.

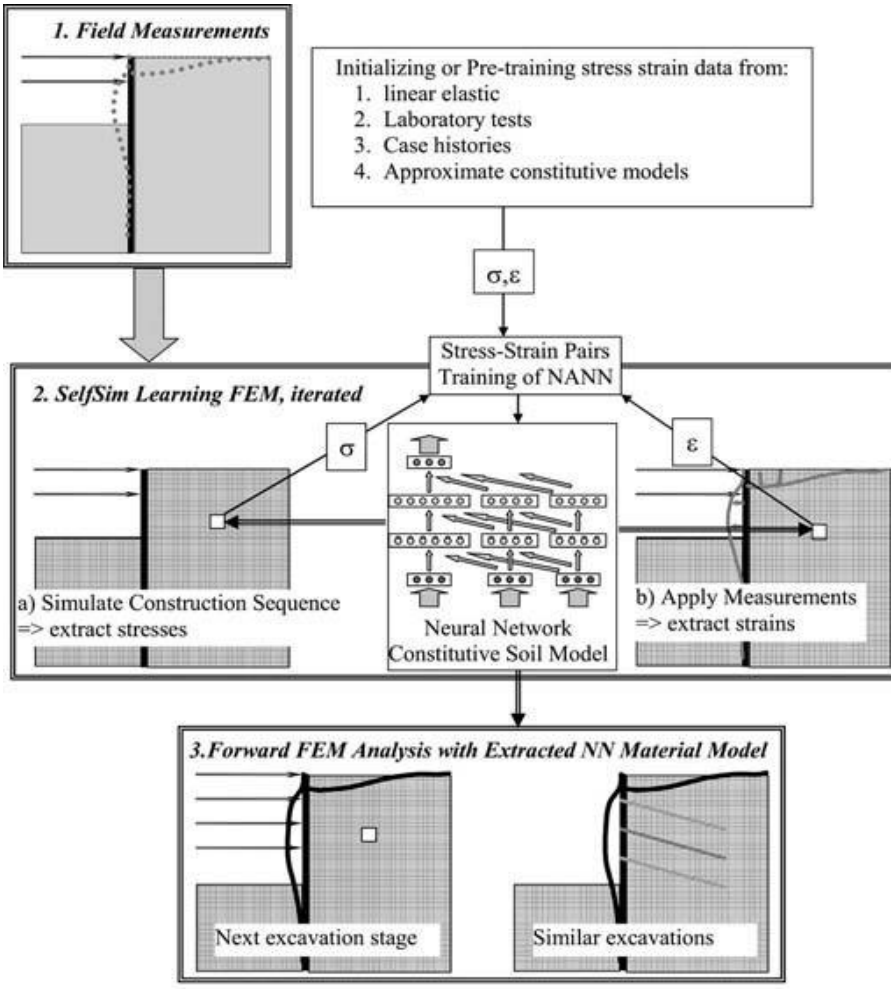

Figure 4-1: Self Sim algorithm applied to a deep excavation problem after (Hashash et al., 2006a).

4.2.2.1 Self-learning simulation for modelling of soil behaviour

In geotechnical engineering applications, the mismatch between field measurements and model simulations is raising concern about the ability of constitutive models in representing the real behaviour of soils under loading condition. Therefore, sophisticated inverse analysis technique has been introduced to model the behaviour of material more accurately.

As mentioned above, Hashash et al, (2006a) applied the Self-Sim modelling approach to analysis of deep excavations to extract the actual behaviour of soil. In this work, the Self-Sim algorithm was validated using a simulated excavation case study. The measurements including lateral wall deformations and surface settlement were obtained using the MIT-E3 soil model in FEA and used to train the ANN model. The capabilities of the Self-Sim algorithm in analysis of a deep excavation was examined through three numerical problems and two field case histories. The results demonstrated that the Self-Sim algorithm can extract the required information to realistically represent the soil behaviour under certain conditions (Hashash et al., 2006a).

(Hashash et al., 2006c) investigated the constitutive behaviour of extra-terrestrial soils using the Self-Sim approach. They applied load-displacement measurements to run the Self-Sim algorithm in which the applied loads and the corresponding displacements were recorded from the in-situ test. Following the same procedure presented in (Hashash et al., 2006a), the behaviour of the soils was captured with reasonable accuracy.

Fu et al., (2007) and (Hashash et al., 2006b) used the Self-Sim methodology to present the integration of laboratory testing and constitutive modelling of soils. Self-Sim was applied to two simulated laboratory tests including a triaxial compression test with no-slip friction ends and a triaxial torsional shear test with no-slip frictional ends. The use of frictional ends was to generate data on non-union states of stress and strain throughout the sample.

This study showed that Self-Sim could establish a direct link between laboratory testing and soil constitutive modelling to capture the soil behaviour under complex loading conditions. The developed ANN model was successfully used to predict the load-settlement behaviour of a simulated strip footing.

Hashash and Song, (2008) employed self-learning simulation (Self-Sim) to extract the underlying constitutive behaviour of soils via training of neural network models. Self-Sim was applied to different practical geotechnical applications to verify the capability of the proposed approach. First, data from triaxial tests on sand with frictional end loading plates were used to create non-uniform states of stress and strain in the sample. Secondly, a deep excavation problem was considered where lateral wall deformation and surface settlement measurements corresponding to the known construction stages were used to extract the anisotropic soil behaviour. The last application was the analysis of site response due to horizontal shaking. The results from the three applications revealed that Self-Sim is able to capture the real behaviour of soils under different loading conditions. For example, the NN model developed from triaxial test simulation was able to accurately capture the underlying soil behaviour after a number of Self-Sim passes as shown in Figure (4-2).

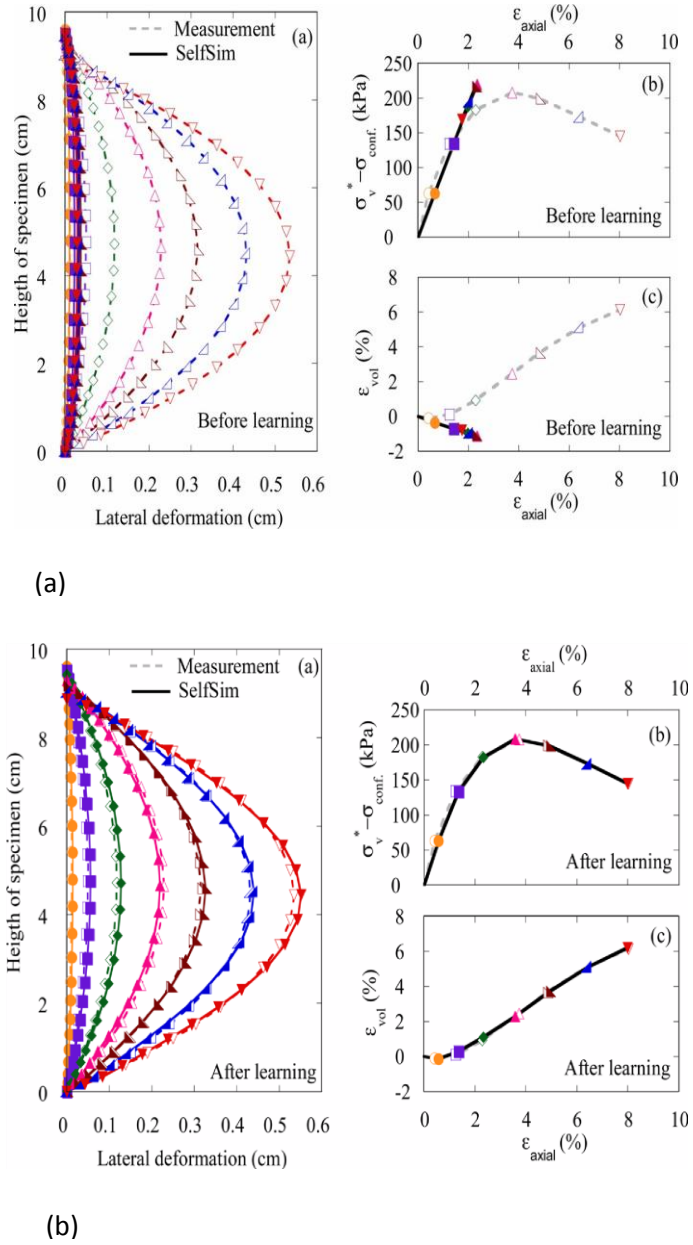

Figure 4-2: Self-Sim learning of triaxial test (a) before Self-Sim learning (b) after 8 passes of Self-Sim learning (Hashash and Song, 2008).

Hashash et al, (2009) presented the Self-Sim inverse analysis approach to investigate the drained behaviour of sandy soil using triaxial compression tests with fully frictional loading platens. Three different series of isotopically consolidated drained triaxial tests were carried out on sand with various particle sizes under confining pressures ranging between 25 to 300 kPa. The Self-Sim was applied using global load-displacement measurements from triaxial tests with up to 8.03 % of axial strain applied on each sample. The results showed that Self-Sim was able to extract the non-uniform stress-strain behaviour of sand. It was also shown that the integration between laboratory modelling and Self-Sim

could reduce the number of experimental tests required, as from a single test, multiple stress paths were generated, and the data were used iteratively to train the NN model. Although the model developed was based on rich information extracted from the real soil behaviour, the model was not applied on a different boundary value problem to verify the practical capability of the developed model.

Field instrumentations were also used in the Self-Sim algorithm for analysis of ground response of a deep excavation in soft soil (Osouli et al., 2010). They utilised the Self-Sim technique during excavation stages to develop a model representing soil behaviour. A synthetically generated set of different instruments were used at different locations to monitor the site response. The soil behaviour was represented synthetically using the MIT-E3 effective stress soil model to create the observed measurements used for the Self-Sim procedure.

Eventually, the developed NN model could be used to predict the ground response around the excavation (given a complete picture of the site), other types of excavation with similar ground condition and later excavation stages. The findings of this comprehensive study were confirmed by using an excavation case study and revealed that implementation of Self-Sim with field instrumentations provides full information of site response inexpensively and reliably. Further, the study presented the use of various instruments in excavation problems and the quality of information that could be gained for excavation modelling. Although all instruments showed their usefulness in the site response analysis, inclinometers placed at some distance behind the wall and measured forces in the struts considerably improved the quality of the represented soil behaviour.

Hashash et al., (2010) introduced two different techniques, based on inverse analysis, for learning the behaviour of soil in deep excavation projects in urban environment. An optimization approach based on genetic algorithm GA and Self-Sim algorithm were presented and compared for the analysis of the deep excavation problems. In the optimization approach PLAXIS (finite element engine) with the implemented hardening soil constitutive model was used in the GA to simulate the excavation problem. Field measurements collected by using inclinometers and surface settlements in Lurie Research Centre USA were considered in both inverse analysis approaches.

The excavation was divided into seven stages and the data from the last stage were only used in the optimization approach. However, lateral wall displacements and surface settlements for all construction stages were used as boundary conditions in the Self-Sim approach. Figure (4-3) illustrates the performance of Self-Sim learning after 12 passes. Although the deformations estimated using the NN models developed through the Self-Sim approach are in close agreement with the field measurements, the analysis involved significant number of Self-Sim passes. Comparison of the estimated lateral wall deformations and surface settlements obtained from GA and Self-Sim for the last construction stage is shown in Figure (4-4). It can be seen that the estimation of lateral wall deformations matches well for both approaches with the field measurements. However, the estimation of surface settlements behind the wall by the GA approach was not captured neither in magnitude nor in shape, although the settlement profile was also considered during the optimization process. This was because the hardening model used in the FE model does include the small strain nonlinearity. The authors claimed that this could be a limitation of using such optimization technique hence the accuracy of GA relies significantly on the constitutive model used, however, another possible non-linear model including small strain range could remove the concern.

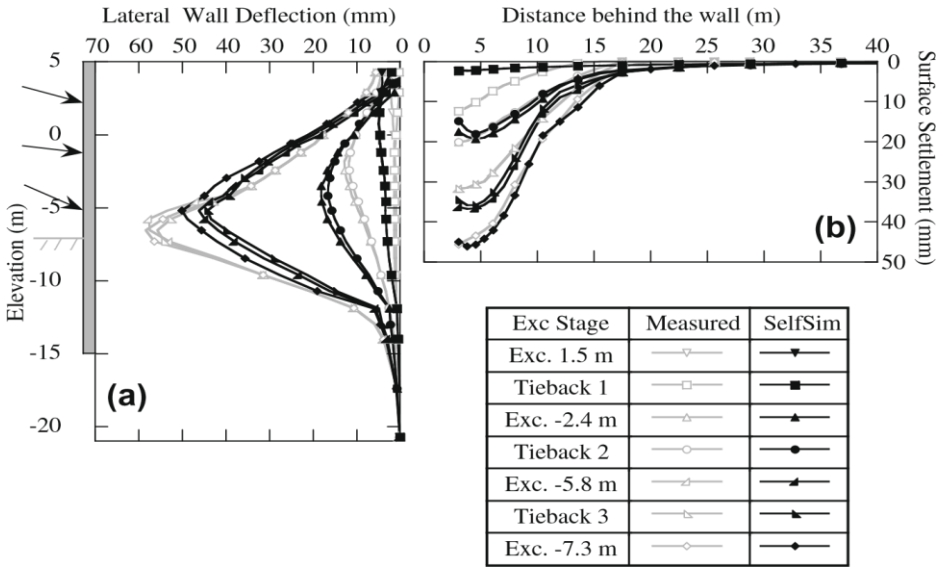

Figure 4-3: Results of the Self-Sim after 12 passes (a) lateral wall deformations; (b) surface settlements (Hashash et al., 2010).

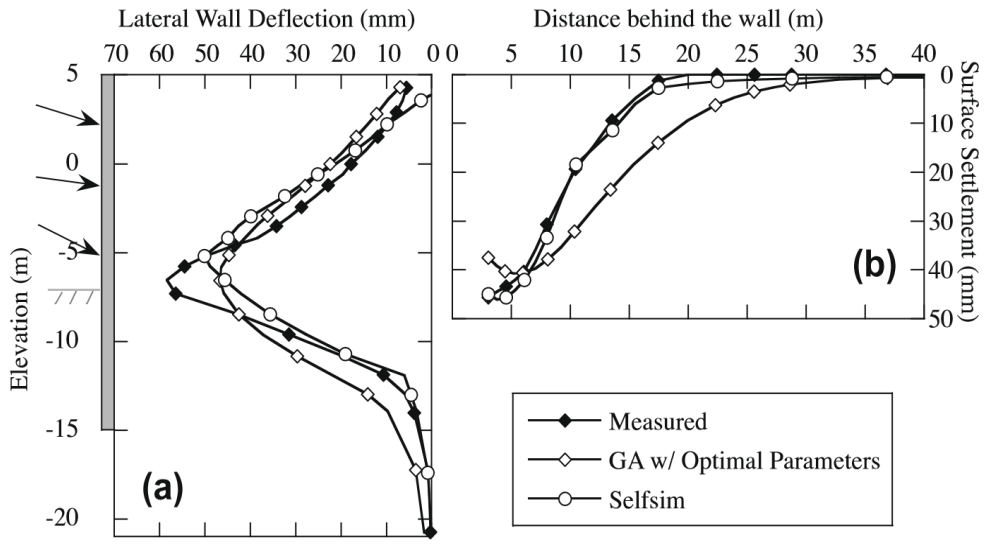

Figure 4-4: Comparison between measured data, GA and Self-Sim approaches of stage 7 of excavation (a) lateral wall deformations; (b) surface settlement (Hashash et al., 2010).

Hashash et al., (2011) adapted the Self-Sim algorithm to capture underlying soil behaviour from field measurements using a three-dimensional (3D) model of a deep excavation in clay soil. A case study involving a site with deep excavation (about 9 m depth) was analysed in 3D to estimate the variation in ground surface elevation around the site. The essential modifications of the FE mesh, the NN model structure and computational cost of 3D analysis within the Self-Sim were presented in detail in this paper. Measurements from inclinometers placed in different locations were used to learn and capture the soil behaviour. The results of the analysis showed that learning from inclinometers at multiple excavation sides was important to capture 3D response of the site excavation. It was also shown that the developed 3D model was generally able to capture the wall deflections and settlements. Although the predicted settlements around the excavation troughs were non-symmetric because of the uneven ground surface around the excavation, the predicted settlements reflected strong 3D effects and the extracted soil model predictions were consistent with the laboratory measurements.

Moon and Hashash, (2015) used the Self-Sim algorithm to link laboratory testing, soil constitutive modelling and numerical modelling, similar to the work presented by Fu et al., (2007) and Hashash et al, (2009). They applied the self-Sim framework to interpret and extract non-uniform stress-strain behaviour of soil using direct shear test (DSS), particularly within K_0 consolidation (with lateral

constraint) undrained direct simple shear (CK_0UDSS) test to generate a soil constitutive model representing the behaviour of Boston blue clay (BBC) soil. They developed different constitutive models based on synthetic and laboratory data. The first model was performed in the Self-Sim framework by simulating 3D FE modelling of direct shear test using the MCC soil model. Figure (4-5) illustrates the simulated DSS based model and boundary conditions. The measurements from the simulated model of horizontal and vertical forces with the corresponding lateral displacements were used in the Self-Sim algorithm. The results showed that as the Self-Sim progressed, the model was able to capture well the first portion of the stress-strain curve (i.e. linear part), but it was not very close in some locations where the curve moved further. This can be clearly seen in Figure (4-6) for different locations.

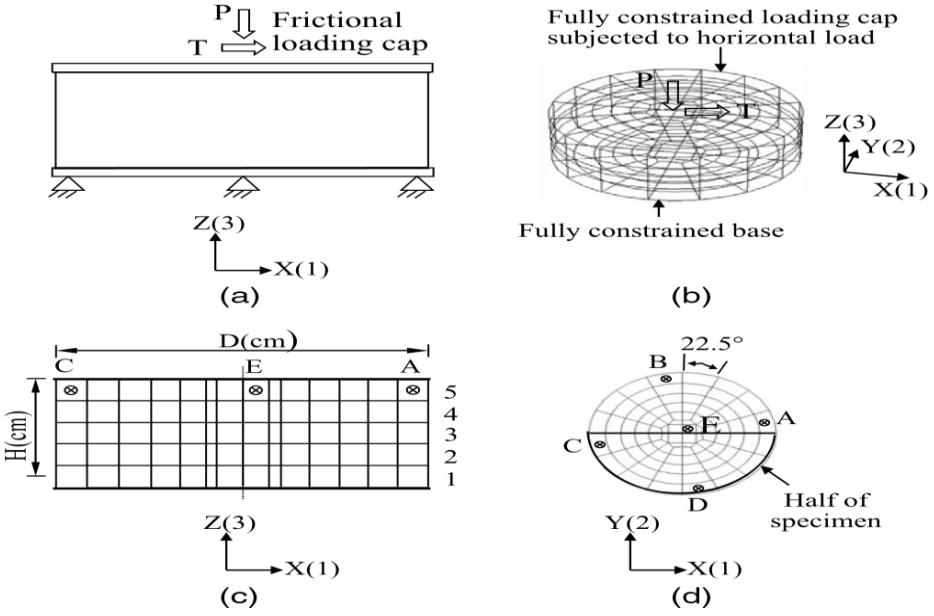

Figure 4-5: Simulated the direct shear test: a) Sample with boundary conditions; (b) 3D FE mesh; (c) Radial cross section; (d) Horizontal cross section after (Moon and Hashash, 2015).

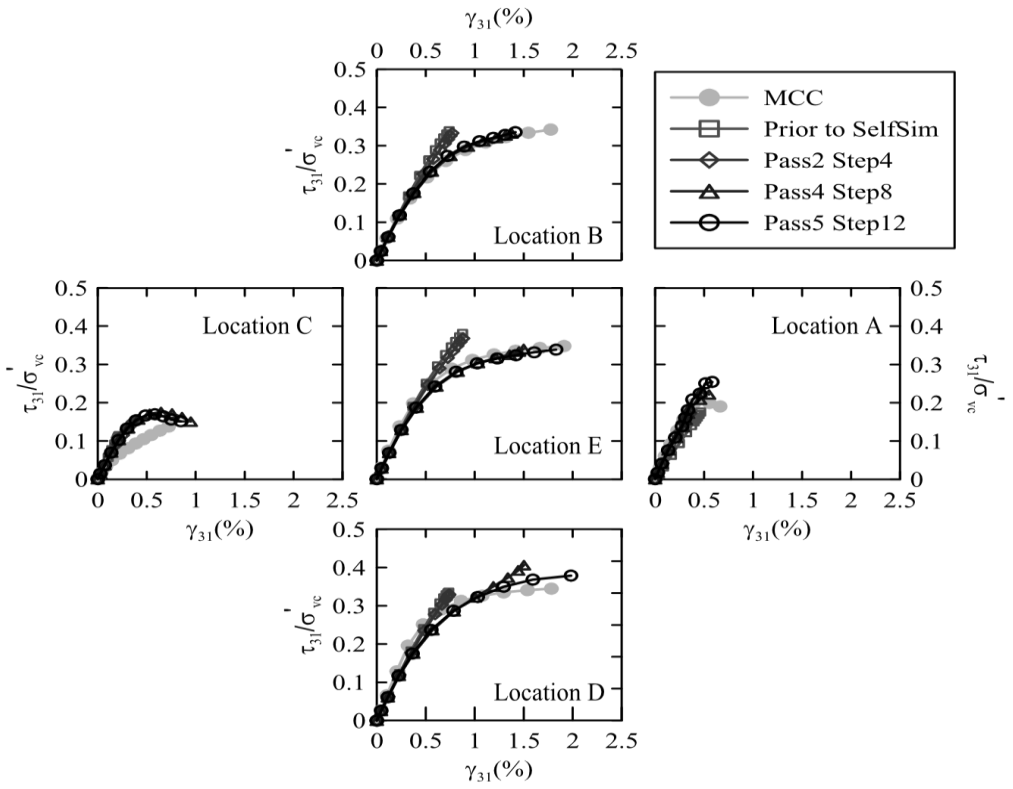

Figure 4-6: Stress-strain relationships generated from DSS and MCC model test at each location shown in Figure (4.5) after (Moon and Hashash, 2015).

The second constitutive model was developed based on data from CK_0UDSS laboratory tests from literature. The same measurements as the previous simulated model were used in the Self-Sim algorithm in several stages. The developed model was compared with the MCC and MIT-E3 constitutive soil models. The results showed that the developed NN based Self-Sim model was in a close agreement with the actual data and performed better than MCC and MIT-E3 models as shown in Figure (4-7).

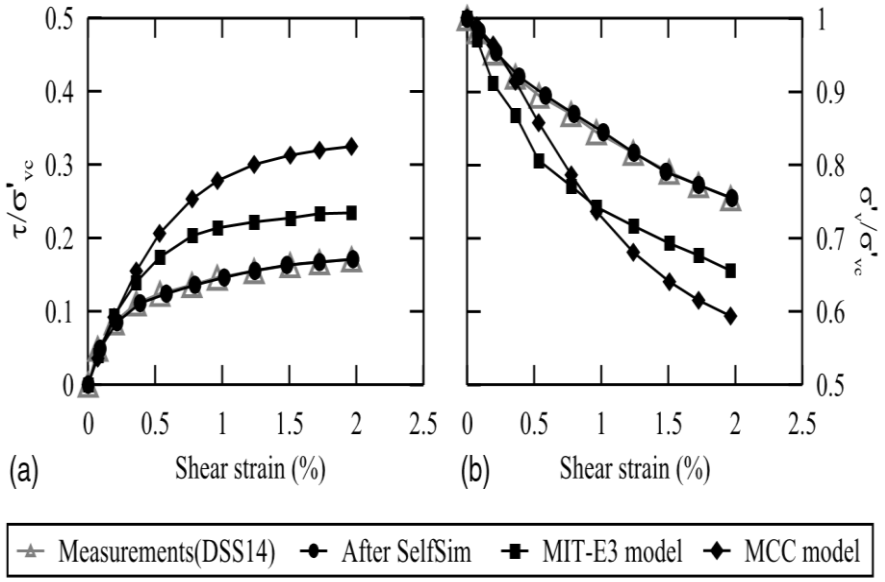

Figure 4-7: Comparison of (a)global share; (b) vertical stress- strain relation, OCR= 1 (Moon and Hashash, 2015).

The developed Self-Sim models were then applied in the analysis of a deep excavation case history. The results revealed that although the outcome showed some discrepancies, the proposed models were reasonably able to capture the global responses (lateral wall deformations and vertical ground surface settlements) of the deep excavation. This is a crucial step towards linking the laboratory measurements with the numerical analysis.

4.2.2.2 Self-learning simulation for cyclic and dynamic material behaviour

Yun et al. (2008c) and Yun et al. (2006) implemented the self-learning simulation methodology to model the cyclic and dynamic behaviour of framed structures. They used 3D beam-column elements, in conjunction with a neural network based material model of hysteretic behaviour proposed by (Yun et al., 2008a, 2008b), for modelling the frame structure system under cyclic loading. The ANN model consisted of two internal variables that could learn the complex hysteretic behaviour of material with only single-valued mapping. The form of the NN model can be expressed as follows (Yun et al., 2008c):

$$M_n = \acute{M}_{NN}(\theta_n, \theta_{n-1}, M_{n-1}, \xi_{\Theta,n}, \Delta\eta_{\Theta,n}) \quad (4\text{-}2)$$

where $\xi_{\Theta,n} = M_{n-1}\,\theta_{n-1}$ and $\Delta\eta_{\Theta,n} = M_{n-1}\,\Delta\theta_n$ are the two internal variables, M = moment, θ = rotation, $\acute{M}_{NN} : R^5 \rightarrow R$ is the functional mapping to be constructed through ANN. n indicates n^{th} time step. Figure (4-8) illustrates the two internal variables included in the analysis.

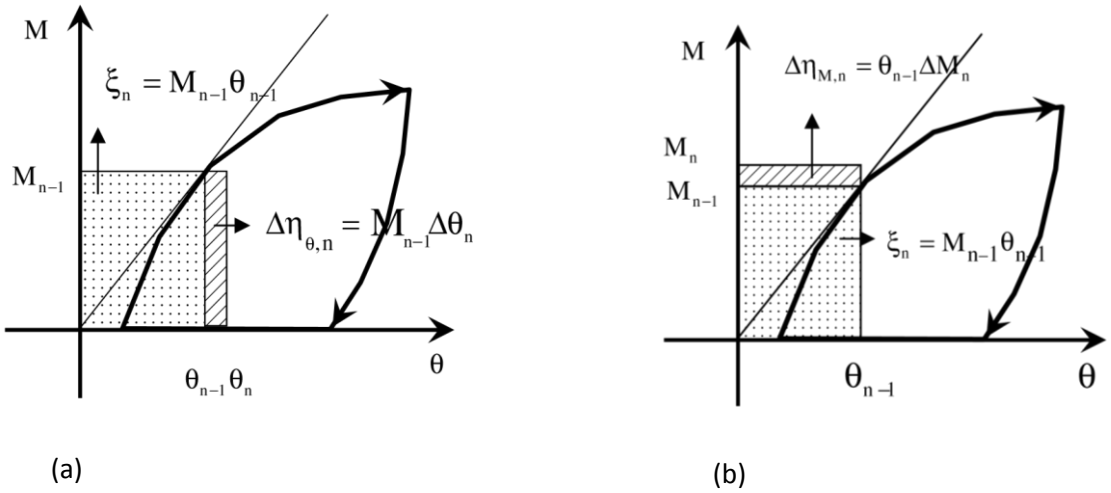

Figure 4-8: Variables for the cyclic model: a) displacement control, b) stress resultant control (Yun et al., 2008c).

The self-learning simulation was improved in this work by employing a new algorithmatic tangent stiffness form with the new NN model within the autoprogressive algorithim. The proposed tangent stiffness of the connection model in FE code was considerd as a relation between the rates of moment and rotation in terms of nonlinear incremental constitutive relations which can be stated as the following equation:

$$\mathrm{K_{con}} = \frac{\partial(^{n+1}\Delta M)}{\partial(^{n+1}\Delta\theta)},\ \text{where}\ n+1_{\Delta M} = -n+1_{\Delta M} - n_{\Delta M}\ \text{and}\ n+1_{\Delta\theta} = n+1_{\Delta\theta} - n_{\Delta\theta} \quad (4\text{-}3)$$

The self-learning procedure was applied to simulate the structure with two parallel finite element models FEM-A and FEM-B. Synthetic (numerically simulated) and actual data were used to learn the real behaviour of connections.

In FEM-A, measured forces were applied while in FEM-B the corresponding displacements were imposed. In this work, two different cases were used to train the NN model and construct the stiffenss matrix in an incremental way. Case I represented the classical way of self-learning simulation in which from FEM-A, moment variables were extracted while the coressponding rotations were extracted from FEM-B. The data were then used to train the NN in an iterative loop as shown in Figure (4-9). In Case II, a different training approach was used in such a way that all input variables from each FEM model were separately used to train the NN model of that finite element analysis (Figure 4-10). Two numerical examples were illustrated to validate the performance of the proposed methodology including three dimensional simulations. The self-learning simulation was verified with real experimental data. The results showed that nonlinear cyclic behaviour of the local connections can be captured from global responses of framed structures within several passes of self-learning simulation. It was also shown that the NN model developed from Case I performs better than the one that was developed from Case II. It appears that using all data sets from the both analyses could reduce the quality of training data.

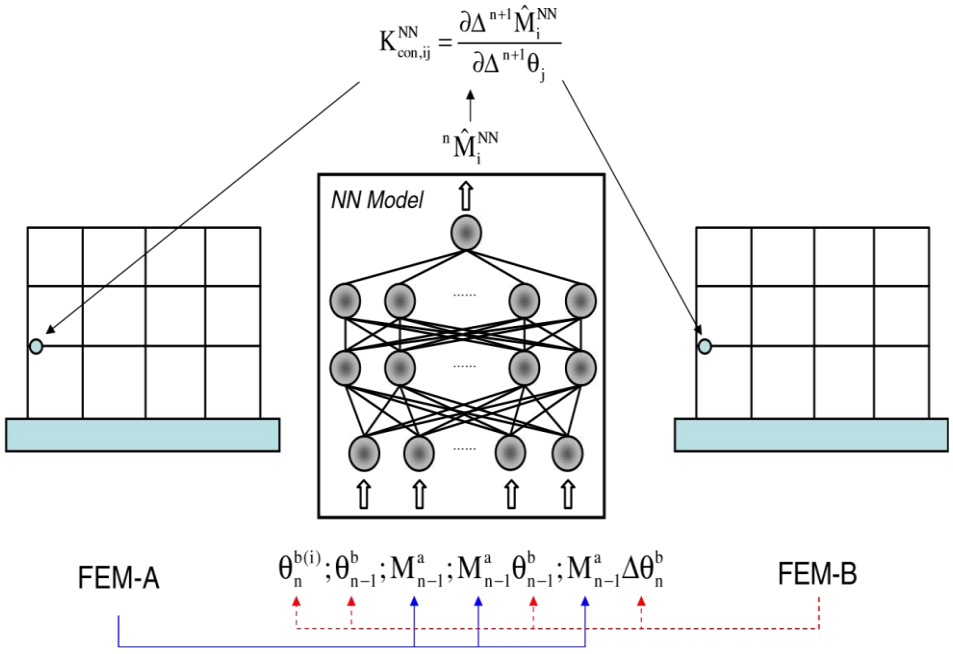

Figure 4-9: The self-learning simulation with algorithmic tangent stiffens formulation in Case I (Yun et al., 2008c).

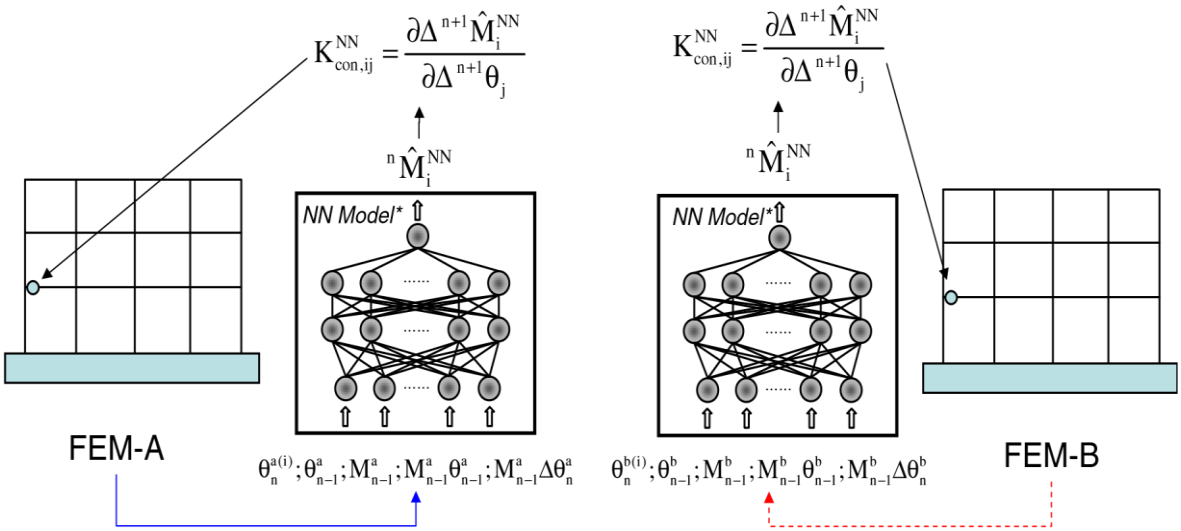

Figure 4-10: The self-learning simulation with algorithmic tangent stiffens formulation in Case II (Yun et al., 2008c).

Yun et al, (2012) stated that Self-Sim with conventional ANN based models required ad hoc data processing that usually caused problem with the Self-Sim training procedure. Consequently, to avoid this issue, they introduced improvements in the Self-Sim algorithm to inversely extract inelastic and nonlinear behaviour of materials through limited measurements under cyclic loading. The new Self-Sim was used in conjunction with a novel ANN hysteretic model for capturing the nonlinear and inelastic behaviour under multiaxial and cyclic stress states. In the hysteresis material behaviour one strain value could be mapped to multiple stresses causing problem with learning of the material behaviour in ANN.

A single valued mapping between inputs and outputs of ANN model via the internal variables was suggested and an explicit incorporation of the ANN based model was presented for finite strain problem to tackle this problem. Numerical and experimental applications were introduced in this paper to verify the performance of the proposed Self-Sim approach. The numerical simulation was applied on a laminated rubber bearing with steel shims using two different constitutive models to synthetically generate data including multi-mechanism-based generalized hysteretic model and the hysteretic neo-Hookean model in ABAQUS library. Figure (4-11) shows the gradual learning of the NN model developed during the Self-Sim compared with the actual data.

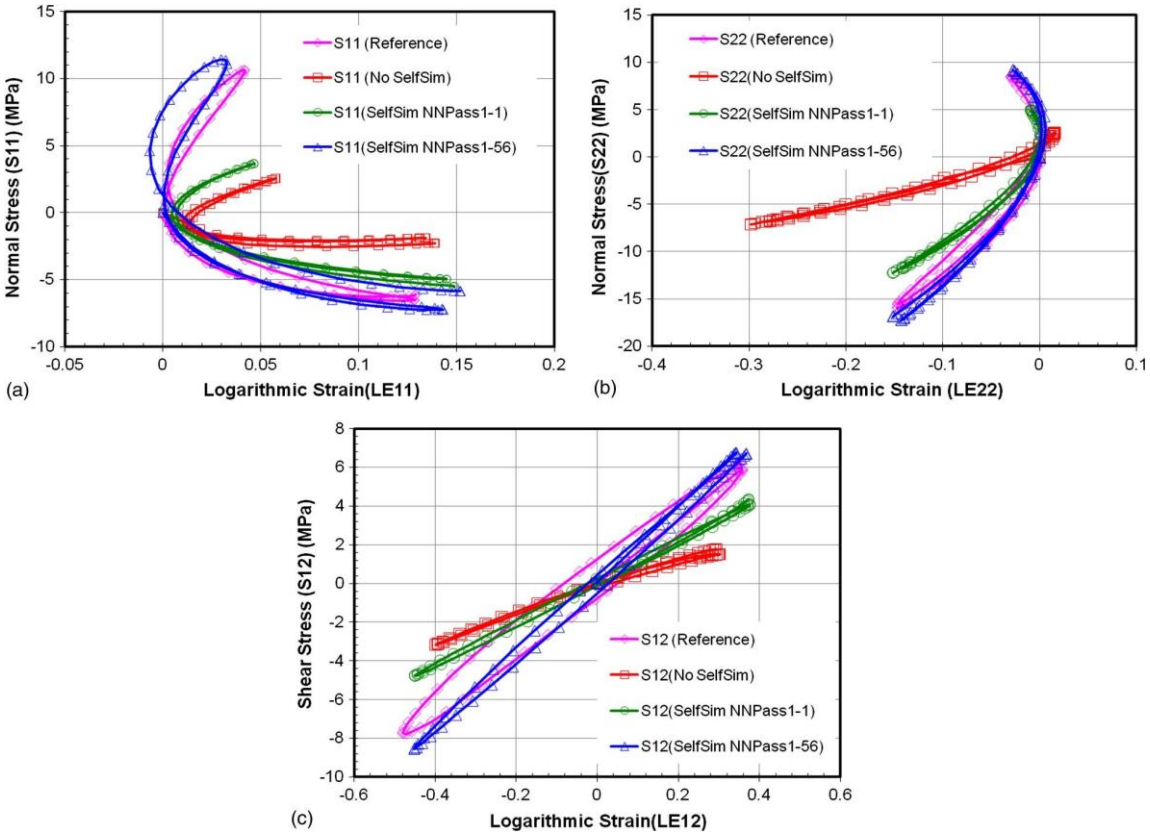

Figure 4-11: Comparison between the actual and Self-Sim results for local stress-strain constitutive response under cyclic loadings (Yun et al., 2012).

Furthermore, experimental tests were carried out on dog-bone type low carbon SAE 1006 specimens to verify the proposed algorithm and to assess the generalization capability of the proposed model. Figure (4-12) illustrates that the model can extract the global load-displacement behaviour, even beyond the range used during the training process. The results showed unexpected extrapolation capability of the ANN model developed based on the experimental data. However, too many load steps and Self-Sim passes were applied to train the ANN model. Also, a clear discrepancy was seen in the shear stress results between the plasticity model and the developed NN model. Although the authors tried to improve the Self-Sim based ANN algorithm, but the developed ANN model with its extracted Jacobian matrix used within FE code could be very complicated.

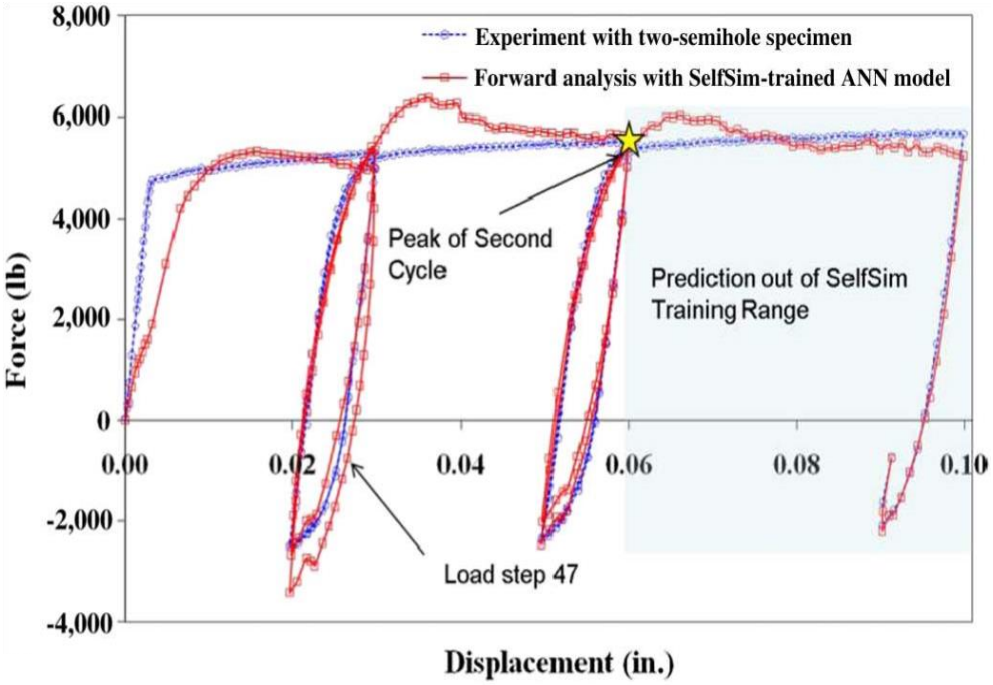

Figure 4-12: Force-displacement relationship of the experimental results and forward analysis using Self-Sim ANN model (Yun et al., 2012).

Tsai and Hashash, (2008) presented the integration of site response analysis and field measurements to extract the undelaying soil behaviour via self-learning simulation (Self-Sim) during shaking. The proposed methodology provided an opportunity for the civil engineers to gain clear insight into the seismic site response by training a NN model to represent the real behaviour of soil under dynamic loading conditions. They extended the Self-Sim methodology to one dimensional seismic site response analysis using base shaking. The corresponding measurements were used as observations in the Self-Sim procedure. Figure (4-13) illustrates the application of the Self-Sim algorithm to seismic site response analysis.

They utilised three different soil profiles generated synthetically including single soil layer, uniform multilayer soil profile and non-uniform multilayer soil profile, to investigate how the Self-Sim can be used to capture dynamic behaviour of soil when the target site response is extracted from downhole arrays. The results showed that Self-Sim is able to provide a close prediction of the site response in all different soil profiles. However, the authors tried to investigate the capability of the developed NN models from each event through a paramedic study in which

the analysis was performed by using material model representing a specific event using input motions of the other events. The results revealed that the NN models could not define the nonlinearity very well and could only predict the site response well within the strain range experienced during the training process.

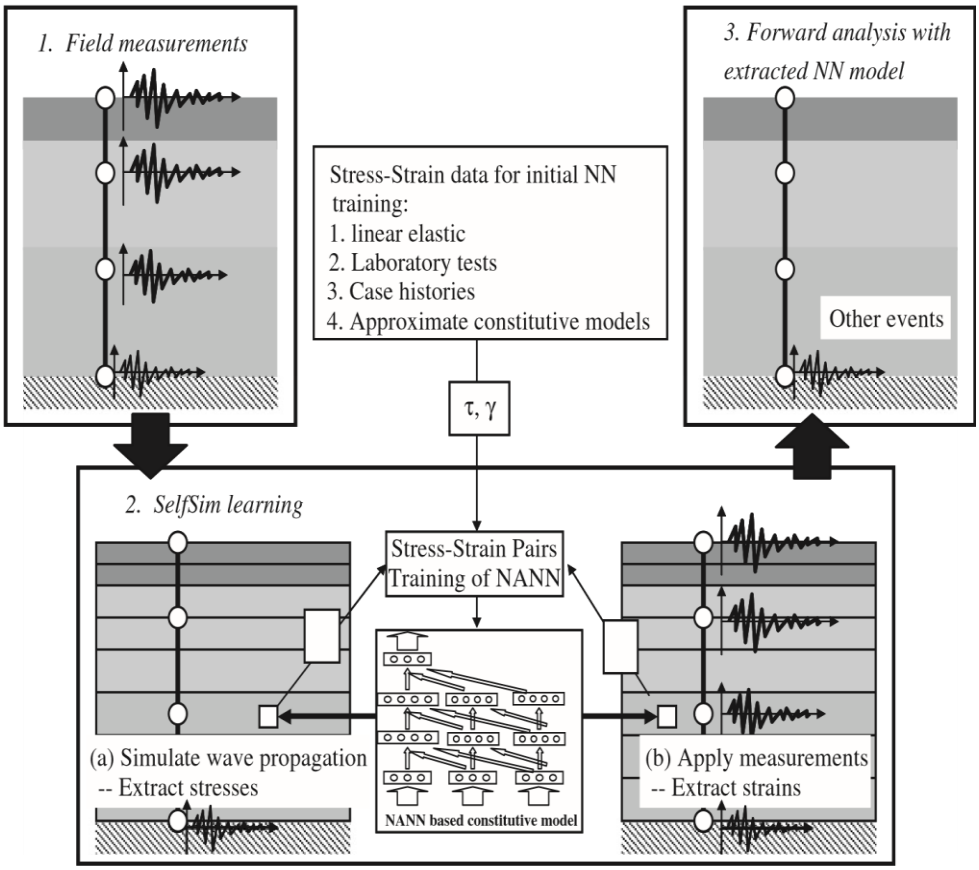

Figure 4-13: Self-Sim algorithm applied to a downhole array application (Tsai and Hashash, 2008).

To enhance and generalize of the proposed material models, the stress-strain behaviour was also extracted by combining the data of all profiles in one single data base which was used to train the NN model. The developed model provided very good agreement with the target response as illustrated in Figure (4-14). It should be mentioned however the combination of the data was done through Self-Sim loop which includes consecutive Self-Sim passes resulting in a very complex training process.

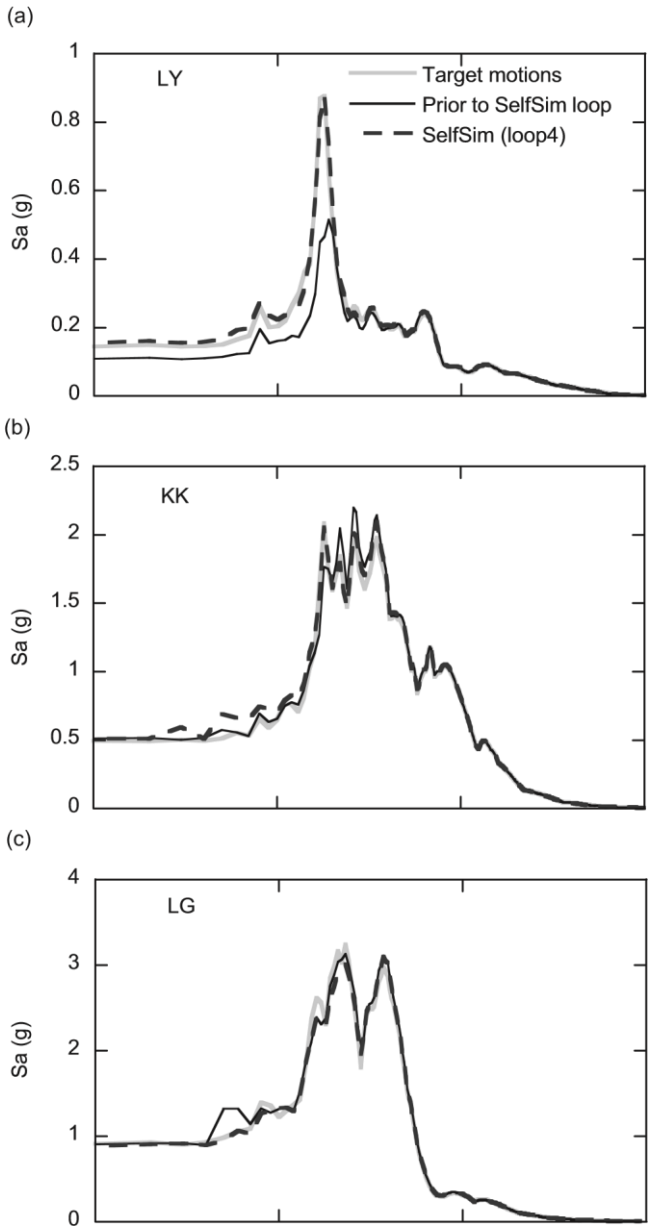

Figure 4-14: Comparison of surface response spectra of three events predicted by the combined NN model after several Self-Sim passes (Tsai and Hashash, 2008).

Tsai and Hashash, (2009) deployed the previously developed Self-Sim approach using field recordings from a number of downhole arrays within the soil profile in the Self-Sim framework for total stress site response analysis to estimate the measured site response while the behaviour of individual soil layers was extracted unconstrained by initial assumptions of soil behaviour. The Self-Sim approach was successfully applied to recordings of two sites, Lotung arrays in Taiwan and La Cienega arrays in Los Angeles case studies.

The results revealed that implementing this approach provides a clear insight into the soil behaviour under seismic events. The extracted soil behaviour could be used to interpret the changes made in the soil properties.

Later, other work employed the same Self-Sim approach but including the effect of the pore pressure generation on the seismic analysis. Groholski and Hashash, (2013) used synthetic downhole arrays to measure motions in the ground and record the pore pressure within soft soil layers during earthquake events. Moreover, Groholski et al. (2014) reintroduced the methodology using field measurements. Self-Sim was applied based on monitoring measurements taken from a real case study, the Wildlife Liquefaction Array (WLA) in California, using accelerometer and piezometer instruments. Figure (4-15) shows the application of the Self-Sim approach to array measurements of ground motion and pore water pressure response. Two earthquake events in the WLA were used in this analysis. The Superstition Hills event was used to build the NN based models and the Elmore Ranch event was used for predictions.

Four sets of NNCMs were developed using Self-Sim analysis representing various type of soils. Each set had a NN model representing soil behaviour and another model representing the pore pressure response of the Superstition Hills earthquake. These NN models were used for the prediction of surface acceleration, surface response and pore pressure for the Elmore Ranch event. The results revealed that the Self-Sim algorithm was able to consider the pore pressure response and learn important characteristics of the natural soil during earthquake event. The developed NN models were also compared with other conventional constitutive models for pore pressure generation embedded in the DEEPSOIL finite element code (strain-based pore pressure D/M and energy-based pore pressure GMP models).

Figure (4-16) shows the model performance at Elmore Ranch event including two directions NS and ES after 13 passes of Self-Learning compared with the recorded data and numerical simulations.

It can be noticed that NN models learned the soil behaviour which was dependent on ground motion direction but with some discrepancy. The authors state that this discrepancy could be due to soil anisotropy or effects of multi-dimensional pore pressure response in this event that was not used during the Self-Sim process. However, the extracted soil behaviour from arrays could be employed to interpret the soil behaviour and pore pressure response.

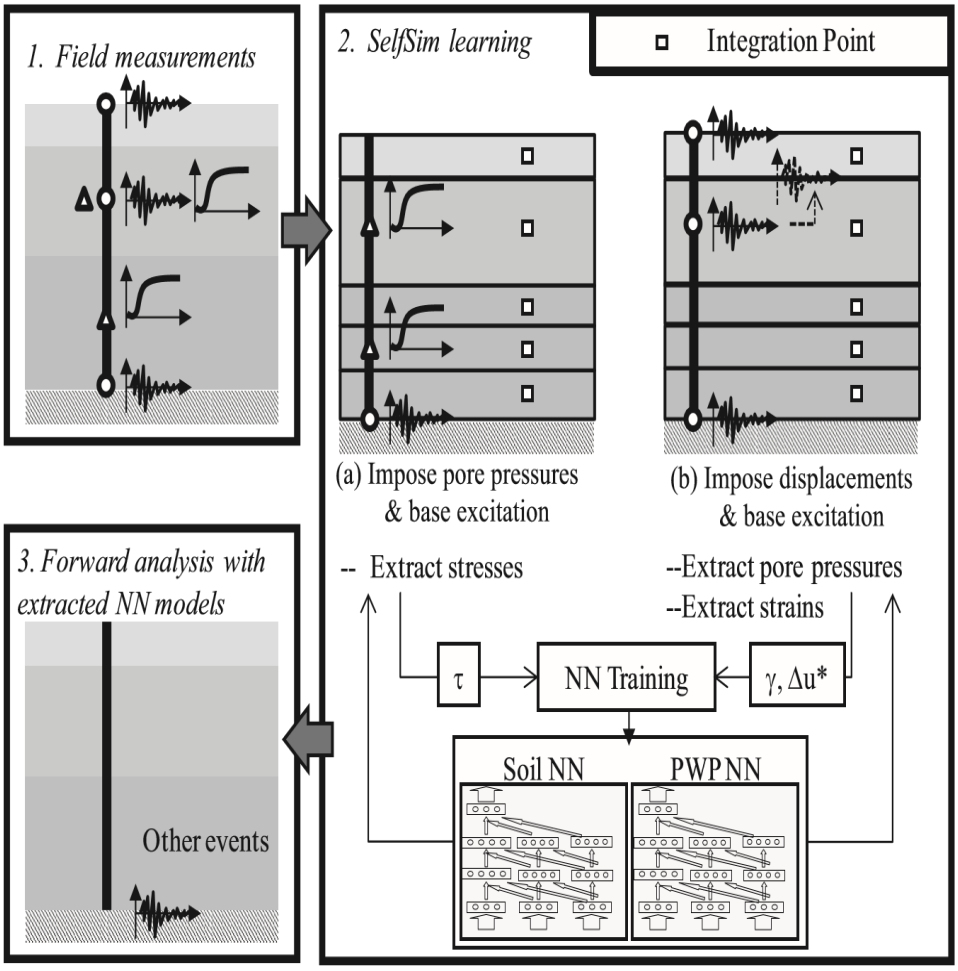

Figure 4-15: Self-Sim procedure applied to array showing pore pressure and acceleration measurements (Groholski et al., 2014).

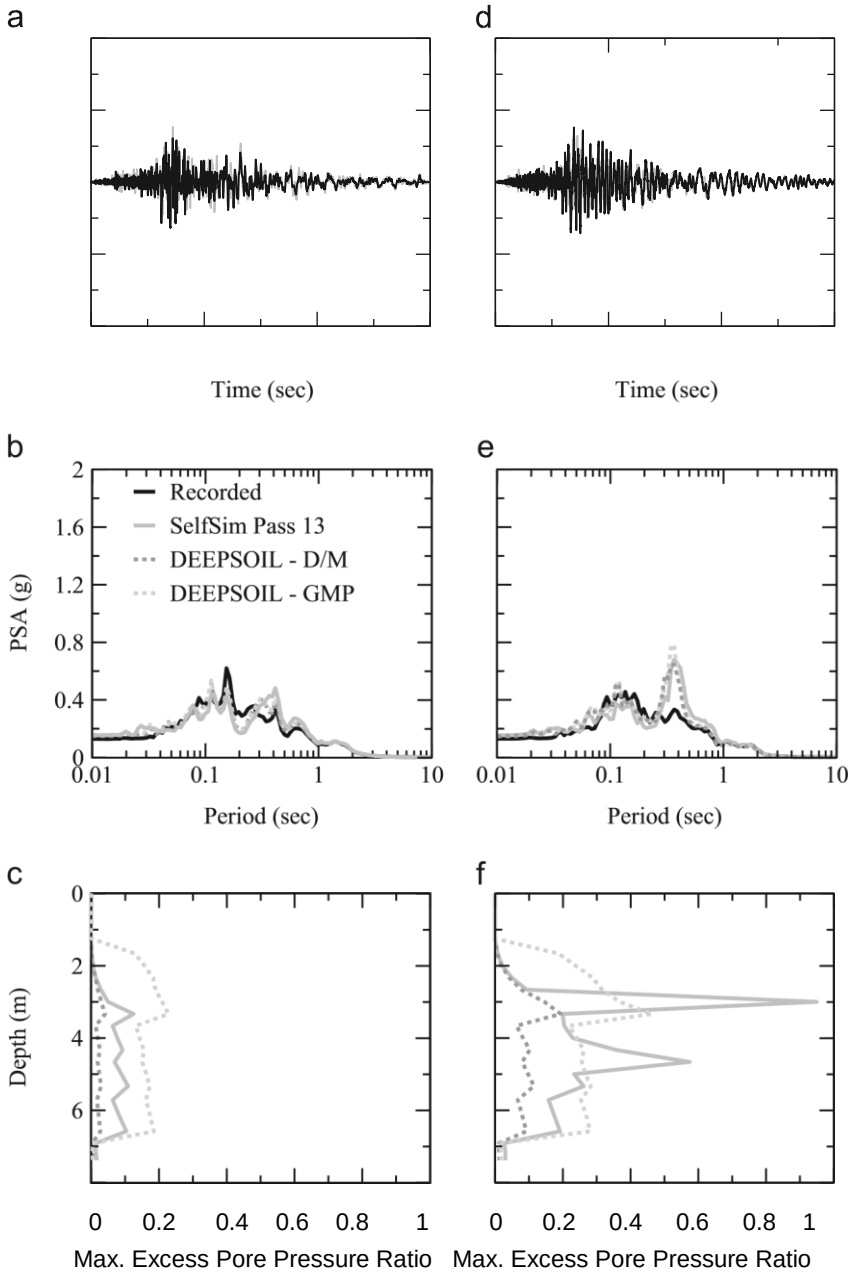

Figure 4-16: Comparison of results of Self-Sim Pass 13 predictions for Elmore Ranch NS (left column) and EW (right column). Event (a and d) surface acceleration, (b and e) surface response, and (c and f) excess pore pressure profile (Groholski et al., 2014).

4.2.2.3 Self-learning simulation for rate dependent material modelling

The self-learning approach was also extended to include the rate-dependent NN based models. Jung and Ghaboussi, (2006) presented the use of self-learning methodology to extract rate-dependent material behaviour via load-displacement boundary conditions from structural tests. This method was developed to overcome the issues from conventional optimization techniques that are used to evaluate the material parameters. The proposed methodology was verified through a synthetic structural test using viscoelastic material with creep function as shown in Figure (4-17a).

The structure was selected as a cylinder with variable diameter and used to generate non-uniform stress distribution within the sample test. The NN model that was created from this analysis was applied to solve another plane strain boundary value problem having the same material (Figure 4-17b). In this work the authors investigated the influence of time step on the NN model learning capability. To improve the performance of the NN model more time steps were required to be included in the self-learning analysis.

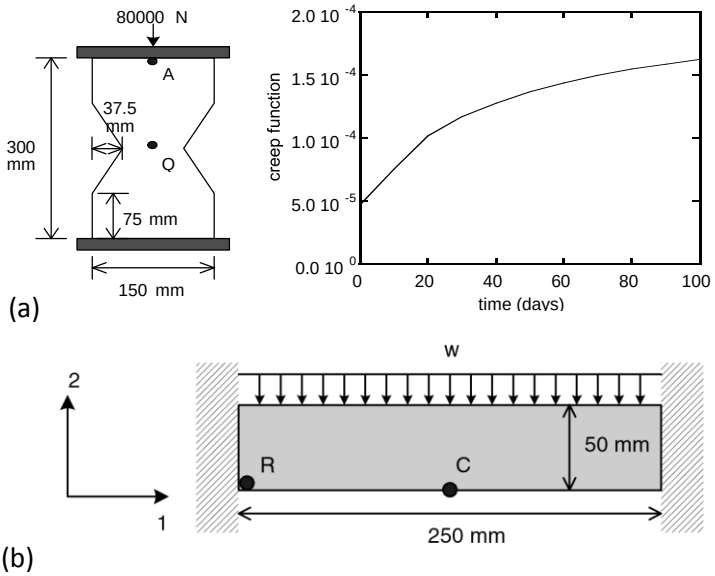

Figure 4-17: (a) The structure and the creep function used in the simulated experiment; (b) the structure of boundary value problem (Jung and Ghaboussi, 2006).

Furthermore, the methodology was applied to a more complex non-linear material behaviour. It was applied to extract the non-linear creep behaviour of a superalloy from experiments data for which was collected from the literature. Although the proposed algorithm worked well, more experimental results were needed to improve the accuracy of the NN model.

Aquino and Brigham, (2006) utilised the Self-Sim to develop a NN thermal constitutive model following the same procedure of previous work. Unlike conventional approaches that are used to find particular material parameters (e.g. thermal conduction), this methodology adopted a thermal constitutive relationship. Figure (4-18a) illustrates the full procedure of the self-learning approach in which two finite element analyses were developed to simulate an experiment. In the first one only heat flux *J* was recorded (as output) whereas in the second FE model, measured temperature was imposed and only the temperature T and temperature gradient ∇T were recorded (as input).

The applicability of the proposed approach was tested through a simulated experiment of simple steel plate as shown in Figure (4-18b). The plate was heated with a surface heat flux in one side while a constant temperature was applied on other sides. The results showed that the methodology was able to develop a NN based thermal constitutive model with good stability even with the existence of noisy data. The authors also mentioned that although the approach was only applied to steady-state problem, it could be easily extended to transient and coupled heat transfer problems. In this paper, the implementation of Jacobian matrix in FE analysis and how the proposed algorithm could be applied to a case study were not clearly presented.

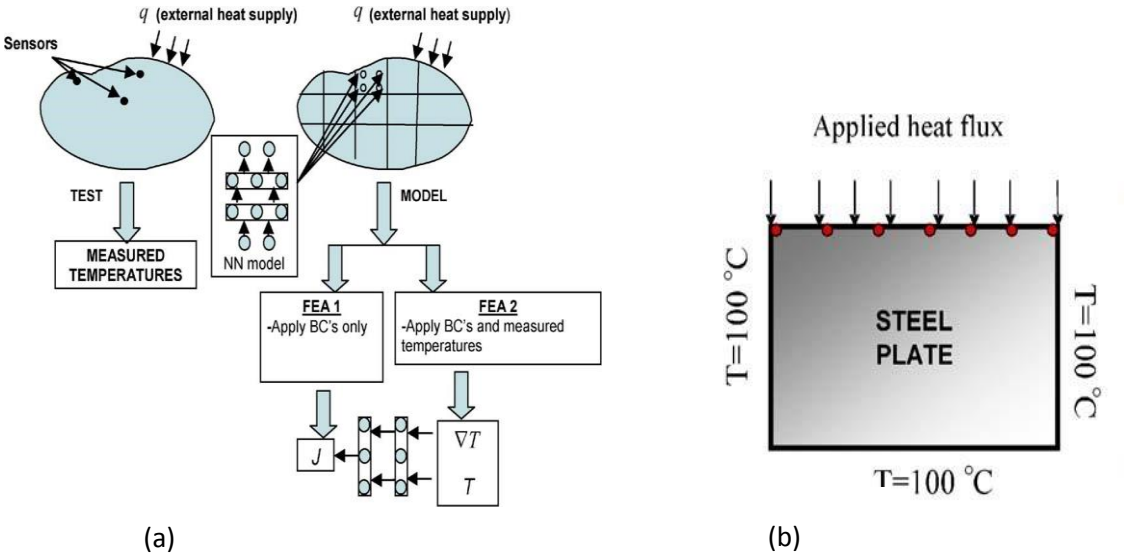

Figure 4-18: (a) Self-learning algorithm; (b) Simulated experimental test (Aquino and Brigham, 2006).

Jung et al., (2007) introduced the Self-Sim approach to predict the time-dependent behaviour of concrete at the time of construction of a segmental bridge. The application of the Self-Sim approach included two steps. In the first step the deflection measurements were collected from a segmental bridge construction at different points from selected construction stages. The NN material model was initialized as a simple visco-elastic model to represents the rate-dependent behaviour of concrete. The second step was to perform two finite element analysis FE-A and FE-B in parallel followed by training the NN model with the data created in the first construction stage. Stresses and the corresponding stress rates were collected from FE-A while strains and the corresponding strain rates were collected from FE-B. The required data were used to retrain the NN model gradually. Eventually, the developed NN model trained from the early stages of construction could be used to predict the response in the remaining stages of the construction or to help having better information for the analysis of similar construction projects. Figure (4-19) shows the Self-Sim algorithm applied to the segmental bridges.

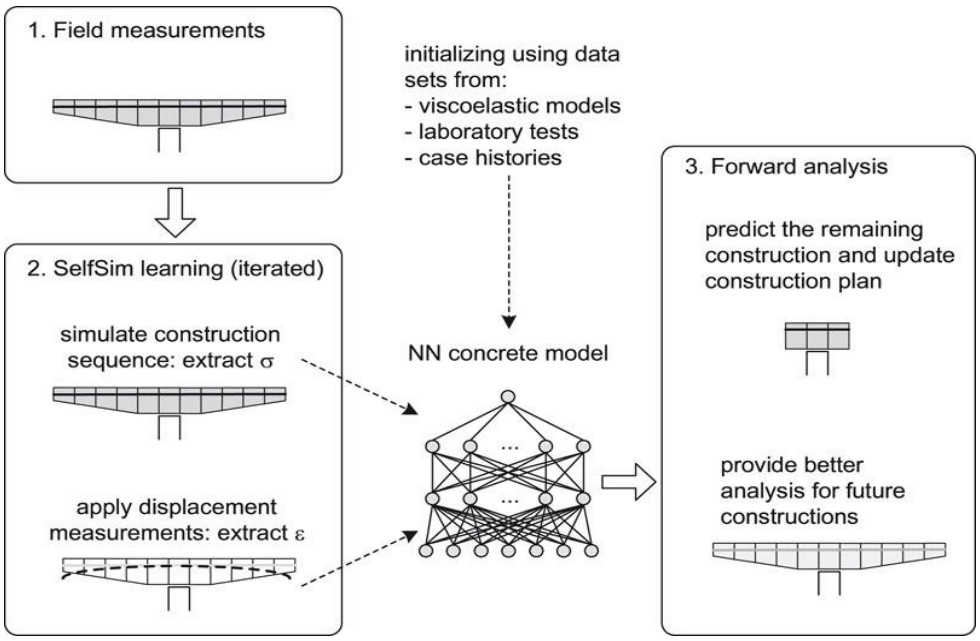

Figure 4-19: Self-Sim used to the field calibration of segmental bridges (Jung et al., 2007).

The proposed procedure was applied to the field calibration of Pipiral Bridge in Colombia as a case study. They used two different ways to predict the deflection of the segmental bridge. In the first one, the construction contained many cantilevers, the NN model could be calibrated using the first two cantilevers, and then casting curves were adjusted for the other cantilevers using the same NN model. However, in the second approach, when high accuracy was required, the NN model was calibrated using observations from early segments and was used to predict the deflections of other segments in the same cantilever as shown in Figure (4-20).

It should be mentioned that NN cannot predict the behaviour beyond the range of data used during training of the NN model. Therefore, an additional source of data was needed such as laboratory tests, field measurements from similar materials etc. The proposed methodology offered a systematic approach of transferring the information stored from each bridge project to the analysis of new projects. It also showed the capability of the Self-Sim approach to be used for different materials.

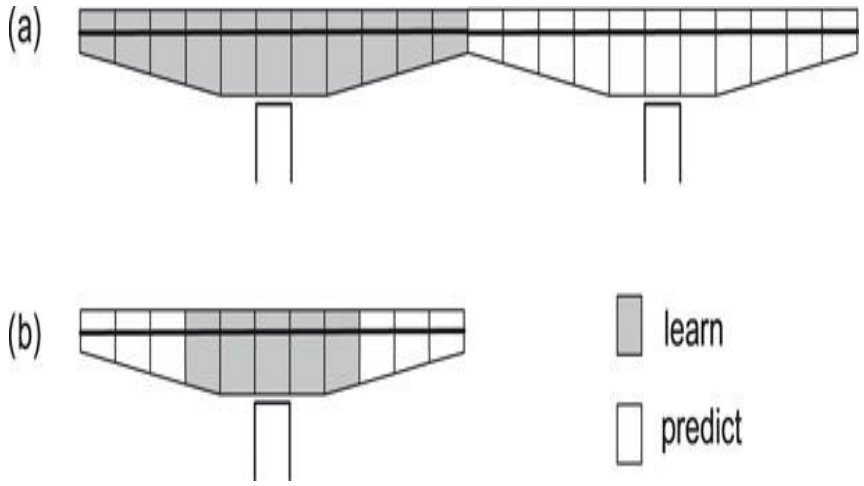

Figure 4-20: (a) training NN model from the current cantilever and predicting deflections of other cantilevers; (b) training from earlier segments and predicting the deflection of the other segments (Jung et al., 2007).

Jung and Ghaboussi, (2010) utilised the self-learning simulation to train a NN based constitutive models that could represent the overall time-dependent behaviour of concrete by using the load-displacement measurements collected from several sensors on a structural test. In this work, the rate-dependent NN based constitutive model was introduced with their training procedure and used to study the creep behaviour of concrete beam. A comparison of the results of the model prediction and the actual data of the concrete beam is illustrated in Figure (4-21).

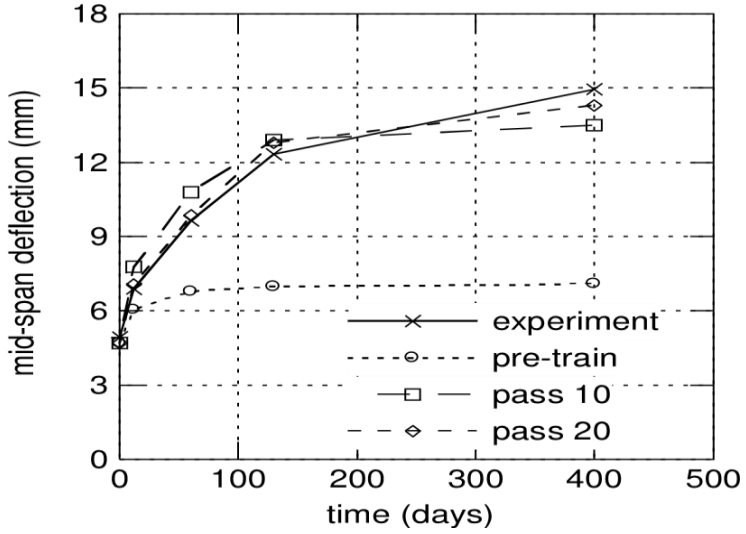

Figure 4-21: Comparison between actual data and model predictions for mid-span deflection of concrete beam (Jung and Ghaboussi, 2010).

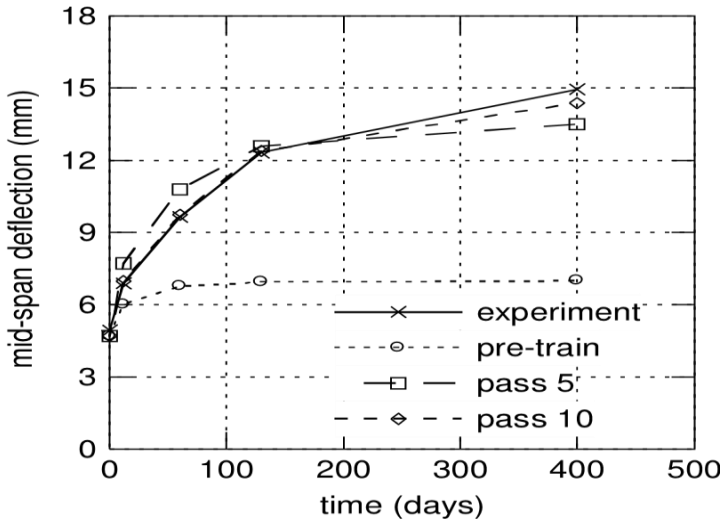

Figure 4-22: Comparison between actual data and model predicted at mid-span deflection of the concrete beam including the shrinkage effect (Jung and Ghaboussi, 2010).

The model was modified to improve its capability in learning the time-dependent creep strains of concrete. The authors added the shrinkage effect to the NN model parameters. The results illustrated that including shrinkage effect to the NN model made no significant improvement in comparison with the previous NN model as seen in Figure (4-22). In addition, the prediction of long-term behaviour with short term measurements was investigated via the auto-progressive algorithm. Data sets from outside the range of training of the NN were added to update the NN model. The calibrated NN model did not clearly show the ability to capture the real behaviour even after several passes. This could be due to the lake of information taken from the short-term measurements.

Gandomi and Yun, (2015) applied a coupled Self-Sim and genetic programming GP framework for the analysis of nonlinear material behaviour. They suggested to combine the recent version of GP called linear genetic programming (LGP) with the Self-Sim based ANN to improve the performance of the methodology and present an explicit model that can be implemented in the FE code. The Self-Sim based ANN was used to extract the comprehensive stress-strain fields while LGP was used for generating the explicit formula of the non-linear material behaviour. The new technique was verified by introducing a simple numerical example that was simulated in FE code (ABAQUS) using non-linear elastic constitutive model.

The results were compared with the actual data and Self-Sim based ANN model. Although the study was to improve the performance of the Self-Sim methodology and apply more effort to be readily applied in the practical engineering field however, the results indicated that the new approach has not added any significant improvements in the Self-Sim algorithm. In addition, using the ANN in the proposed framework was still valid for data preparations.

4.3 EPR based Self-learning FEM

The self-learning simulation (Self-Sim) methodology has been successfully applied to various aspects of engineering problems including modelling the material behaviour from experimental/field data. The main feature of using Self-Sim in material modelling is that it learns directly from the real measurements and provides accurate predictions under static and dynamic loading conditions. Therefore, it works as a comprehensive model to link the field or experimental data to numerical modelling. As mentioned above, Self-Sim has been applied in conjunction with ANN to capture the material behaviour. However, as mentioned in Chapter 3, ANNs suffer from a number of drawbacks. Although there has been some limited work to improve the effectiveness of the ANN based Self-Sim framework, the heart of the framework still includes the NNCM in all the developments. An alternative data mining tool called evolutionary polynomial regression (EPR) has shown robustness in material modelling and it provides an explicit equation that can be easily implemented in FE models. This has motivated this research to use EPR in the Self-Sim framework instead of ANN.

The implementation of an EPR based constitutive model in FE code was first developed by Rezania, (2008) as discussed in Chapter 3 (Figure. 3-14). It was shown that the incorporation of a suitably trained EPR model in a FE code is a straightforward step in material modelling in numerical analysis (Faramarzi, 2011; Rezania, 2008). In this thesis an EPR-based self-learning FE model has been developed using ABAQUS as the finite element engine. The developed approach implements EPR based constitutive model in the FE code. The multi-objective function in EPR was used. The linking of ABAQUS with EPR was effectively done in MATLAB environment in a fully automated iterative loop.

The entire procedure of the EPR-based self-learning FEM is shown in Figure (4-23). The process starts by running two finite element analyses (FE-A and FE-B) in parallel, initialized with an elastic model. A finite element model (FE-A) simulates the behaviour of the structure under applied forces and determines stresses and strains at each integration point. Since the applied boundary forces are accurate and the equilibrium condition is satisfied, the computed stresses will be accurate approximation of actual stresses that are experienced throughout the test. However, the computed strains form this analysis could be poor approximation of actual strains, due to the difference between the computed and measured displacements.

In parallel, another finite element model (FE-B) analyses the structure using the same initial elastic model in which the measured boundary displacements are imposed. The strains obtained from this analysis are assumed to be accurate approximation of the actual strains, whereas the stresses may be a poor approximation of the actual stresses due to the difference between the computed and measured boundary forces. The stresses obtained from FE-A and the strains obtained from FE-B are collected to form stress-strain pairs of data and used to retrain the EPR model. The analyses of the finite element models A and B and subsequent training of the EPR model form the Self-Sim learning cycle. The analyses of finite elements A and B are repeated and an EPR model is developed from the results which is updated at each iteration. Convergence is considered to be achieved when the results of both analyses (FE-A and FE-B) are approximately matched. Each cycle of Self-Sim that accomplishes the applied load is called a pass. More than one pass may be required to extract the accurate material behaviour by retraining of the EPR model.

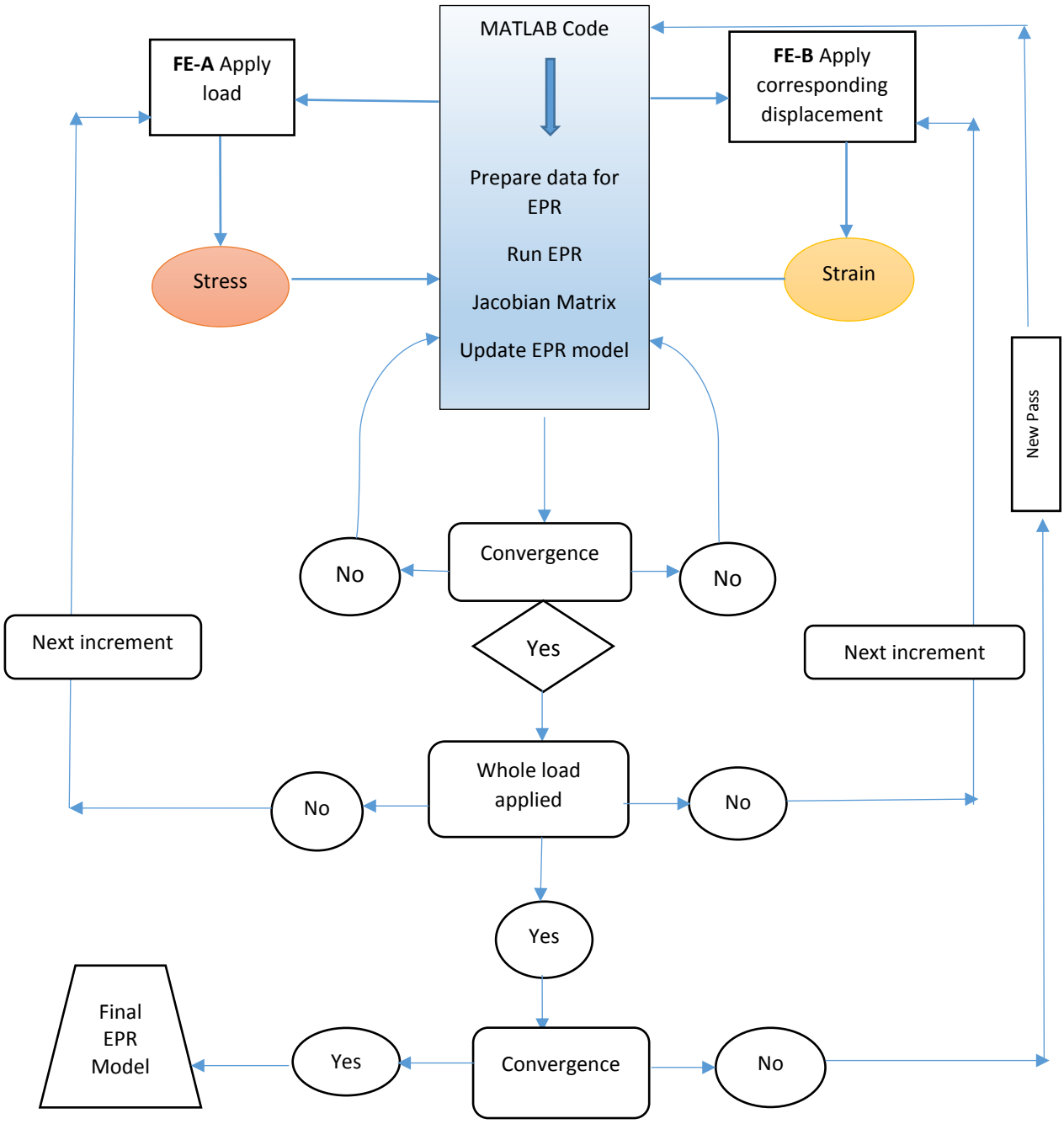

Figure 4-23: Flow chart of the proposed automation process of EPR-based self-learning algorithm (Nassr et al., 2018).

4.3.1 EPR based Self-Sim code

ABAQUS is a widely used FE engine to simulate different engineering applications including civil, mechanical, aerospace, biomechanical and more (ABAQUS, 2016). One of the several useful features of ABAQUS is that the constitutive model for material can be implemented via its user defined subroutine UMAT which is coded in FORTRAN language. Moreover, the postprocessing capabilities are quite useful to interpret the outcomes. Linking ABAQUS with the EPR based constitutive model has been done in MATLAB environment as follows:

1- The required boundary value problem is set up in ABAQUS. Two simulation models (FE-A and FE-B) are created in parallel.
2- The number and location of the monitoring points are specified where the load and the corresponding displacement are applied.
3- MATLAB calls ABAQUS to run FE-A and FE-B sequentially and the required results from them are written in MATLAB as text files.
4- MATLAB prepares the data (shuffles and removes duplicated data) and prepares the input and output parameters to be all written in the EPR Excel sheet.
5- MATLAB runs EPR and selects the best model according to the highest *CoD*.
6- The Jacobian matrix is constructed and written in a Fortran file as a UMAT used in both FE-A and FE-B analyses.
7- ABAQUS simulations are run again implementing the new UMAT. The process is repeated iteratively in a loop until the whole load is applied and through the necessary cycles and/or passes until the termination criteria are satisfied.

The above steps have been programmed to run automatically in a MATLAB code. The whole analysis takes a relatively short amount of time to complete, depending on the type and size of the problem being analysed.

4.3.2 Training strategy of EPR based Self-Sim

There are two main strategies (total stress-strain strategy and incremental stress-strain strategy) that can be employed to train ANN or EPR to generate a constitutive model representing the material behaviour. There are several factors that should be taken into account in choosing the best strategy and specifying the input and output parameters to train the EPR based constitutive model. These include the source of data, the way the trained EPR is to be used, and the training procedure (Faramarzi et al., 2012). Unlike ANN, in the EPR training process, the input parameters that do not have any effect on the output can be automatically discarded from the EPR models. Therefore, it is useful to include all possible input variables in the training process of EPR.

4.3.2.1 Total stress-strain strategy

This technique can be considered as a direct training in which strains are used as inputs and stresses as output. The total stress-strain strategy can be utilised for modelling of materials that show no significant difference in behaviour in loading and unloading (i.e., are not path dependent). This algorithm has been applied to different boundary value problems by several researchers to train ANN based model (Ghaboussi and Sidarta, 1998; Shin, 2001). This technique considers strain variables $(e.g., \ \varepsilon_x, \varepsilon_y, \varepsilon_z, \gamma_{xy})$ that represent the strain components in a two dimensional (2D) continuum as input variables and the corresponding stresses variables (e.g., $\sigma_x, \sigma_y, \sigma_z, \tau_{xy}$) as output. In the ANN, one model could have more than one output with the corresponding inputs, however, EPR constructs one mathematical equation for each output. For instance, in the 2D problem we may have four equations representing one material model as shown below.

$$\sigma_x = f(\varepsilon_x, \varepsilon_y, \varepsilon_z, \gamma_{xy})$$

$$\sigma_y = f(\varepsilon_x, \varepsilon_y, \varepsilon_z, \gamma_{xy})$$

$$\sigma_z = f(\varepsilon_x, \varepsilon_y, \varepsilon_z, \gamma_{xy})$$

$$\tau_{xy} = f(\varepsilon_x, \varepsilon_y, \varepsilon_z, \gamma_{xy})$$

This strategy has been deployed in the training procedure of some applications to train the EPR model within the Self-Sim framework.

4.3.2.2 Incremental stress-strain strategy

EPR can also be trained incrementally where input variables provide the EPR model with the behaviour corresponding to the current state (i.e., current stresses and current strains) and an output which predicts the next state of stress or strain corresponding to an input strain or stress increment. This technique was mainly used to train EPR based models with experimental data by several researchers (Faramarzi et al., 2012; Javadi and Rezania, 2009a; A. A. Javadi et al., 2012). The same approach was utilised to train most of ANNs based constitutive models (Ghaboussi et al., 1998). The difference between the two strategies is that in the incremental strategy, invariants of stresses and strains are used instead of using their values in the spatial directions. For example, the input variables can be selected as the current state of mean effective stress p'^i, deviator stress q^i, volumetric strain ε_v^i, axial strain ε_y^i and increment of axial strain $\Delta\,\varepsilon_y^i$ corresponding to the current state of stresses and strains in a load increment i, while deviator stress q^{i+1} corresponding to the input increment of the axial strain $\Delta\varepsilon_y^i$ can be used as the output parameter. For instance, the form of the inputs and output for a triaxial test simulation would be:

Input variables: $\varepsilon_v^i, \varepsilon_y^i, \Delta\varepsilon_y^i, q^i, p'^i$

Output variable: q^{i+1}

The input variable for deviator stress q^i, is the variable that should be updated incrementally during the EPR training stage, according to the output variable passed from the previous increment of the training stage. Using such training strategy seems to be useful for soils due to their incremental nature, therefore for modelling soil behaviour this technique has been used in this thesis.

4.3.2.3 Jacobian matrix in EPR-based Self-Sim

When implementing a constitutive model in finite element analysis, the material stiffness (Jacobian) matrix must be determined as:

$$J = \frac{\partial(d\sigma)}{\partial(d\varepsilon)} \tag{4-4}$$

where, σ and ε are the stress and strain vectors respectively. Jacobian matrix is explicitly formed for various constitutive models. For example, the Jacobian matrix for a linear elastic model following the Hooke's law in plane stress condition is stated as follows (Stasa, 1986):

$$D = \frac{E}{1+\mu^2}\begin{bmatrix} 1 & \mu & 0 \\ \mu & 1 & 0 \\ 0 & 0 & (1-\mu)/2 \end{bmatrix} \tag{4-5}$$

where, D is the stiffness matrix, E is the elastic modulus and μ is the Poisson's ratio. The direct derivation of ANN was proposed by Shin and Pande, (2003) to calculate the Jacobian stiffness matrix using the following equation:

$$D_{ANN} = \frac{\partial\sigma}{\partial\varepsilon} \tag{4-6}$$

In the EPR based Self-Sim, this procedure was adopted within the total stress strain strategy to construct the Jacobian matrix. The above equation can be applied in elastic and inelastic behaviour. The Jacobian matrix constructed in this way can be readily implemented in ABAQUS instead of a conventional built in constitutive model. The form of EPR based Jacobian matrix for plane stress condition can be presented as:

$$\boldsymbol{J_{EPR}} = \begin{bmatrix} \frac{\partial\sigma_x}{\partial\varepsilon_x} & \frac{\partial\sigma_x}{\partial\varepsilon_y} & \frac{\partial\sigma_x}{\partial\gamma_{xy}} \\ \frac{\partial\sigma_y}{\partial\varepsilon_x} & \frac{\partial\sigma_y}{\partial\varepsilon_y} & \frac{\partial\sigma_y}{\partial\gamma_{xy}} \\ \frac{\partial\tau_{xy}}{\partial\varepsilon_x} & \frac{\partial\tau_{xy}}{\partial\varepsilon_y} & \frac{\partial\tau_{xy}}{\partial\gamma_{xy}} \end{bmatrix} \tag{4-7}$$

The Jacobian matrix provided by EPR model is constructed in a different way when the incremental stress-strain technique is utilised to train EPR in the Self-Sim framework. This technique utilises the advantage of the standard elastic stiffness matrix which is presented in terms of elastic parameters (e.g. E, μ).

Owen and Hinton, (1980) derived the constitutive stress-strain relationship as described below:

$$\delta\sigma = D\delta\varepsilon \tag{4-8}$$

where D is the stiffness matrix which for isotropic and elastic materials can be constructed using only two elastic parameters (E, μ). To describe the elastic stress-strain curve of materials, there are four more elastic parameters that can be utilised for material modelling: G (shear modulus), K (bulk modulus), λ (Lame's first parameter) and M (P-wave modulus) (Timoshenko and Goodier, 1970). For isotropic materials, any two of the above parameters are enough to construct the stiffness (Jacobian) matrix hence all parameters are related to each other as stated in the following equations:

$$K = \frac{E}{3(1-2\mu)} \tag{4-9}$$

$$\lambda = \frac{E\,\mu}{(1-2\mu)(1+\mu)} \tag{4-10}$$

$$G = \frac{E\,(1-\mu)}{3(1+\mu)} \tag{4-11}$$

$$M = \frac{E\,(1-\mu)}{(1+\mu)(1-2\mu)} \tag{4-12}$$

The Jacobian matrix provided by the EPR based Self-Sim model trained incrementally was constructed based on calculating and updating the E at each increment in the Self-Sim framework while the value of μ was assumed constant for simplicity. The calculation of E can be described in two steps:

Step (1): for the $i+1^{th}$ load increment, the input variables ε_v^i , ε_y^i , $\Delta\varepsilon_y^i$, q^i, p'^i have already been calculated in the previous increment. The new value of the output variable q^{i+1} is calculated for the next step based on the EPR model.

Step (2): The value of Young's modulus E is calculated through the stress-strain curve. For instance, in case of axisymmetric problem:

$$E = \frac{\Delta q^i}{\Delta \varepsilon_y^i} \tag{4-13}$$

By assuming the value of Poisson's ratio to be constant, the Jacobian matrix can be constructed and iteratively implemented in ABAQUS via its user subroutine UMAT at every load increment. Every step of the framework has been automated in a MATLAB code using its comprehensive functions.

4.4 Summary

Self-Sim approach has proven to be a robust technique for material modelling. This has been shown by application to a number of engineering applications under static and dynamic loading conditions. This approach builds a bridge between experimental or field measurements and numerical analysis, providing deep insight into material behaviour and widening the knowledge on how materials behave in a more realistic sense. Therefore, in general, improving the capabilities of this inverse approach would be highly valuable in engineering and science fields.

One of the main drawbacks of the Self-Sim algorithm is that it usually uses ANN in representing the material behaviour. However, ANNs are known to suffer from a number of drawbacks that make them difficult to work within numerical analysis. The complex structure of the ANN models that are generated within the traditional Self-Sim approach is probably the reason why this approach has not gained more interest from other researchers in different fields. EPR as an alternative machine learning technique has proven to be a powerful tool that overcomes most of the shortcomings of ANNs.

In this thesis EPR has been utilised in the framework of Self-Sim with some important modifications to the whole algorithm which make it much simpler to extract and represent the material constitutive behaviour.

Like ANN, an EPR based model does not require to define the yield function, plastic potential function, failure, flow rule, etc (Rezania, 2008) . Two different strategies of training EPR based Self-Sim are implemented in this work. The next two chapters will demonstrate and verify the new Self-Sim framework in modelling some structural and geotechnical applications.

CHAPTER 5

Structural Applications of EPR Based Self-learning FEM

5.1 Introduction

Simulation algorithms, and in particular the FEM, have been used successfully in different fields of engineering including structural and geotechnical engineering, aerospace, biomedical engineering, chemical engineering, among many others. In FEA the behaviour of the real material is approximated with that of an idealised material that behaves in accordance of some theoretical relations (i.e. constitutive models). It is generally known that the successful application of FEM in engineering applications is mainly dependent on the choice of a suitable constitutive model that is able to describe the material behaviour (e.g., stress-strain relationship). Many constitutive models have been developed for various materials such as concrete, soils, rocks, polymers, etc. In spite of the large number of constitutive models with different degrees of complexity, it has been indicated that these models are not able to fully capture the real material behaviour of some complex materials under different loading conditions. In addition, incorporation of such complex models in finite element codes could be challenging, consequently delimiting their functionality in engineering applications.

The rapid developments in the computer hardware and software has enabled scientists and engineers to include the data mining technique in this important field. For example, the use of ANN in representing the constitutive behaviour of different materials has gained a lot of attention in the last 3 decades, as discussed in chapter 3. The conventional procedure for training of ANN involves using data from many experimental tests which is costly, time consuming and may not be available in some cases.

Therefore, a new methodology, called auto-progressive training or Self-Sim, was developed to train ANN through finite element analysis of boundary value problems (Fu et al., 2007; Shin and Pande, 2000; Sidarta and Ghaboussi, 1998).

However, it is well known that ANNs have some drawbacks as described in chapter one. EPR has been developed, as an alternative data mining technique, to avoid most of the ANNs' drawbacks (Giustolisi and Savic, 2006). EPR has been applied successfully to represent the constitute behaviour of different materials (Rezania; et al., 2008). Although EPR has been shown to be a robust tool for capturing and learning the material behaviour, again as in the conventional training of ANN, the way that EPR is trained requires considerable amount of experimental (or field) data to build a reliable material model.

To address this problem, the self-learning algorithm has been introduced in this thesis for training of EPR models (see Chapter 4). In this chapter, the methodology of EPR-based self-learning simulation (EPR-Self-Sim), developed in the previous chapter, will be used for the analysis of different structural engineering applications using the total stress-strain training strategy.

5.2 MATLAB Environment

MATLAB (Matrix Laboratory) is a proprietary programming language developed by MathWorks. It has many functions that can be used directly. MATLAB has series of mathematical processes that work on arrays or matrices which are built-in to the MATLAB environment. In this research, the automation process utilises the interesting facilities available in the MATLAB environment. These are included in the following steps which are coded in MATLAB.

- Running the finite element analyses (FE-A and FE-B) sequentially in an iterative loop.
- Generally, EPR produces the developed models in LaTeX form. In the MATLAB, the best model was selected based on the *CoD* value and the EPR formula was transformed to a symbolic form based on the exponent and constants matrixes. This would ensure that the mathematical

expressions developed by the EPR model are ready to be differentiated and incorporated in finite element code appropriately.

- The model is prepared, differentiated and written in a FORTRAN file (UMAT) using a set of functions in the MATLAB code. It should be mentioned that the way that the model is written in the Fortran file is automatically simplified and arranged to be calculated easily using the MATLAB function [fortran (Input,'file','UMAT.f')].
- The results from finite element analyses are written in text files: MATLAB prepares the requested data, shuffles the data and removes the duplicated data and implements them into the EPR file.
- The EPR is run repeatedly in a loop process.
- Scaling of the data: EPR is quite sensitive with the small numbers as the precision of MATLAB (which is behind the EPR) is about (10^{-16}). Therefore, when the analysis deals with small numbers, the input and output data should be normalized and denormalized at each EPR run between [0 1]. Normalizing and denormalizing the data is done in the EPR and MATLAB codes respectively using the scaling equations:

$$X_{input} = \frac{X - X_{min}}{X_{max} - X_{min}} \tag{5-1}$$

$$Y_{output} = \frac{Y - Y_{min}}{Y_{max} - Y_{min}} \tag{5-2}$$

- Termination criterion: During the analysis, the results of displacements at FE-A and FE-B models are compared. When the difference between the results of the two models becomes less than a pre-defined tolerance, the EPR based self-learning simulation is terminated.

5.2.1 Numerical examples

The automation process of implementation of the multi-objective EPR model in the self-learning procedure is presented in this chapter. The methodology is applied on several structural applications including truss elements and plane stress conditions following the framework presented in Figure (4-23).

To verify the capability of the developed algorithm, the developed procedure is examined for linear elastic, nonlinear elastic and elastic-plastic behaviour of structural materials. The choice of the training strategy is dependent on the application that needs to be analysed. The total stress-strain strategy is suitably selected to train the EPR through the self-learning process in these applications. In the proposed framework, choosing the appropriate number and locations for the monitoring points could significantly influence the quantity and quality of the training data. Hypothetical and experimental data are used to run the EPR-based self-learning procedure. The results of the developed EPR models are compared with the actual data and showed the capabilities of the proposed algorithm in representing the constitutive behaviour of materials.

5.2.1.1 Application 1: Aluminium plate (linear elastic model)

A 2D plane stress panel subjected to in-plane compression is considered. The geometry of the plate, boundary conditions and loading are shown in Figure (5-1). Due to the symmetry, only a quarter of the plate is modelled, and appropriate boundary conditions are applied on the left and bottom boundaries. The material of the plate is linear elastic with Young's modulus E = 500 Pa and poison's ratio μ = 0.3 and the pressure applied is 20 Pa. The load was applied on a rigid surface to make sure that the plate is deformed uniformly. This example has been deliberately kept simple in order to verify the process of EPR based self-learning simulation. The measurement data are generated synthetically from a standard FE model in ABAQUS. The plate is analysed with 80 isotropic 8-node elements. It is assumed that during the experiment the displacements at the node on the top right corner of the plate, N_1 (monitoring point, shown in Figure 5-1) are recorded as experimental measurements and used in the self-learning process.

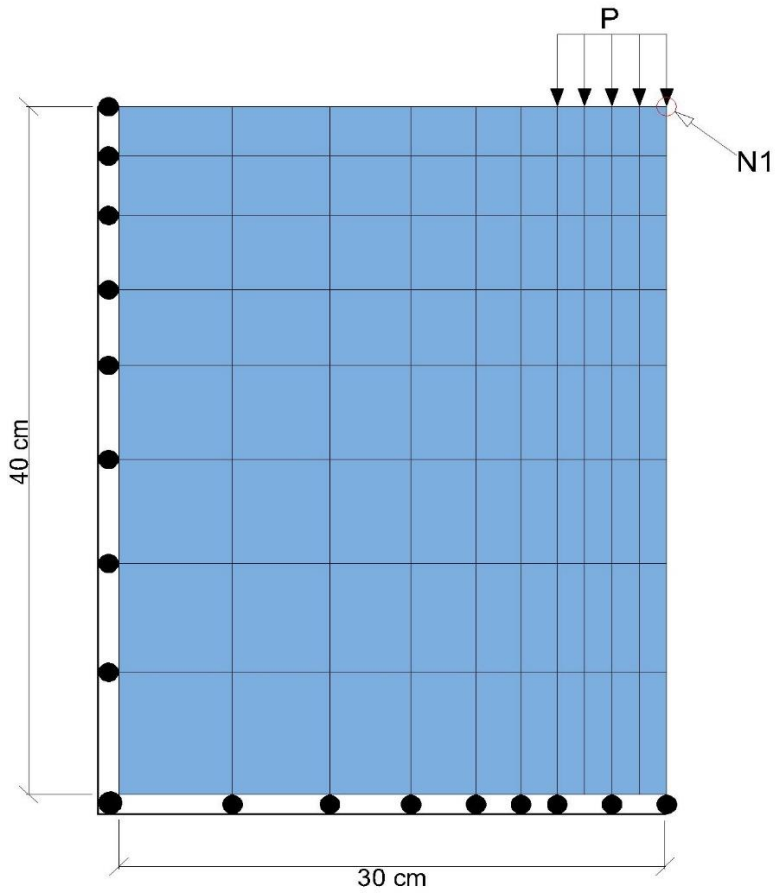

Figure 5-1: Geometry, loading, mesh and BCs of the plate.

The EPR-based self-learning framework is applied where two finite elements analyses are created (FE-A and FE-B) and run in parallel. The procedure starts from an initial (usually a linear elastic model) only for the first increment of load in the first iteration however in this case the same linear elastic model is used. The following input and output variables are used in the total stress-strain training strategy to train and develop the EPR models.

$\sigma_x = f(\varepsilon_x, \varepsilon_y, \gamma_{xy})$

$\sigma_y = f(\varepsilon_x, \varepsilon_y, \gamma_{xy})$

$\tau_{xy} = f(\varepsilon_x, \varepsilon_y, \gamma_{xy})$

In the EPR setting, the maximum number of terms is set to be 5 and the exponents are limited to [0 1]. After completing the training process within the self-learning algorithm, three sets of EPR models are generated and the best models are selected based on *CoD* values and used for the analysis of the plate. These models with the highest *CoD* (99.99% for each model) are sequentially generated within the MATLAB code. The Jacobian matrix is then formulated by the differentiation of the following EPR constitutive equations and transferred via UMAT to the FE analysis: *

$$\sigma_x = 549.48\,\varepsilon_x + 164.64\,\varepsilon_y - 5.134 \times 10^{-12} \tag{5-3}$$

$$\sigma_y = 549.41\,\varepsilon_x + 164.67\,\varepsilon_y - 1.235 \times 10^{-11} \tag{5-4}$$

$$\tau_{xy} = 0.0064\varepsilon_x + 192.32\,\gamma_{xy} - 7.159 \times 10^{-13} \tag{5-5}$$

The Jacobian matrix that is implemented in the FE model is as follows:

$$J = \begin{bmatrix} \frac{\partial \sigma_x}{\partial \varepsilon_x} & \frac{\partial \sigma_x}{\partial \varepsilon_y} & \frac{\partial \sigma_x}{\partial \gamma_{xy}} \\ \frac{\partial \sigma_y}{\partial \varepsilon_x} & \frac{\partial \sigma_y}{\partial \varepsilon_y} & \frac{\partial \sigma_y}{\partial \gamma_{xy}} \\ \frac{\partial \tau_{xy}}{\partial \varepsilon_x} & \frac{\partial \tau_{xy}}{\partial \varepsilon_y} & \frac{\partial \tau_{xy}}{\partial \gamma_{xy}} \end{bmatrix} = \begin{bmatrix} 549.48 & 164.64 & 0.00 \\ 164.67 & 549.41 & 0.00 \\ 0.0064 & 0.00 & 192.32 \end{bmatrix} \tag{5-6}$$

The above Jacobian matrix is the same as the standard stiffness matrix for an isotropic elastic material under plane stress condition (equation 4-5) with E = 500 Pa and μ = 0.3 as follow.

$$D = \begin{bmatrix} 549.45 & 164.83 & 0.00 \\ 164.83 & 549.45 & 0.00 \\ 0 & 0.00 & 192.31 \end{bmatrix} \tag{5-7}$$

* Unit: Stresses in N/m^2

It can be seen that equation (5-6) developed through EPR based self-learning and (5-7) based standard elastic matrix are in an excellent agreement. The convergence is achieved from one pass of the self-learning. This is because the behaviour is simple and EPR has enough data to capture the behaviour. Figures (5-2) and (5-3) show the convergence of FE-A and FE-B models. It can be seen that the contours of vertical stress and strain are similar. This clearly shows the capability of the proposed algorithm in general. It should be mentioned that the running time for such a simple application is very short within the automation process.

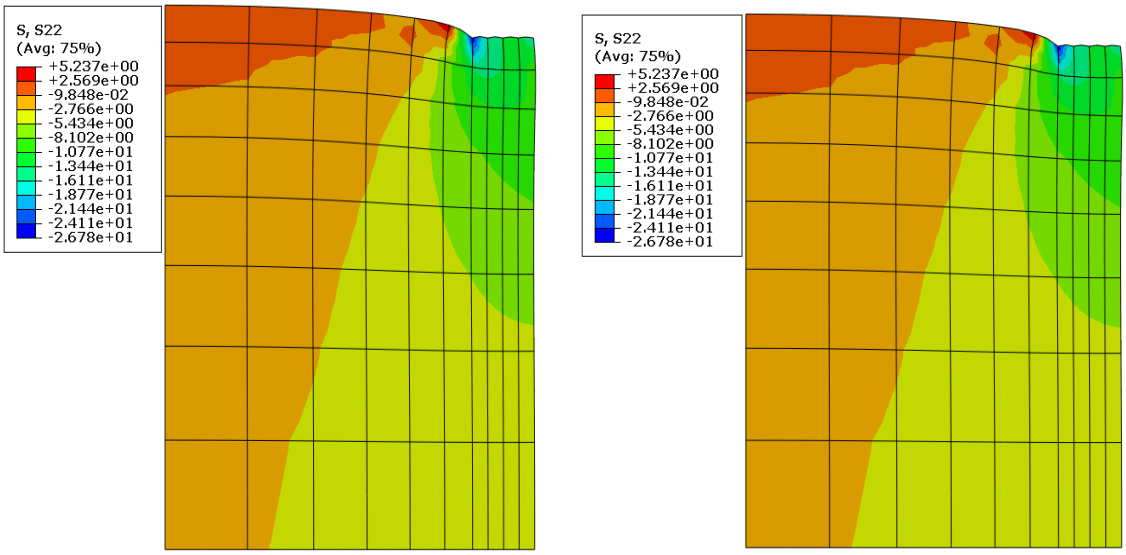

(a) (b)

Figure 5-2: Comparison between vertical stress contours (S22) of (a) FE-A (b) FE-B of EPR based self-Learning model showing the convergence state.

* Unit: Stress (S22) in N/m^2

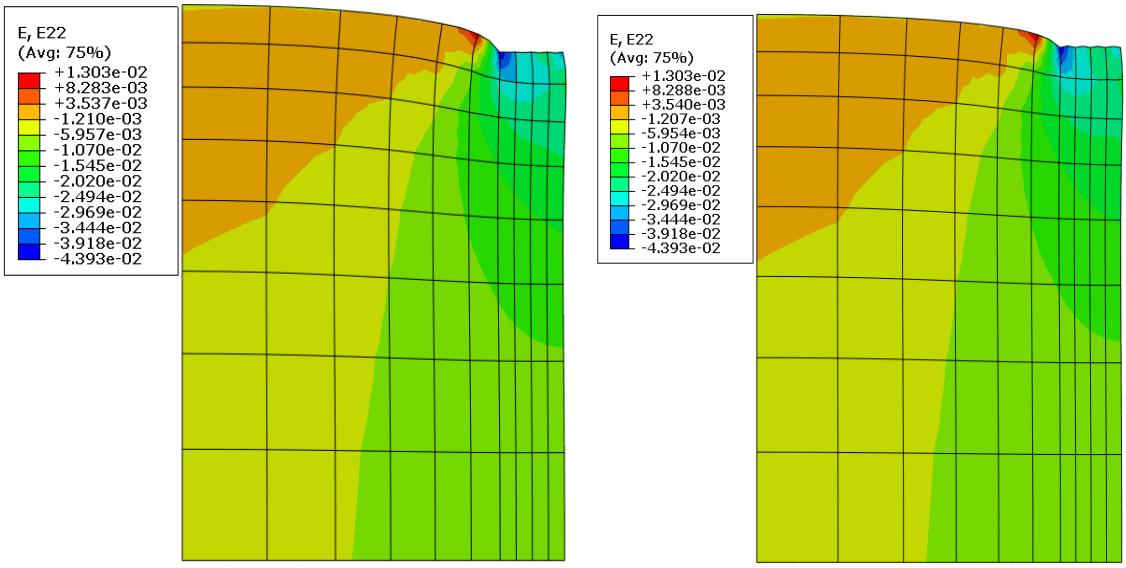

Figure 5-3: Comparison between vertical strain contours (E22) of (a) FE-A (b) FE-B of EPR based self-Learning model showing the convergence state.

Figure (5-4) shows the prediction of the developed EPR-based self-learning FE model for the displacement at the monitoring point (N_1). Comparison is made between the results of the actual (linear elastic) model and the EPR based self-learning FEM. It can be seen that the EPR-based FEM is able to provide an excellent agreement with the actual data.

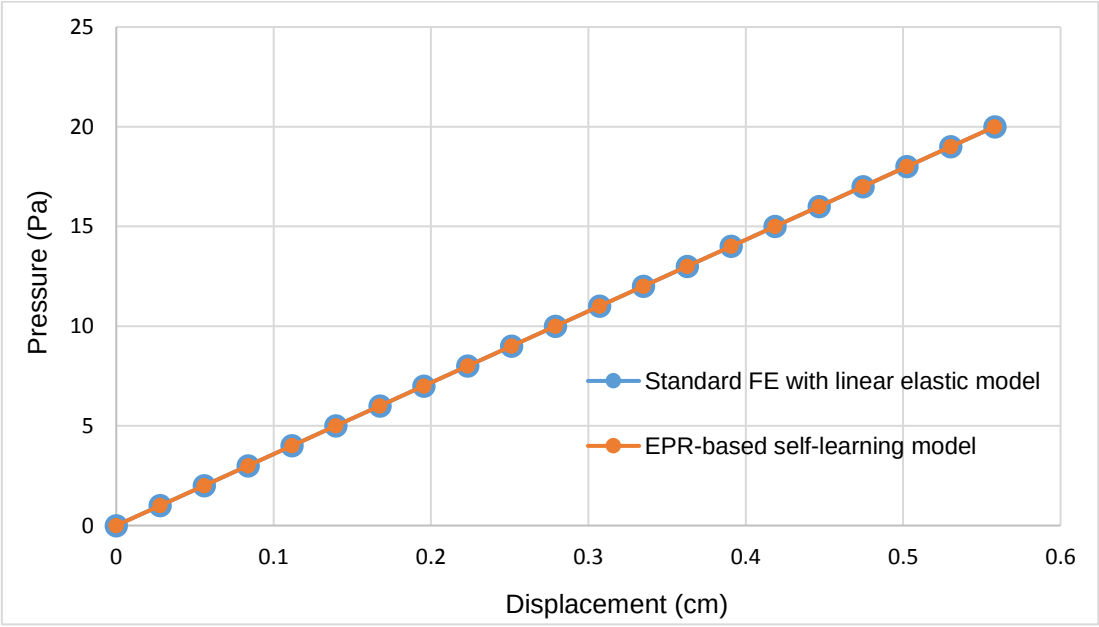

Figure 5-4: EPR based self-learning FEM prediction at node N1 and actual model prediction.

5.2.1.2 Application 2: Truss structure (non-linear elastic model)

A 2D truss structure with 13 axial force elements is considered in the second application. The geometry, boundary conditions and loading are illustrated in Figure (5-5). The truss is subjected to a concentrated load (100 KN) at node 3 (n_3). The simulation is carried out with 13 truss elements considering non-linear elastic behaviour (Ramberg-Osgood model) for the material to generate the synthetically measured data. The maximum displacement is expected to be at node 3 (n_3) therefore it is convenient to choose this node as a monitoring point.

The self-learning framework is used in which the load is applied in FE-A and the corresponding displacement at n_3 is enforced on FE-B. The load and the corresponding displacement at n_3 are considered as the experimental measurements (monitoring data) used in the self-learning process. The training variables are axial stress and axial strain.

The general form of the Ramberg-Osgood model (Ramberg and Osgood, 1943). is:

$$\varepsilon = \frac{\sigma}{E} + \frac{2\beta\sigma_\circ}{3E} \times \left(\frac{\sigma}{\sigma_\circ}\right)^n \tag{5-8}$$

The model parameters are presented in Table (5-1). In this application only the values of the axial strain are output, and the values of axial stress are input which is similar to the original model formulation. EPR models are developed with these variables using the self-learning FEM framework. After selecting the best EPR model, the equation is transformed and differentiated to the axial strain. This step is included in the MATLAB code taking very short time to be solved.

Table 5-1: The Ramberg Osgood model parameters.

Young's modulus (E)	20 x 10^9 Pa
β	2.34
$\sigma_\circ$	1.0×10^7 Pa
n	3

The procedure starts with an initial simple linear elastic model with E = 20 x 10^9 Pa. This is to ensure that the initialised step is not run with a random. In the EPR setting, the maximum number of terms is set to 5 and the exponents are set to be in range [0 1 2 3]. After training and completing the load increments applied, an EPR model with the highest *CoD* (99.97%) is chosen. *

$$\varepsilon_{11} = 1.5899\,\sigma_{11} - 3.7333\,\sigma_{11}^2 + 3.1443\,\sigma_{11}^3 - 9.0355\ \times 10^{-5} \qquad (5\text{-}9)$$

where ε_{11}, σ_{11} are the axial strain and stress respectively.

The developed EPR model is able to capture the material behaviour from the first pass of the self-learning procedure. The convergence of the FE-A and FE-B models of the structure is shown in Figure (5-6) through the stress-strain curves. It can be seen that the two analyses are in very good agreement.

The vertical displacements (U2) at the monitoring point n_3, obtained using the Ramberg-Osgood model and the EPR based self-learning model, are presented in Figure (5-7). Comparison of the results shows that the EPR model can capture the behaviour very accurately.

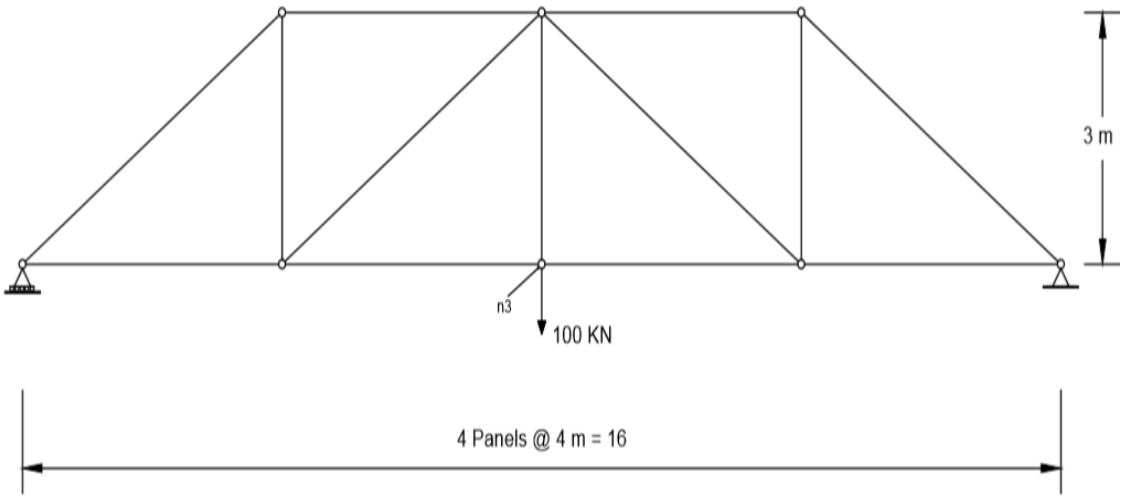

Figure 5-5: Truss structure and the applied load.

* Unit: Stress (σ_{11}) in N/m^2

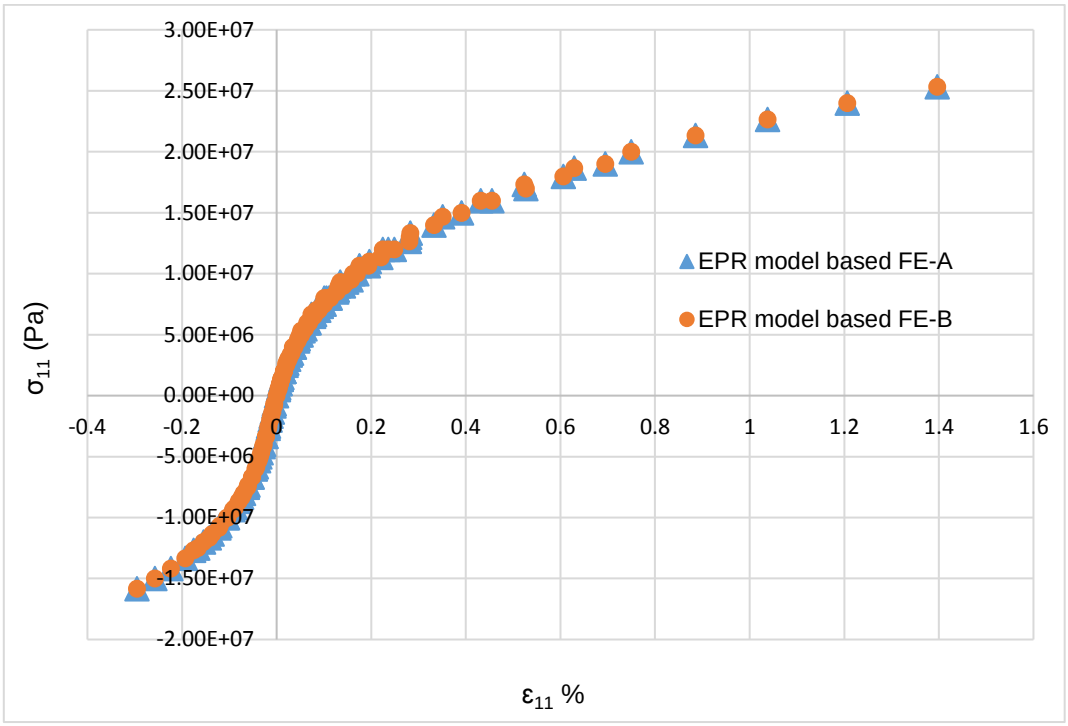

Figure 5-6: Convergence of FE-A and FE-B of EPR-based Self-learning model predictions.

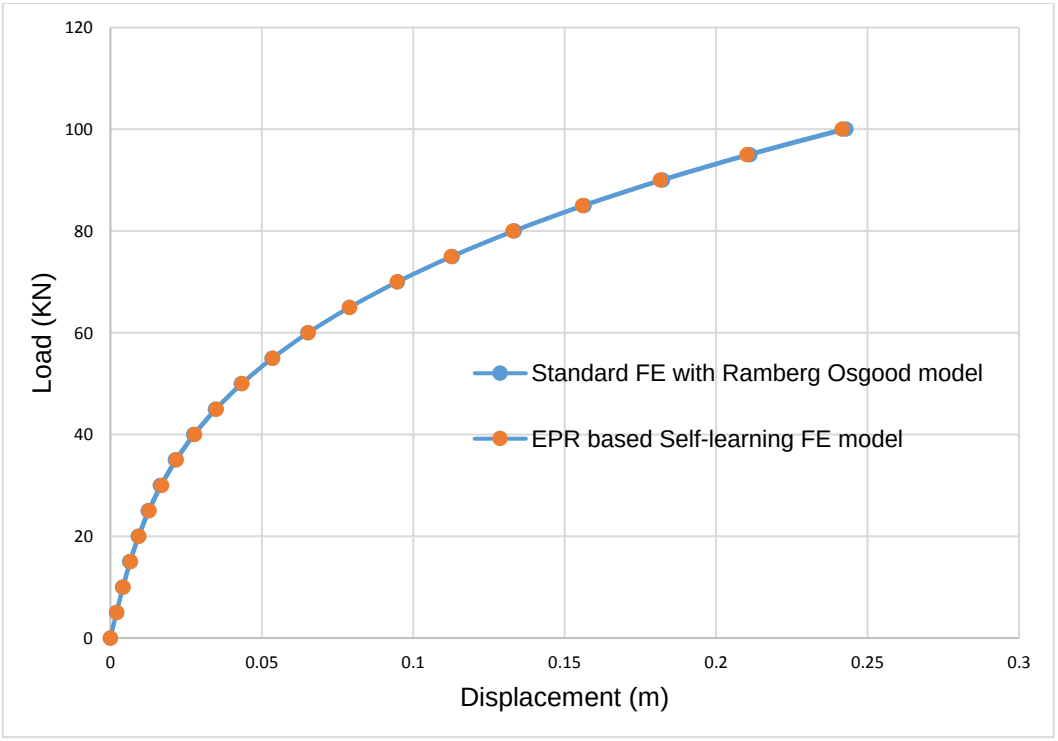

Figure 5-7: Comparison between the Ramberg Osgood model and the EPR-based self-learning FE model (displacements U2 at node n_3).

5.2.1.3 Application 3: Truss structure (elastic-plastic model)

The same truss structure presented in the previous application (Figure 5-5) is used in this analysis. The truss is subjected to a concentrated load (100 KN) at node 3 (n_3). The load–displacement data were synthetically generated within FE simulation using an elastic-plastic model with hardening (using tabulated data option of the material module) in ABAQUS. In this application, one monitoring point was considered enough to represent the response of the structure to the loading. The load and the corresponding displacement at n_3 are considered as the experimental measurements (monitoring data) and used in the self-learning process. Two finite element models FE-A and FE-B are created, and the self-learning process was initialized first with a linear elastic model with Young's modulus of 3×10^6 Pa. Again, the total stress-strain strategy is employed in this application in which the values of axial strain and axial stress are considered as input and output respectively:

$$\sigma_{11} = F(\varepsilon_{11}).$$

In the EPR settings, the maximum number of terms is set to 6 and the exponents are set to be in range of [0 1 2 3 4 5]. These settings are specified following a trial and error procedure of EPR runs. Following the developed framework of EPR based self-learning simulation, the load was applied in increments and at each load increment, an EPR model with highest *CoD* is chosen and forwarded for the next increment. Convergence of the FE-A and FE-B models is achieved after two cycles of self-learning (within a single pass). The final EPR model developed is as follows: *

$$\sigma_{11} = 73.38 \times 10^5\, \varepsilon_{11}^5 - 8.82 \times 10^3\, \varepsilon_{11}^4 + 71.28 \times 10^5\, \varepsilon_{11}^3 + 43.59\, 10^3\, \varepsilon_{11}^2 + 3 \times 10^3\, \varepsilon_{11} \quad (5\text{-}10)$$

The above EPR model has *CoD* of 99.86 %. From Figure (5-8) it can be seen that during the self-learning procedure, the prediction capability of the developed EPR model was improved gradually towards the expected behaviour within two cycles of self-learning. The convergence criteria between the FE-A and FE-B models is introduced in Figure (5-9). It can be seen that the two finite element analyses converged.

* Unit: Stress (σ_{11}) in N/m^2

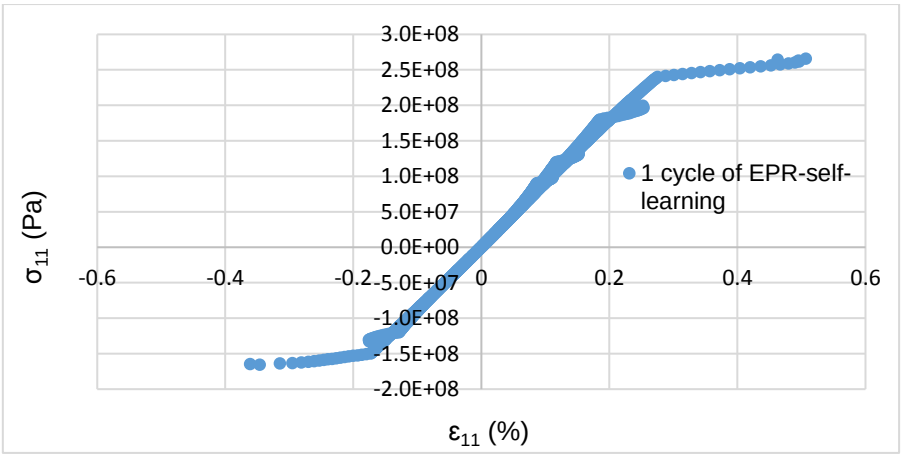

(a)

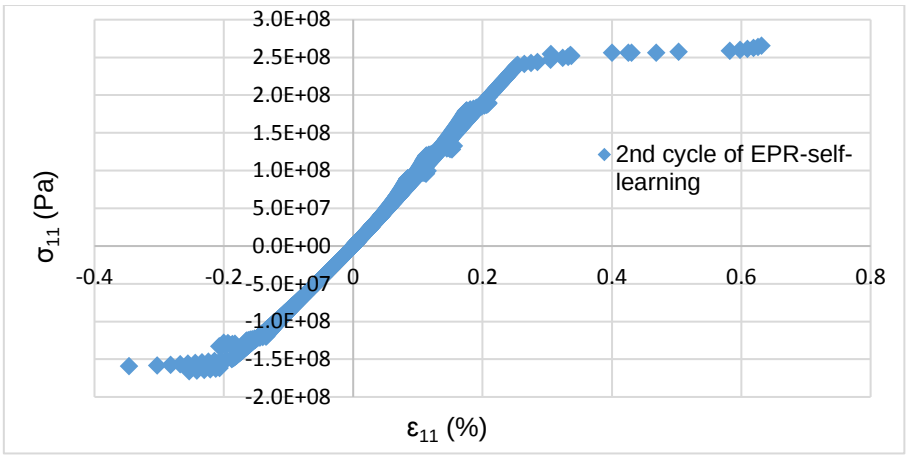

(b)

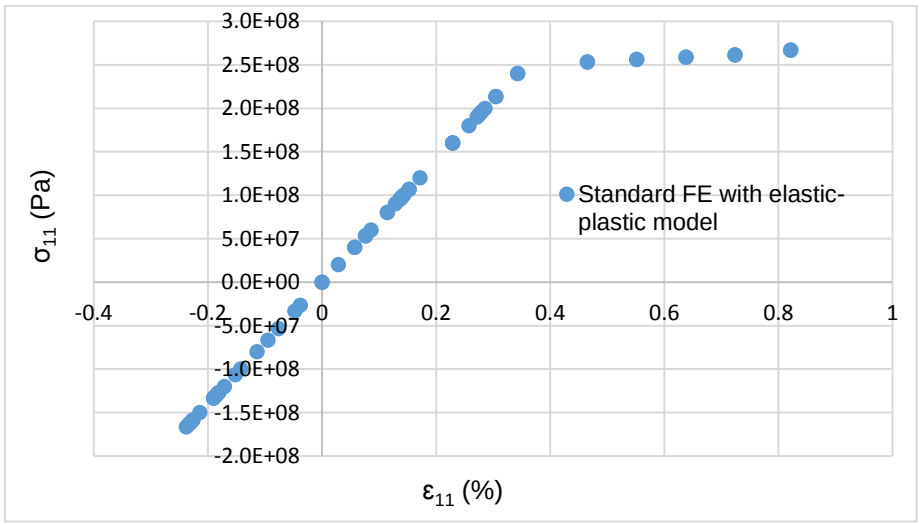

(c)

Figure 5-8: Stress-strain results of the EPR-based self-learning model and the original model (a) 1st cycle of self-learning, (b) 2nd cycle of self-learning (c) the elastic-plastic model prediction.

To verify the developed EPR model, the results of load and displacement at node (n_3) in the EPR-based self-sim model and the original model are compared. It can be seen from Figure (5-10) that the developed EPR model is able to predict the deformation of the truss with one pass of self-learning with very good accuracy within both elastic and plastic regions.

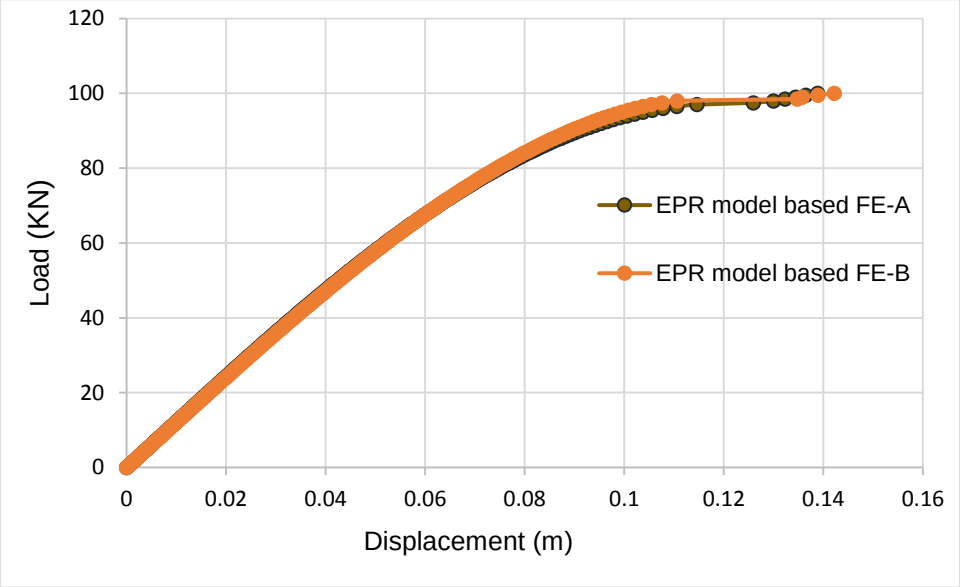

Figure 5-9: Convergence of the load-displacement curves of the FE-A and FE-B models after completion of the self-learning simulation.

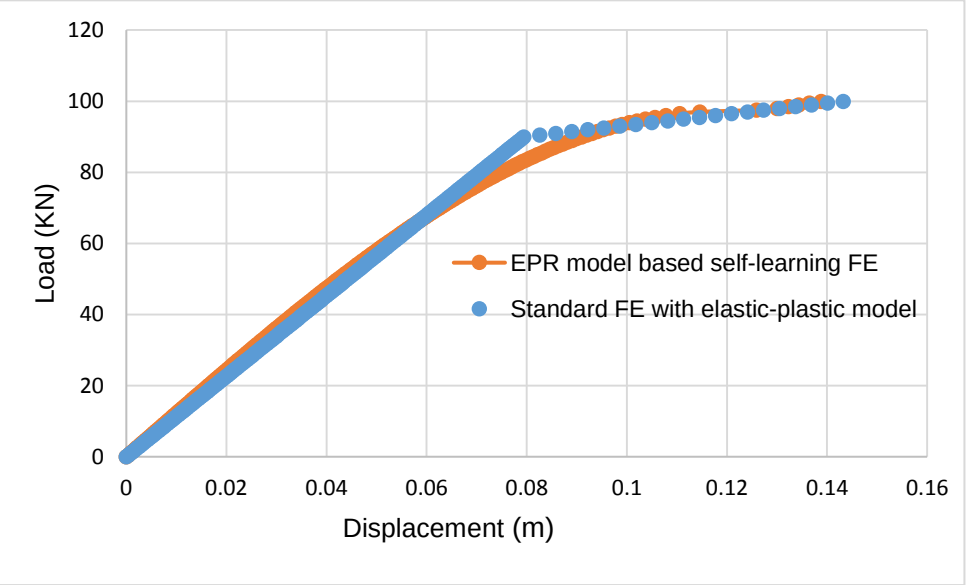

Figure 5-10: Deformation of node (n_3) predicted by the EPR-based self-learning model and the original elastic-plastic model.

5.2.1.4 Application 4: Aluminium plate (non-linear elastic model)

A 2D plane stress square plate subjected to a biaxial tensile loading is considered in this application. The geometry of the plate, boundary conditions and loading are shown in Figure (5-11). Due to the symmetry, only a quarter of the plate is simulated. The experimental measurements are generated synthetically by using a non-linear elastic model implemented in the FE simulation (Faramarzi, 2011).

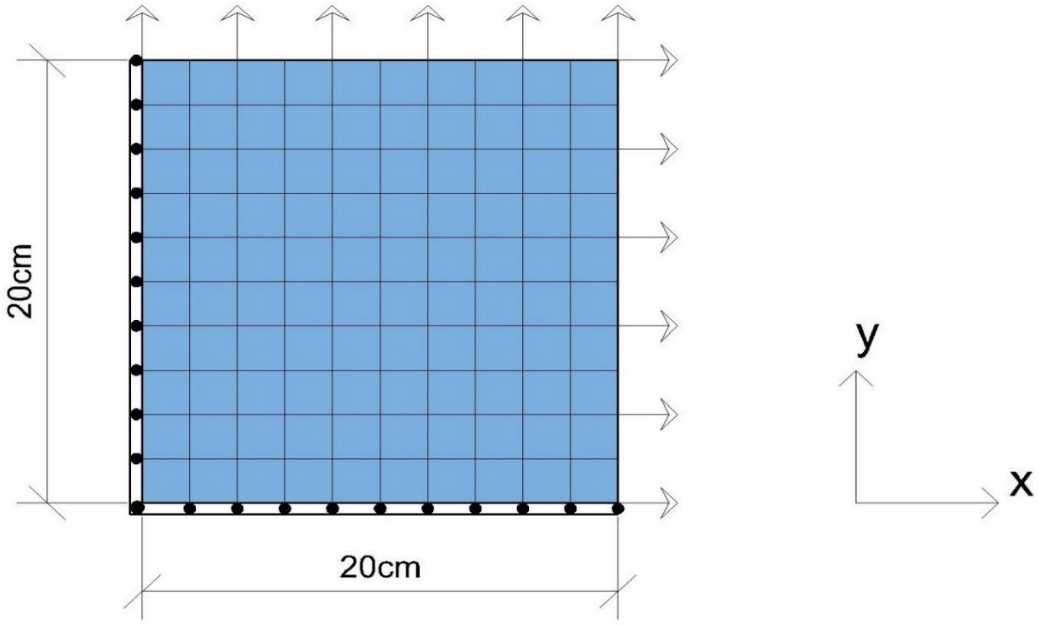

Figure 5-11: Geometry, loading, mesh and boundary conditions of the plate.

The applied pressures are 17.5 Pa and 25 Pa along the x and y axes and the corresponding strains are 5% and 10% respectively. The finite element simulation of the plate is carried out using 100 (8-node biquadratic plane stress) elements. This application has a different approach in the way that the training data are generated within the self-learning procedure. This is because the stress-strain values represent loading along the principal axes only (shear strains and shear stresses are zero) which are not enough to train the EPR-based self-learning model.

Consequently, a strategy is applied to generate more data with non-zero shear stresses and strains. This strategy has been utilised by several researchers to generate more data to train ANN and EPR models when the material being analysed is isotropic (Faramarzi, 2011; Shin, 2001). In this strategy, the material is assumed to be isotropic and the EPR is trained with the global axes having non- zero shear stress values.

The strategy of data extension utilises the isotropic assumption, hence it allows to exchange the normal components. Figure (5-12) illustrates the transformation of the stress components. The transformation of stress-strain components is achieved by rotating the local axes (x-y) from the global axes (1-2) and based on Mohr's circle and using (2θ) angle. The transformation of stress and strain components can be calculated from the following equations:

$$\sigma_x = \frac{\sigma_1 + \sigma_2}{2} + \frac{\sigma_1 - \sigma_2}{2}\cos(2\theta) \quad (5\text{-}11)$$

$$\sigma_y = \frac{\sigma_1 + \sigma_2}{2} - \frac{\sigma_1 - \sigma_2}{2}\cos(2\theta) \quad (5\text{-}12)$$

$$\tau_{xy} = \frac{\sigma_1 - \sigma_2}{2}\cos(2\theta) \quad (5\text{-}13)$$

$$\varepsilon_x = \frac{\varepsilon_1 + \varepsilon_2}{2} + \frac{\varepsilon_1 - \varepsilon_2}{2}\cos(2\theta) \quad (5\text{-}14)$$

$$\varepsilon_y = \frac{\varepsilon_1 + \varepsilon_2}{2} - \frac{\varepsilon_1 - \varepsilon_2}{2}\cos(2\theta) \quad (5\text{-}15)$$

$$\gamma_{xy} = \frac{\varepsilon_1 - \varepsilon_2}{2}\cos(2\theta) \quad (5\text{-}16)$$

The above equations were coded in MATLAB in the process of preparing data for the EPR.

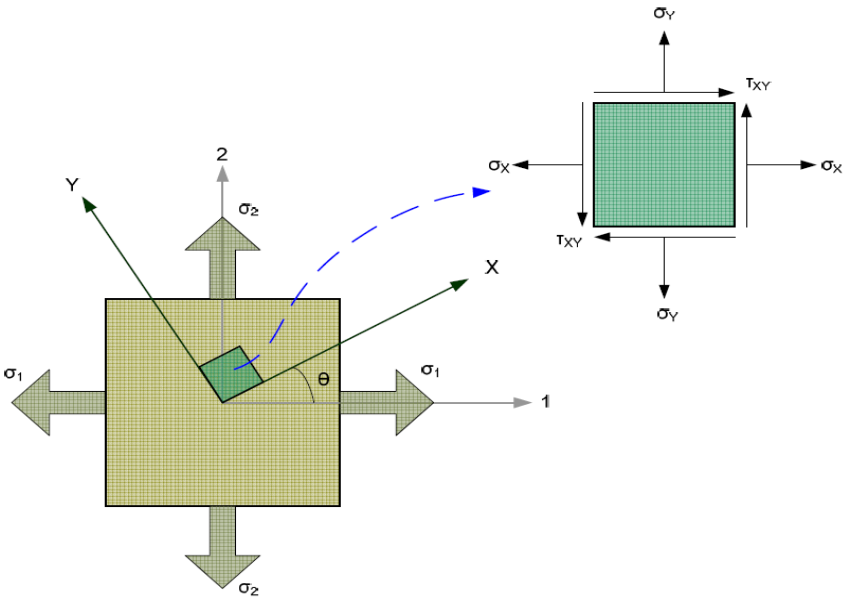

Figure 5-12: Stress components transformation in plane stress (Faramarzi, 2011).

The pressures and the corresponding displacements on the edges of the plate are selected as monitoring data; they are considered as the experimental measurements and used in the self-learning process. Two finite element models, FE-A and FE-B are created and the self-learning process is initialized first with an elastic modulus of 500 Pa and Poisson's ratio 0.3. The total stress-strain strategy is employed in which the values of strains and stresses are used as input and output respectively as:

$$\sigma_x = f(\varepsilon_x, \varepsilon_y, \gamma_{xy})$$

$$\sigma_y = f(\varepsilon_x, \varepsilon_y, \gamma_{xy})$$

$$\tau_{xy} = f(\varepsilon_x, \varepsilon_y, \gamma_{xy})$$

In the EPR setting module, the maximum number of terms is set to be 10 and the range of exponents is [0 1 2]. After training, in each run, three EPR models with the highest *CoD* values are chosen and Jacobian matrix is calculated from the partial derivation of these equations. The final EPR equations used in the analysis have *CoD* = 99.96% and are as follows: *

$$\sigma_x = 26365\ \varepsilon_y\ \varepsilon_x^2 - 7965.5\ \varepsilon_y\ \gamma_{xy}^2 - 26336\ \varepsilon_x\ \gamma_{xy}^2 - 7318\ \gamma_{xy}^2 + 7924\ \varepsilon_x\ \varepsilon_y^2 - 4752.5\ \varepsilon_x^2 - 2564\ \varepsilon_y^2 + 166.2\ \varepsilon_y + 554\ \varepsilon_x \quad (5\text{-}17)$$

$$\sigma_y = 26372.4\ \varepsilon_x\ \varepsilon_y^2 + 7917\ \varepsilon_y\ \varepsilon_x^2 - 26362.5\ \varepsilon_y\ \gamma_{xy}^2 + 1241.4\ \varepsilon_x^2\ \gamma_{xy}^2 - 8119.2\ \varepsilon_x\ \gamma_{xy}^2 + 4230\ \gamma_{xy}^2 - 2188\ \varepsilon_y^2 - 6410.6\ \varepsilon_x\ \varepsilon_y + 166.2\ \varepsilon_x + 554\ \varepsilon_y \quad (5\text{-}18)$$

$$\tau_{xy} = 3366\ \varepsilon_x^2\ \varepsilon_y^2\ \gamma_{xy} + 4100\ \varepsilon_x^2\ \gamma_{xy} + 4095\ \varepsilon_y^2\ \gamma_{xy} + 8167\ \varepsilon_x\ \varepsilon_y\ \gamma_{xy} - 2188\ \varepsilon_x\ \gamma_{xy} - 2187.2\ \varepsilon_y\ \gamma_{xy} + 387\ \gamma_{xy} \quad (5\text{-}19)$$

Figure (5-13) shows the stress-strain relations prior to the self-learning process, using the linear elastic model. During the self-learning process, accurate stresses and strains (from FE-A and FE-B models respectively) are used to train the EPR models. The availability of data used through the self-learning algorithm gradually enables the EPR to learn and capture the elastic material behaviour within a single pass.

Figure (5-14) shows the convergence between the FE-A and FE-B models in the self-learning process presenting the vertical and horizontal stress-strain curves. The results show an excellent convergence between both FE analyses until the softening behaviour occurred when the FE-A model was stopped.

To verify the capability of the EPR-based self-learning model, a comparison is made between the prediction of the actual model and the EPR-based model applied on FE-B (see Figure 5-15). The results show an excellent agreement between the EPR-based FE analysis and the actual data and demonstrate the excellent ability of the developed EPR-based self-learning model to capture the nonlinear behaviour of the plate. Furthermore, the comparison between the EPR-based model developed and the actual model is introduced via the horizontal and vertical displacement contours as shown in Figures (5-16) and (5-17). In this analysis, the developed model is applied on FE-A. The EPR model shows good approximation to the actual displacement results.

* Units: Stresses in N/m^2

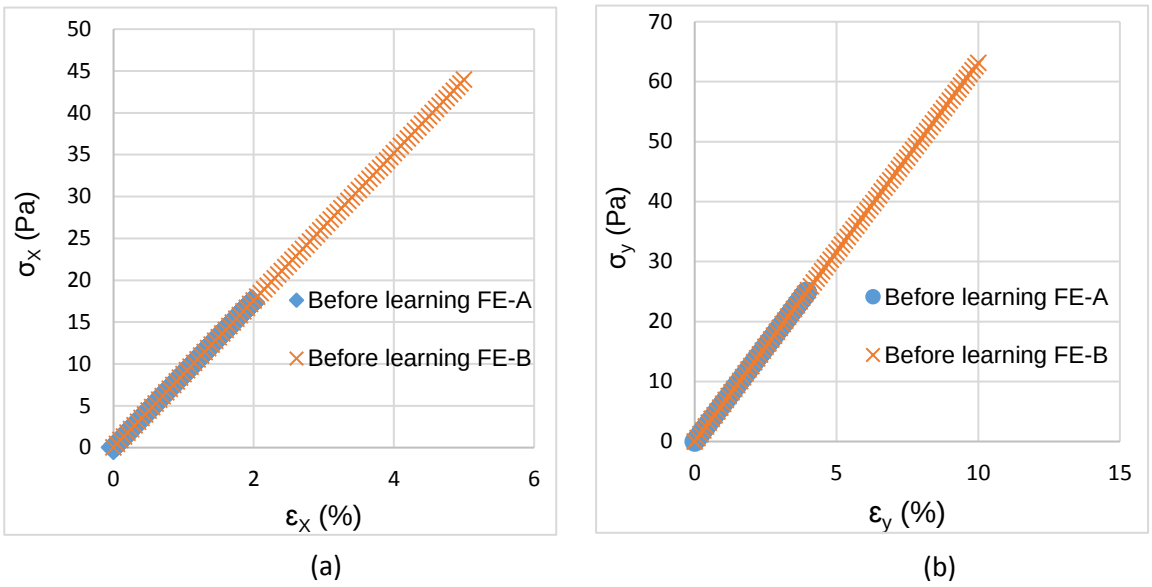

Figure 5-13: The stress-strain relations prior the self-learning process of FE-A and FE-B (a) horizontal stress-strain; (b) vertical stress-strain.

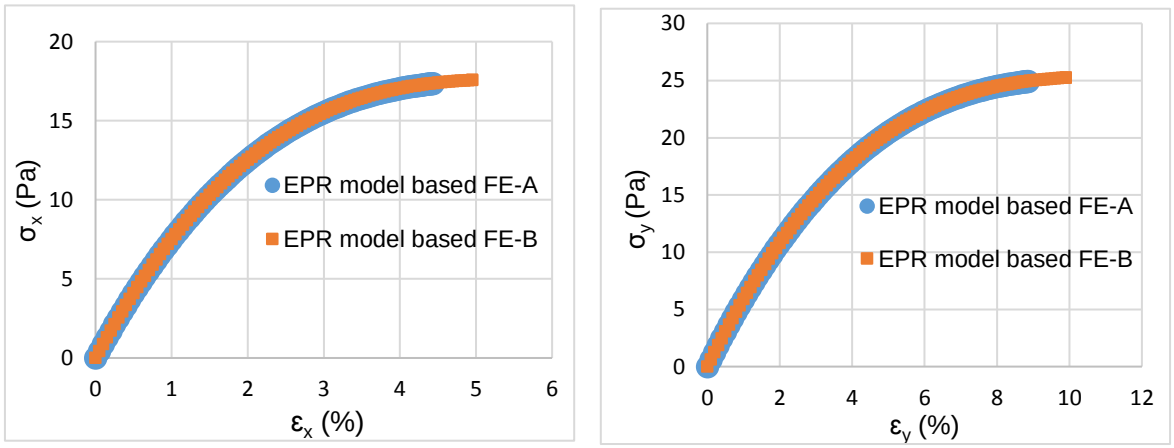

Figure 5-14: Convergence of FE-A and FE-B of the stress-strain results, (a) horizontal stress-strain; (b) vertical stress-strain.

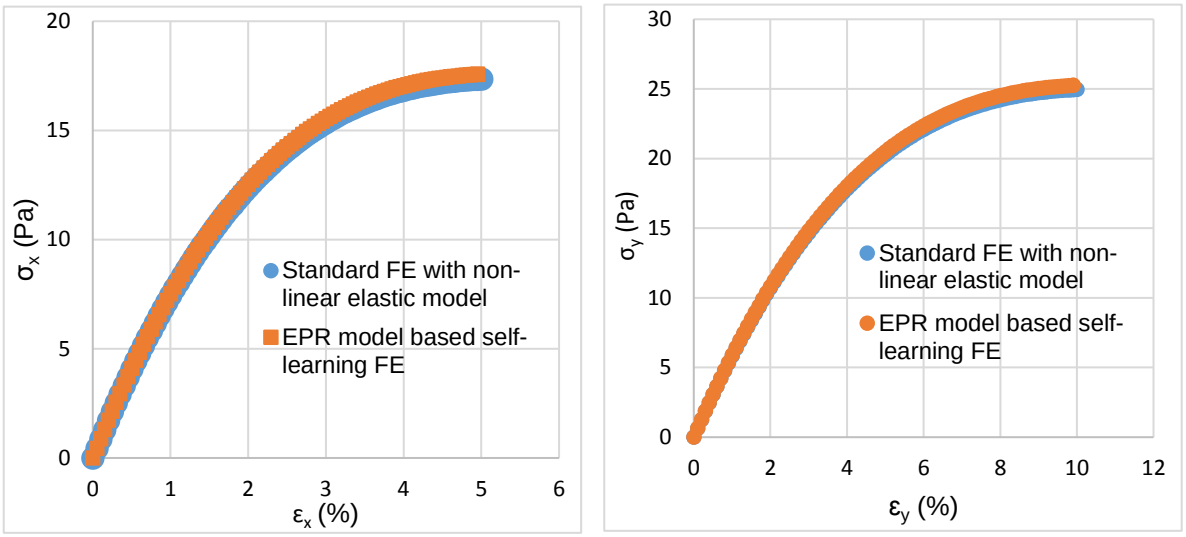

Figure 5-15: Stress-strain curves of EPR-based model applied on FE-B and the actual model, (a) horizontal stress-strain; (b) vertical stress-strain.

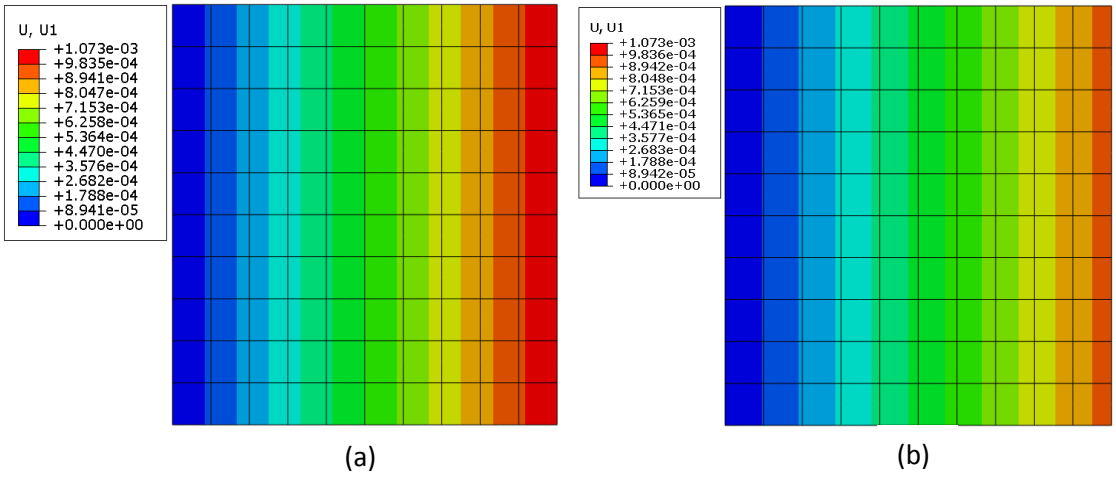

(a) (b)

Figure 5-16: Comparison between contours of horizontal displacements in (a) actual model; (b) EPR based self-learning model applied on FE-A. *

* Unit: displacement (U1) in m

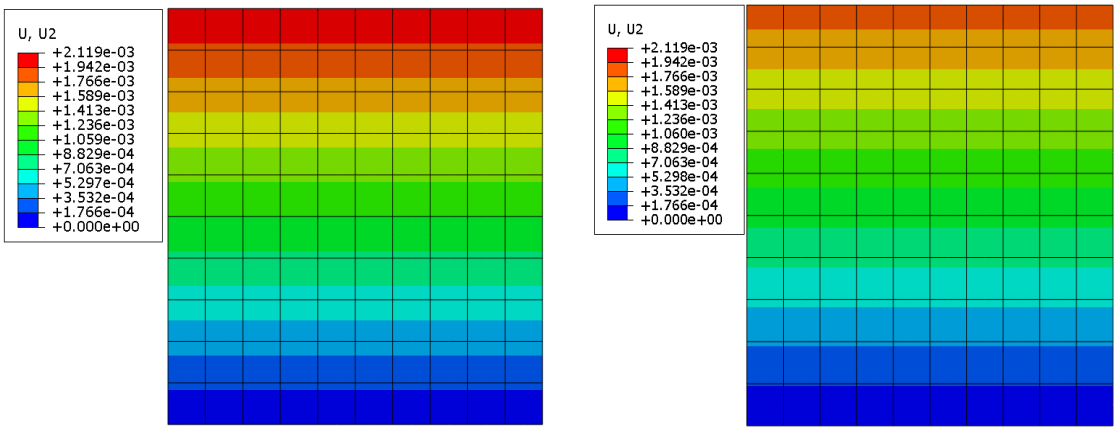

(a) (b)

Figure 5-17: Comparison between contours of vertical displacements in (a) actual model; (b) EPR based self-learning model applied on FE-A. *

5.2.1.5 Application 5: Aluminium plate (elastic-plastic behaviour)

In this application the same plate illustrated in the previous application (Figure 5-11) with the same geometry and the boundary conditions, is analysed considering elastic-plastic behaviour. The experimental data are generated synthetically using an elastic-plastic model. The model is assumed to represent the elastic-plastic material behaviour in which elastic and plastic parts are defined clearly and implemented in finite element analysis (ABAQUS) through the UMAT subroutine. Tensile strains are applied on x-y edges of the plate in which horizontal and vertical strains are 15% and 30% respectively. After generating the experimental data, the self-learning procedure is carried out by running two finite element models, FE-A and FE-B. Figure (5-18) shows the square plate under the tensile strains. The self-learning process was initially started with a linear elastic model (Young's modulus of 250 Pa and Poisson's ratio of 0.33). The same procedure as presented in the previous application (including the way that EPR model was trained, the contributing variables and the training strategy) is used here.

* Unit: displacement (U2) in m

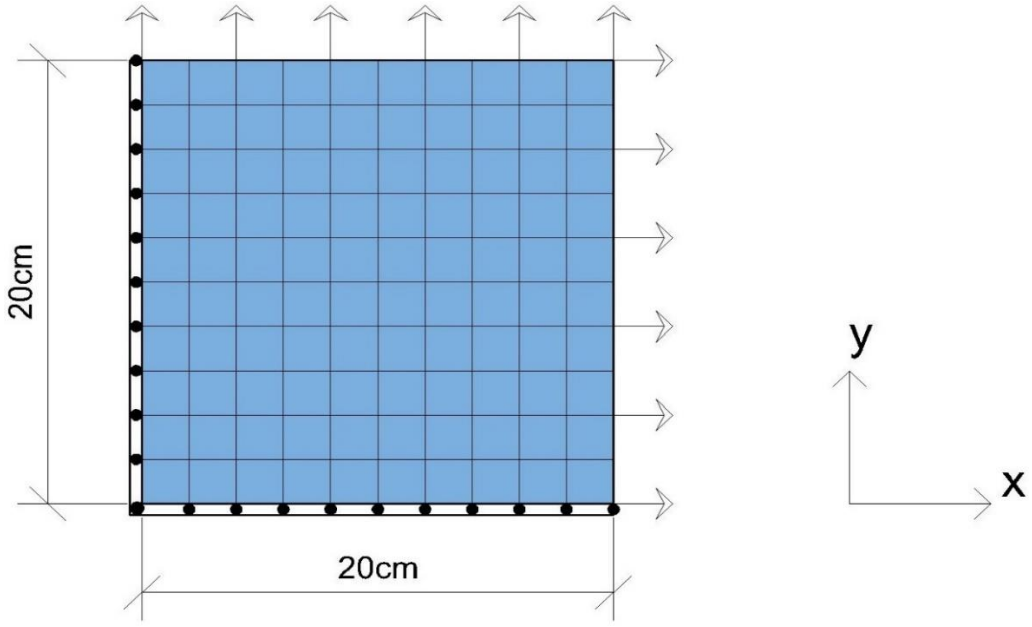

Figure 5-18: Geometry, loading, mesh and boundary conditions of the plate.

In the EPR setting, the maximum number of terms is set to 10 and the range of exponents is [0 1 2 3 4 5]. After training, in each run, three EPR models with the highest values of *CoD* are chosen and the Jacobian matrix is calculated from the partial derivatives of these models. The final EPR models used in the analysis have *CoD* = 99.26%, 99.27% and 99.72% for the vertical, horizontal and shear stresses respectively. These models are: *

$$\begin{aligned}\sigma_x = {} & 164.4\,\varepsilon_y - 2522.5\,\varepsilon_y^2 + 1465.7\,\varepsilon_y^3 - 37436\,\varepsilon_y^4 + 35049\,\varepsilon_y^5 \\ & + 420\,\varepsilon_x - 5559\,\varepsilon_x^2 + 40256.7\,\varepsilon_x^3 - 135049\,\varepsilon_x^4 \\ & + 183206\,\varepsilon_x^5\end{aligned} \tag{5-20}$$

$$\begin{aligned}\sigma_y = {} & 427\,\varepsilon_y - 4090\,\varepsilon_y^2 + 20340\,\varepsilon_y^3 - 47058\,\varepsilon_y^4 + 40366\,\varepsilon_y^5 + 183\,\varepsilon_x \\ & - 4596\,\varepsilon_x^2 + 41475\,\varepsilon_x^3 - 163422\,\varepsilon_x^4 + 426439\,\varepsilon_x^5\end{aligned} \tag{5-21}$$

$$\begin{aligned}\tau_{xy} = {} & 245\,\gamma_{xy} - 30433\,\gamma_{xy}^3 - 1308.6\,\varepsilon_y\gamma_{xy} + 150378\,\varepsilon_y\gamma_{xy}^3 \\ & - 465\times10^5\,\varepsilon_y^3\,\gamma_{xy}^5 - 9575\,\varepsilon_y^4\,\gamma_{xy} - 1069\,\varepsilon_x\gamma_{xy} \\ & + 9979\,\varepsilon_x\varepsilon_y\gamma_{xy} - 27\times10^5\,\varepsilon_y^2\,\gamma_{xy}^3 \\ & + 23\times10^8\,\varepsilon_x\,\varepsilon_y^4\,\gamma_{xy}^5\end{aligned} \tag{5-22}$$

* Unit: Stresses in N/m^2

The above EPR models are generated within the self-learning framework in one pass. This is because sufficient amount of data is generated. The results of this analysis show that EPR-based self-learning model is able to capture the elastic and plastic parts of the material response with reasonable accuracy. Figures (5-19) and (5-20) show the convergence between the FE-A and FE-B models for the horizontal stress-horizontal strain and vertical stress-vertical strain curves respectively. It can be seen that the developed EPR model is able to present a good match between the analyses. To verify the ability of the proposed EPR model, the results of stress-strain curves in the x and y directions are presented for the original model and the EPR models applied on FE-A and FE-B. Figures (5-21) to (5-24) illustrate the comparison between their predictions. The EPR model shows very good agreement with the actual data in both axes using the developed EPR model.

It should be mentioned that the EPR model is a polynomial function that may have some limitations when the experimental data are in the form of straight lines as in this application. Also, in reality the elastic-plastic material behaviour usually introduces some curvature at yield point which appears in the EPR model predictions. Therefore, it can be claimed that using EPR based modelling, is able to reflect the real material behaviour under certain conditions.

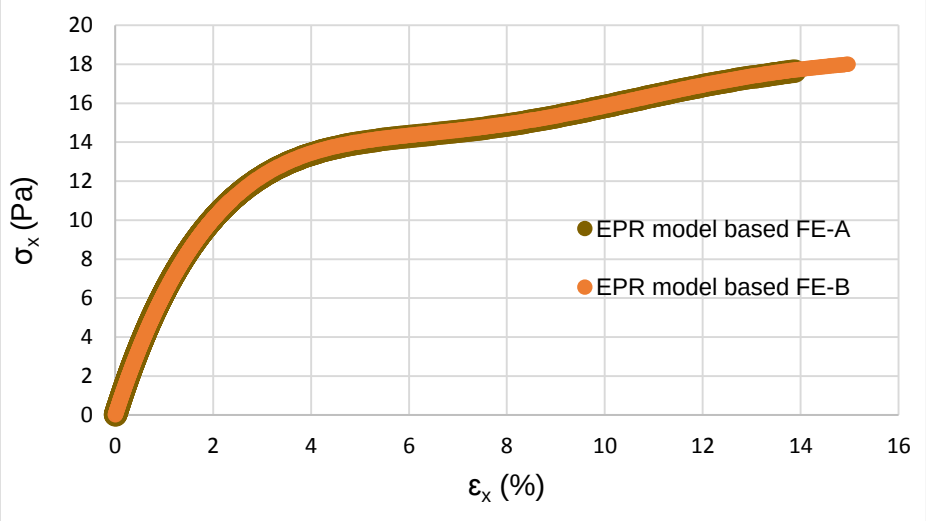

Figure 5-19: Convergence of FE-A and FE-B based self-learning simulation for horizontal stress-strain relation.

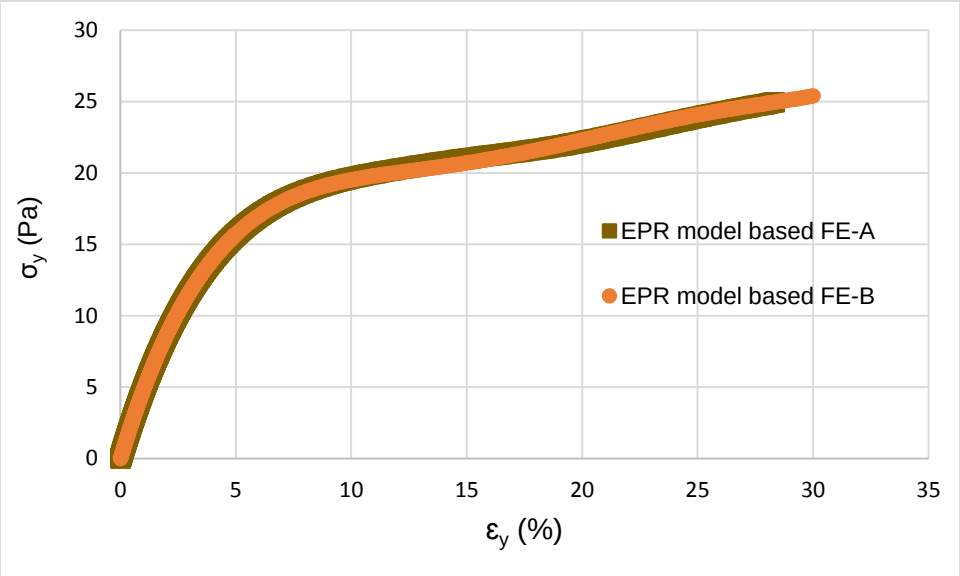

Figure 5-20: Convergence of FE-A and FE-B based self-learning simulation for vertical stress-strain relation.

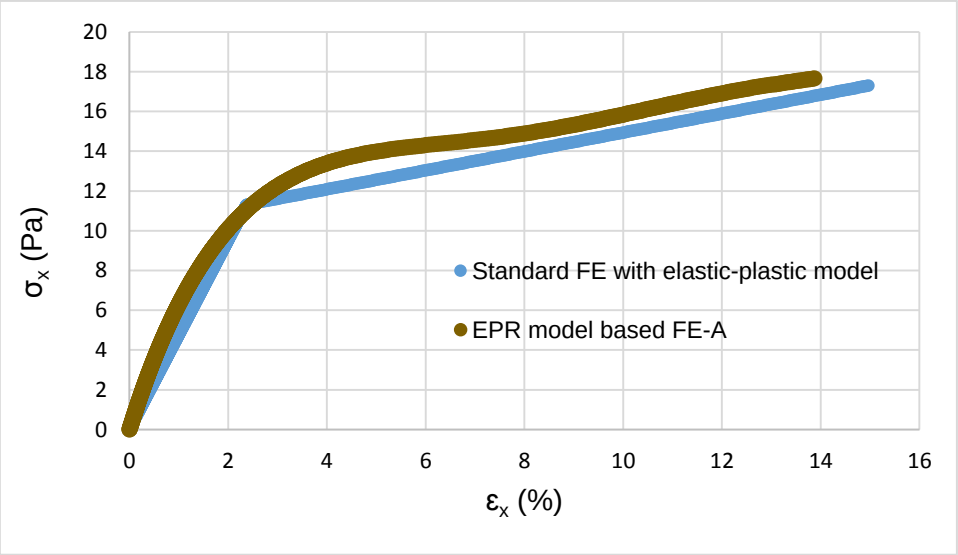

Figure 5-21: Result of the horizontal stress-strain curve showing the comparison between the actual elastic-plastic model and the EPR based self-learning model applied in FE-A.

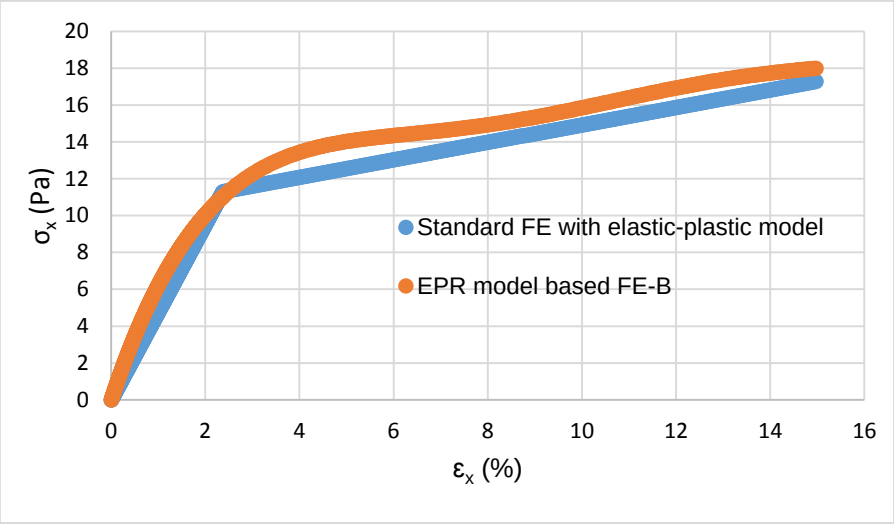

Figure 5-22: Result of the horizontal stress-strain curve showing the comparison between the actual elastic-plastic model and the EPR based self-learning model applied in FE-B.

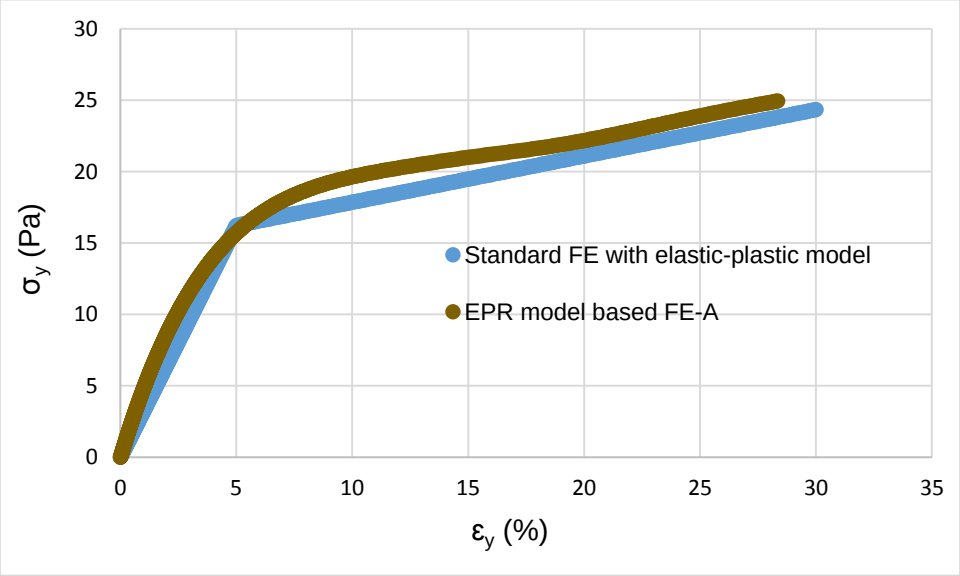

Figure 5-23: Result of the vertical stress-strain curve showing the comparison between the actual elastic-plastic model and the EPR based self-learning model applied in FE-A.

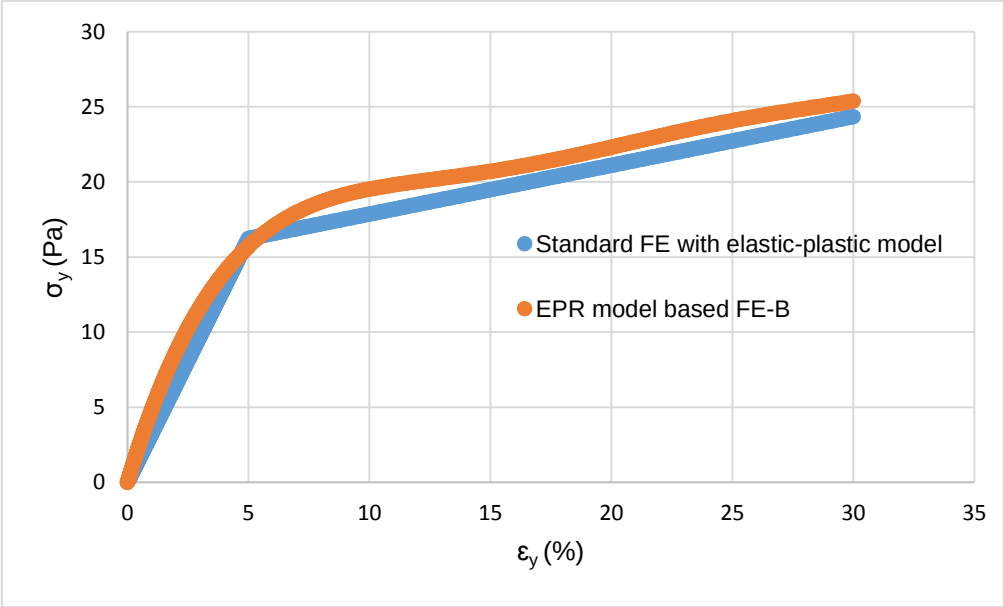

Figure 5-24*:* Result of the vertical stress-strain curve showing the comparison between the actual elastic-plastic model and the EPR based self-learning model applied in FE-B.

5.3 Summary

Self-learning finite element method is a new approach that can link between field measurements and numerical analysis. This field in particular needs significant improvement and development. Training EPR with experimental data is not the ultimate goal of using EPR in constitutive modelling. Improving the way that EPR is trained and is implemented in FE codes would encourage researchers to use EPR in the constitutive modelling of different engineering materials and in numerical modelling of various boundary value problems. The proposed methodology has been developed as a full framework, coded in MATLAB environment. In the EPR-based self-learning approach, the real behaviour of material is approximated by the EPR-based constitutive models. This provides a unified approach to constitutive modelling that can be used in the analyse of different boundary value problems. The efficiency and capabilities of the proposed approach have been illustrated by application to a number of structural engineering applications. The EPR based self-learning procedure has been applied to a range of material behaviour, including linear elastic, nonlinear elastic and elastic plastic behaviour.

The synthetic data generated using these models were considered as experimental data and were used in the self-learning simulations. This was to verify that the developed model is working correctly by comparing the results with those of the conventional models. The results revealed that the methodology can be effectively used as an alternative approach to train the EPR-base models. The developed EPR-based constitutive models were successfully applied to analyse a number of basic structures. The comparison between EPR models and the actual material models was presented to verify the ability of EPR in constitutive modelling. The total stress-strain strategy was utilised to train the EPR models within the framework of self-learning simulation in all the applications.

The developed automation process simplifies the way that EPR is trained, significantly reducing the time required for training and implementation of EPR in finite element code.

CHAPTER 6

Geotechnical Applications Based on EPR Material Modelling

6.1 Introduction

Modelling of behaviour of some materials such as soils and rocks is a challenging due to their erratic and complex nature. In recent decades, with the advancements in computer hardware and software, numerical modelling has progressed rapidly. Some researchers have introduced the use of data mining techniques for constitutive modelling of materials (including soils and rocks) under different loading conditions. ANNs offer great potential for representation of complex material behaviour, however, it is also well known that ANNs have some shortcomings.

As mentioned in Chapter 4, EPR based material modelling was introduced as an alternative algorithm to represent the complex behaviour of soils including saturated and unsaturated soil states. EPR has several features that enable it to be used in modelling of such complex materials. For example, its learning capability, ability to generalise the behaviour, learning directly from raw data without any assumption and more importantly one of the key advantages of EPR it generates explicit and transparent equations/models that can be easily understood and implemented in numerical analysis (e.g., FEA) by the users. Through a wide range of engineering applications, EPR-based constitutive modelling has proven to be a robust tool that can be utilised as a unified framework to represent the material response under different loading conditions.

Furthermore, as discussed in Chapter 5, EPR-based Self-Sim approach has been introduced that uses EPR as an alternative data mining technique in the

heart of the self-learning framework. This methodology improves the way EPR is trained, provides the required data and offers the possibility to be used in simulation of different engineering problems. In Chapter 5, a number of structural applications were analysed using the developed methodology. It was shown that the methodology has the ability to construct constitutive models representing different material behaviour. In this chapter, the use of EPR based constitutive modelling is presented for two geotechnical applications: (1) modelling of the behaviour of a very challenging material (frozen soil), and (2) analysis of the stress-strain behaviour of a clay soil in triaxial experiments using laboratory test data from literature. The incremental stress-strain strategy is used to train the EPR in both geotechnical applications. The selection of an appropriate procedure for training EPR models depends on several factors such as the source of data and the way the data are used to train EPR. The incremental strategy is more appropriate for modelling materials that are path dependent such as soils and rocks. The results of both applications are presented and compared with the actual data to verify the ability of EPR in material modelling.

6.2 Frozen soil

Artificial ground freezing (AGF) has been frequently used in underground engineering. It has no effects on the volume change of ground, adjacent buildings, groundwater, surrounding soil and environment (Chamberlain, 1981). Accurate determination of the shearing behaviour of frozen soils under different conditions and stress paths plays an important role in the geotechnical construction projects such as open excavations, underground subway stations and tunnels. Improper determination of the behaviour of frozen soils could have disastrous consequences as it could lead to underestimation of the allowable shear strength under loading conditions of a particular application. In AGF, artificial withdrawal of heat temporarily freezes the in-situ soil which leads to stabilization of the soil mass such that the closed frozen bodies are watertight (Ziegler et al. 2013). One of the main advantages of AGF is that frozen bodies can be produced in all soil conditions such as heterogeneous, soft and loose soils. AGF is an eco-friendly method, because during implementation, there is no environmental impact on the soil and groundwater (Esmaeili-Falak, 2017; Harris,

1995). It should be noted that AGF in geotechnical engineering should not be mistaken for natural earth freezing or permafrost freeze-thaw cycles (Wang et al. 2016). AGF is the deliberate freezing of pore water of soil which leads to increase in shear strength and reduction in permeability. The mechanical behaviour of unfrozen soils has been extensively investigated by many researchers, however, there has been limited research on the behaviour of frozen soils. Frozen soils exhibit higher strength under loading compared with unfrozen soils (Czurda, K. A., & Hohmann, 1997). They also show similarity with ice behaviour in terms of a time dependent creep and their frictional properties like unfrozen phase (Ma and Chang, 2002).

Frozen soil can be considered as a complex multiphase material consisting of soil particles, frozen water, unfrozen water and air (Lackner et al., 2005). Over the last few years, with the rapid development in the equipment and theoretical implementation of thermomechanical procedures, several attempts have been made to develop constitutive and numerical models for frozen soils based on experimental results. These models followed the non-linear elastic-plastic theory to represent the approximate mechanical behaviour of frozen soils (Xu et al., 2011; Yang et al., 2010).

Recently, with the developments in the computational field (software and hardware) some researchers (e.g. Jahed Armaghani et al., 2015; Momeni et al., 2014) have emphasized on the use of soft computing techniques such as the Simple Regression Analysis (SRA), Multiple Regression Analysis (MRA) and Artificial Neural Network (ANN) in geotechnical engineering problems. Data-driven models provide reasonable, quick and rigorous tools for solving wide range of engineering problems, in particular when the relations between independent and dependent parameters are unknown and complex. Furthermore, from the cost viewpoint, these methods are helpful as direct determination of behaviour of frozen soils in laboratory is costly. To the author’s knowledge, no previous research has been reported on the application of artificial intelligence techniques to describe the constitutive behaviour of frozen soils. However, extensive research has been done on the use of artificial intelligence in modelling the behaviour of unfrozen soils and rocks (A. Ahangar-Asr et al., 2011; Javadi and Rezania, 2009a; Johari et al., 2011; Millar, 2008).

6.2.1 Modelling of frozen soil

6.2.1.1 Data preparation

Triaxial testing can be used to determine the mechanical behaviour of unfrozen and frozen soils. Triaxial equipment is widely used by geotechnical researchers to investigate the shear behaviour of various types of soils. In this application the triaxial data collected from literature (Esmaeili-falak et al., 2017) is utilised to model the stress-strain behaviour of frozen soil using EPR. Esmaeili-falak et al., (2017) conducted a comprehensive program of tests using a triaxial compression apparatus, made specifically for frozen soils under special conditions and using standard procedures according to ASTM D4083. The particle size distribution curve of the soil used in the tests is shown in Figure (6-1). The soil can be classified as poorly graded sand (SP). The physical properties of the soil are presented in Table (6-1) (Esmaeili-falak et al., 2017).

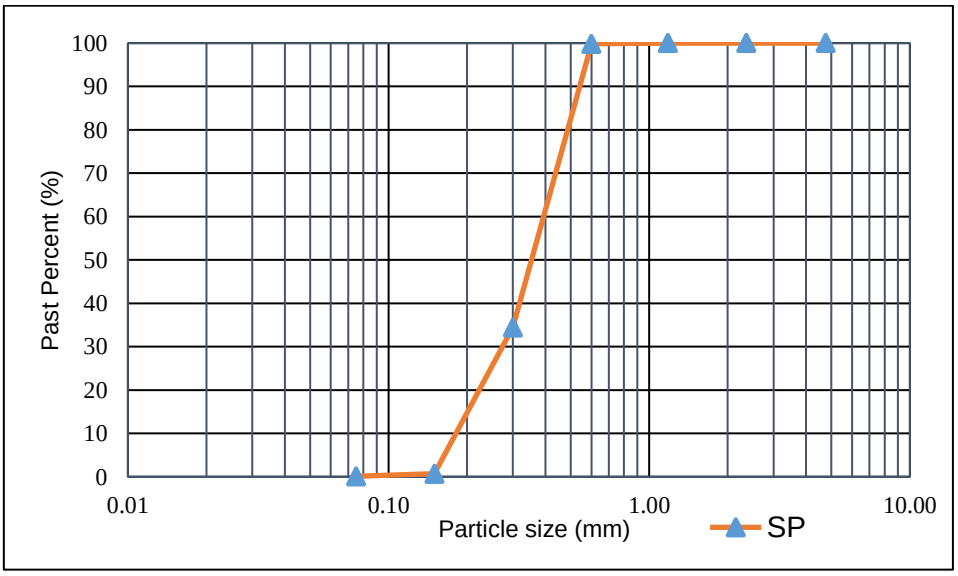

Figure 6-1: Particle size distribution of frozen soil.

Table 6-1: Physical properties of SP soil.

Soil classification	SP
Saturated density (Mg/m^3)	1.98
Angle of friction (degree)	33
Specific gravity (Gs)	2.635
Gravel (%)	0
Sand (%)	98.8
Clay and silt (%)	1.2
Coefficient of uniformity (Cu)	2.17
Coefficient of curvature (Cc)	1.04

The experimental data from a comprehensive set of triaxial tests on samples of the frozen soil are used to train an EPR-based model to predict the stress-strain behaviour of the soil. The tests were performed on samples of a sand compacted in the laboratory under different confining pressures, temperatures and strain rates. The testing program included unconsolidated undrained (UU) triaxial tests where the axial strain was applied increasingly to shear the sample under constant confining pressure. In the experiments, the samples were tested at temperatures ranging between -0.5 ^{o}C to -11 ^{o}C and strain rates between 0.1 %/min to 2 %/min (Esmaeili-falak et al., 2017). The applied confining pressures varied between 0 to 800 kPa.

The dataset is divided into two groups, the first group (80% of the data) is used for training of the EPR model, while the remaining (20% of the) data, which is not used in the training stage, is used to validate the prediction capability of the developed EPR model. In general, if a larger portion of data is used for training, the accuracy of the training will improve. Many researchers have used about 80% of the data for training and 20 % for testing (e.g. Ahangar-Asr et al., 2015; Alangar-Asr; and Javadi, 2011; Rezania; et al., 2008). It is ensured that all parameters in the testing dataset lied between the minimum and maximum values in the training dataset to avoid extrapolation.

The incremental stress-strain strategy is utilised in developing the EPR model. In this strategy, the input and output data are used incrementally in which the input data provide the EPR model with adequate information on the current state of stresses and strains while the output parameter represents the next state of stress corresponding to an input strain increment. The EPR model has six input variables as shown in Table (6-2). The input variables of the model are the temperature, confining pressure, strain rate, current axial strain and current deviator stress, and the models were developed to predict the deviator stress in the soil (model output) related to an increment of axial strain.

The deviator stress and axial strain are updated incrementally through the training and testing stages based on output of the model at the end of each increment.

Table 6-2: The Input and output parameters used for developing the EPR model.

Type	Contributing Parameters	Range
Input	Temperature (T)	-0.5 to -11˚C
	Confining pressure (σ_3)	0 to 800 kPa
	Strain rate ($\dot{\varepsilon}$)	0.1 to 2 %/min
	Axial strain (ε_y)	0 to 10%
	Axial strain increment ($\Delta\varepsilon_y$)	0.1 to 0.4%
	Deviator stress (q)	0 to 12500 kPa
Output	Deviator stress for next increment ($\boldsymbol{q_{i+1}}$)	0 to 12500 kPa

In the EPR settings, the number of terms is set to 15 and the exponents are set to be in the range [0 1 2 3]. These settings are specified following a trial and error process of EPR runs. Before running the EPR, all the datasets are randomly shuffled to ensure that the obtained EPR model is not biased towards a particular part of the training data. To reduce the required time for EPR training, duplicated data are removed.

These steps are implemented through a code written in MATLAB in order to simplify the training and reduce the time required for analysis.

The best EPR model with the highest *CoD* (which is 99.88%) is selected as: *

$$\begin{aligned} \boldsymbol{q_{i+1}} = {} & 1.1053\, q + 154078.5\, \Delta\varepsilon_y - 477650.84\, T\, \Delta\varepsilon_y^2 \\ & - 994036.26\, \sigma_3\, T\, \Delta\varepsilon_y^3 - 27993.26\, \varepsilon_y - 1.449\, \varepsilon_y\, q \\ & + 12415.7\, \dot{\varepsilon}\, \varepsilon_y + 242790.28\, \varepsilon_y^2 - 4446986.22\, \Delta\varepsilon_y\, \dot{\varepsilon}\, \varepsilon_y^2 \\ & - 2784857.5\, \Delta\varepsilon_y\, \dot{\varepsilon}\, T\, \varepsilon_y^2 + 57959.6\, T\, \varepsilon_y^3 \\ & - 0.0817\, \sigma_3\, \dot{\varepsilon}\, q^2\, \Delta\varepsilon_y^3 - 34.09 \end{aligned} \qquad (6\text{-}1)$$

Figure (6-2) shows the deviator stress-axial strain curves predicted using the developed EPR model (equation 6-1) together with the actual experimental data used for the training process. It can be clearly seen that the proposed EPR model is able to extract the behaviour of the frozen soil under different temperatures, strain rates and confining pressures with excellent accuracy.

To verify the generalization capability of the developed EPR model, the experimental results are compared with the EPR model predictions for the unseen (testing) data in Figure (6-3). The results show that the model is able to extend the learning and predict the behaviour of the frozen soil under different temperatures, strain rates and confining pressures with very high accuracy.

*Units: q, σ_3 in KN/m^2, $\dot{\varepsilon}$ in %/min, T in °C

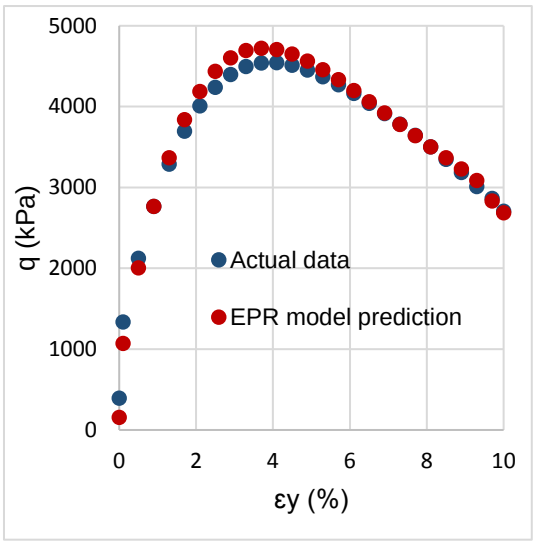

(a)

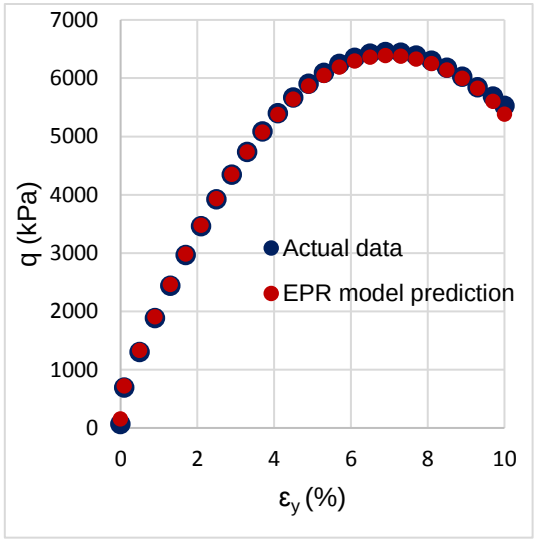

(b)

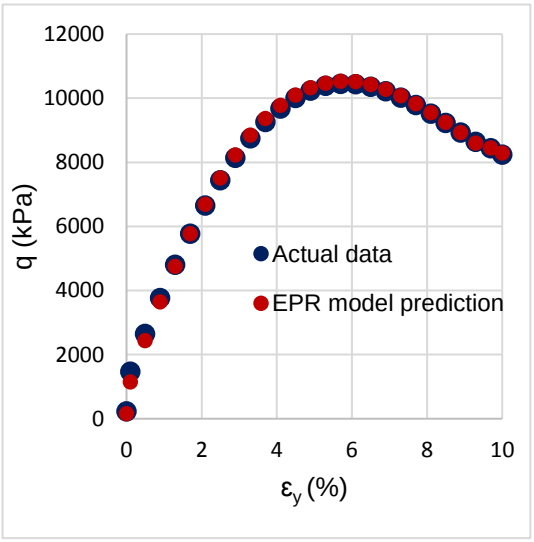

(c)

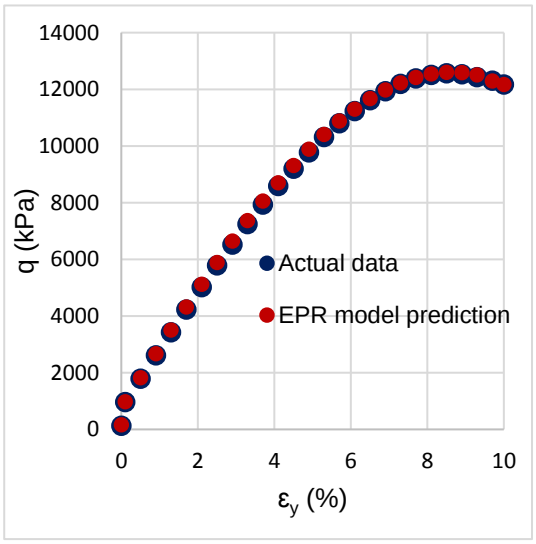

(d)

Figure 6-2: Comparison between the EPR model predictions and the experimental data for different confining pressures, temperatures and strain rates: (a) 100 kPa, -3 °C and 0.2 %/min, (b) 50 kPa, -5 °C and 0.5 %/min, (c) 800 kPa, -5 °C and 1.0 %/min, (d) 200 kPa, -11 °C and 1.0 %/min.

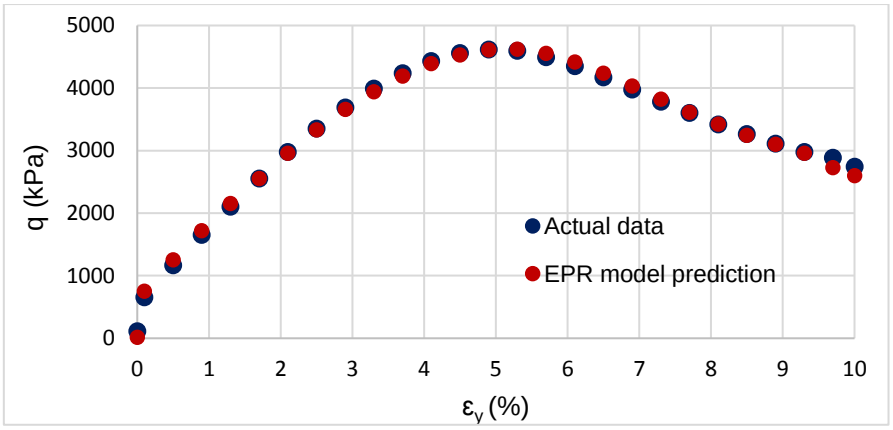

(a)

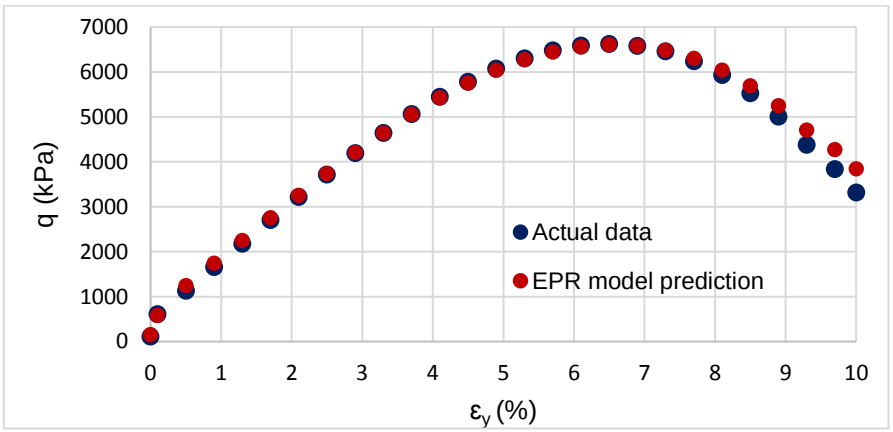

(b)

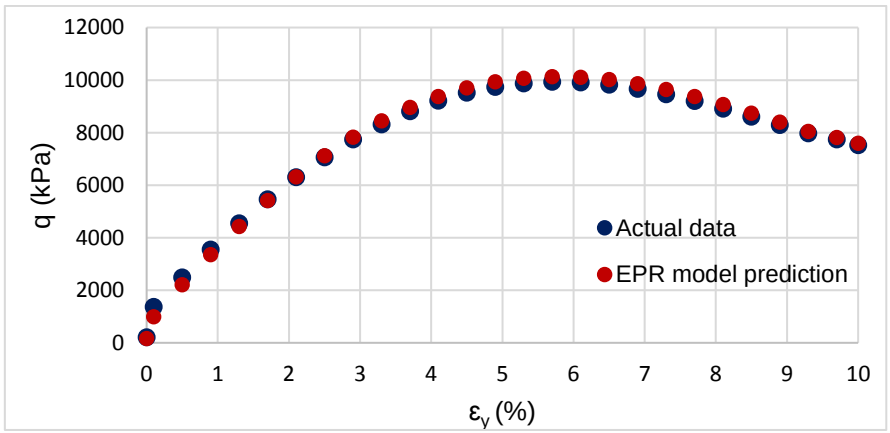

(c)

Figure 6-3: Comparison between the EPR model predictions and the (unseen) experimental data for different confining pressures, temperatures and strain rates: (a) 0 kPa, -5 °C and 0.2 %/min, (b) 100 kPa, -2 °C and 1 %/min, (c) 400 kPa, -5 °C and 1.0 %/min.

6.2.1.2 Predicting the entire stress-strain curve using the EPR model

Further to the model validation described in the previous section, the EPR model is used to predict the entire stress-strain curve in the q: ε_y space incrementally, point by point. The results from various sets of unseen (testing) data are used to measure the ability of the developed model to predict the behaviour of the frozen soil, point by point, through the entire stress-strain curve. For each experiment, the magnitudes of temperature, strain rate and confining pressure are kept constant and the other parameters are updated incrementally based on the axial strain increment.

Figure (6-4) shows the proposed procedure to update the input variables and build the whole stress-strain curve for the shearing stage of a triaxial experiment. Starting the procedure with zero axial strain and zero deviator stress (representing the starting point of the shearing stage) and using a prescribed axial strain increment, the values of the deviator stress q_{i+1} are calculated using the developed EPR model (Ahangar-Asr et al., 2015; Faramarzi et al., 2012). For the next increment, the values of axial strain (ε_y) and deviator stress (q) are updated as:

$$q_i = q_{i+1}$$

$$\varepsilon_{y,i} = \varepsilon_{y,i} + \Delta\varepsilon_y$$

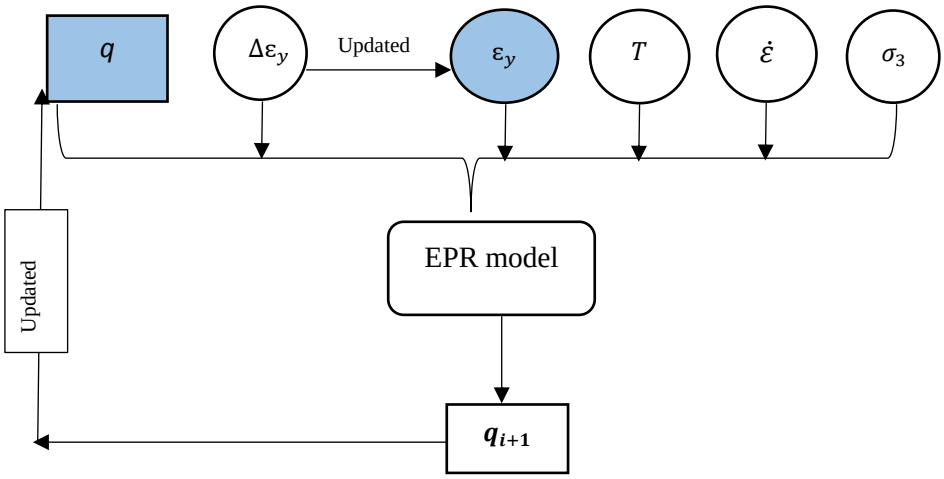

Figure 6-4: Procedure for predicting the entire stress-strain curve.

In this way, the next point on the deviator stress-axial strain curve is predicted. This algorithm is applied until all the points on the curve are predicted. Figure (6-5) shows the comparison between the three stress-strain curves predicted (point by point) by the EPR model and the experimental data. The results show very good agreement with the experimental results. The key point of such EPR model validation is that, while the errors are accumulated at every single point during the predictions, the entire curve is predicted very accurately. This is a strong testament of the robustness of the proposed EPR model in capturing and representing the real behaviour of the frozen soil.

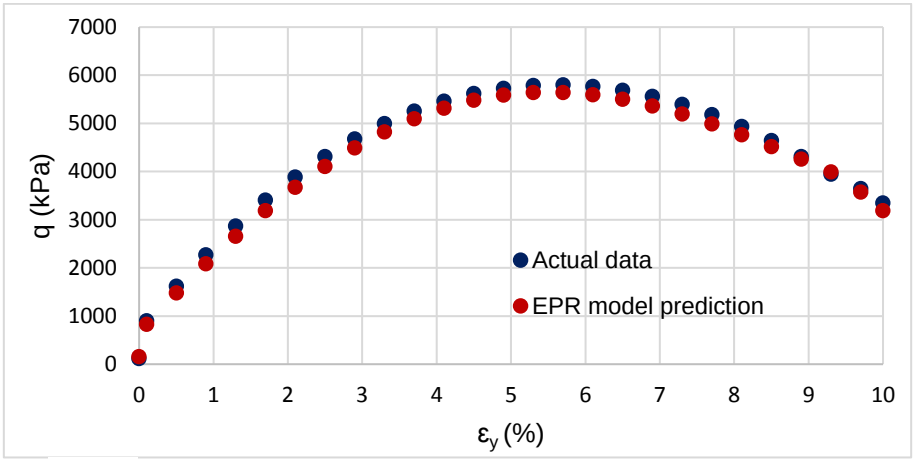

(a)

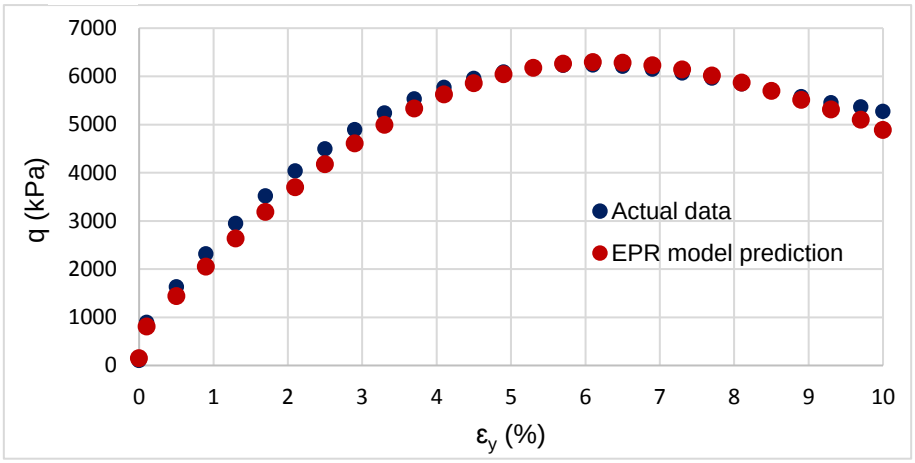

(b)

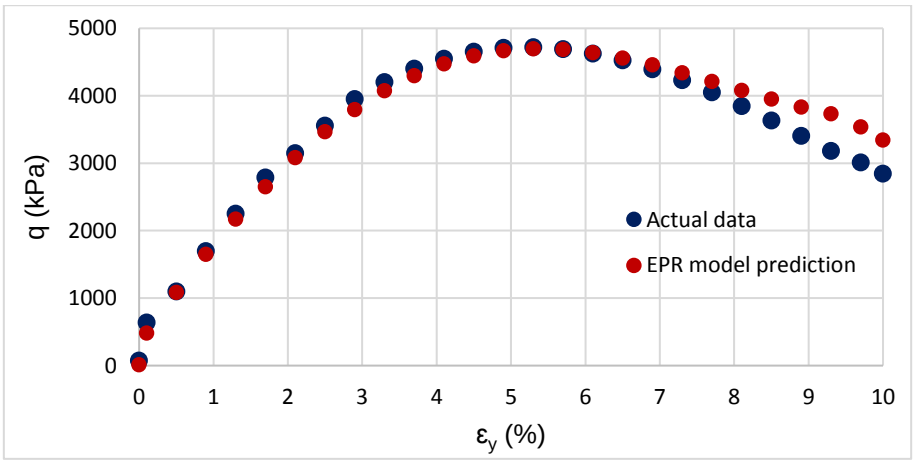

(c)

Figure 6-5: Comparison between the EPR model prediction (point by point) and the experimental data for confining pressures, temperatures and strain rates of (a) 0 kPa, -9 °C and 0.2 %/min, (b) 50 kPa, -4 °C and 0.5 %/min, (c) 200 kPa, -3 °C and 0.2 %/min.

6.2.1.3 Sensitivity analysis

A sensitivity analysis is conducted on the sets of validation (unseen) data. In this analysis, changes are applied to the values of one selected input variable (within its maximum and minimum range) while other input variables are fixed to their mean values. The analysis includes the effects of changes in confining pressure, temperature and strain rate on the deviator stress - axial strain curve. Figures (6-6 to 6-8) show the effect of each input parameter on the soil behaviour. It can be seen that, as expected, decrease in temperature results in increase in the deviator stress. Any increase in the confining pressure or strain rate would cause an increase in the deviator stress. These results are expected and consistent with the trends noticed in the experimental tests. The results of the sensitivity analysis indicate that the EPR model has been able to extract and correctly predict the patterns of mechanical behaviour of the frozen soil.

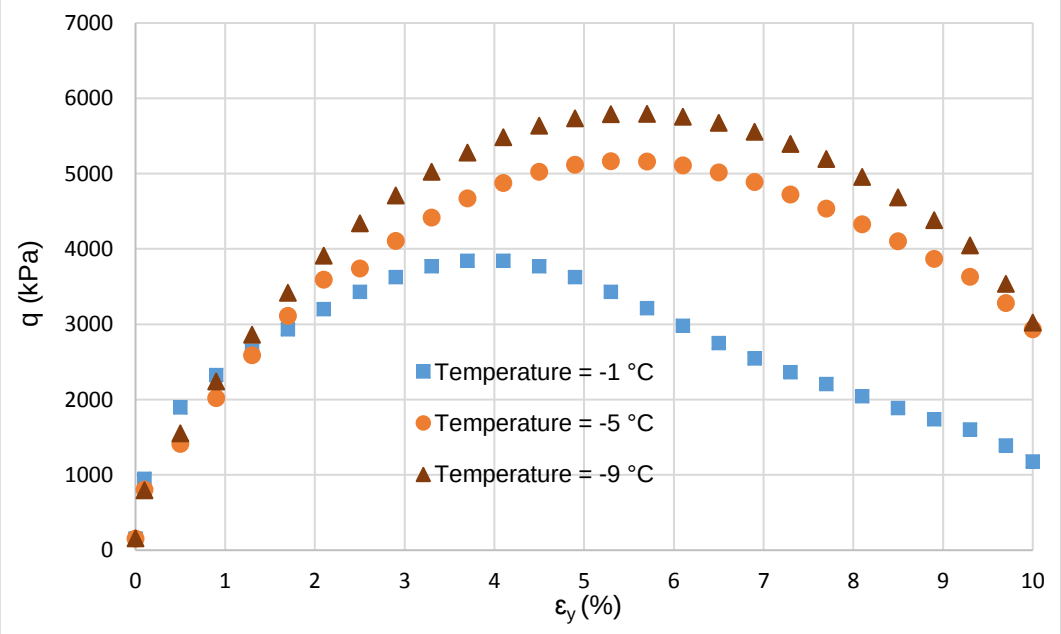

Figure 6-6: Effect of temperature on the behaviour of the frozen soil.

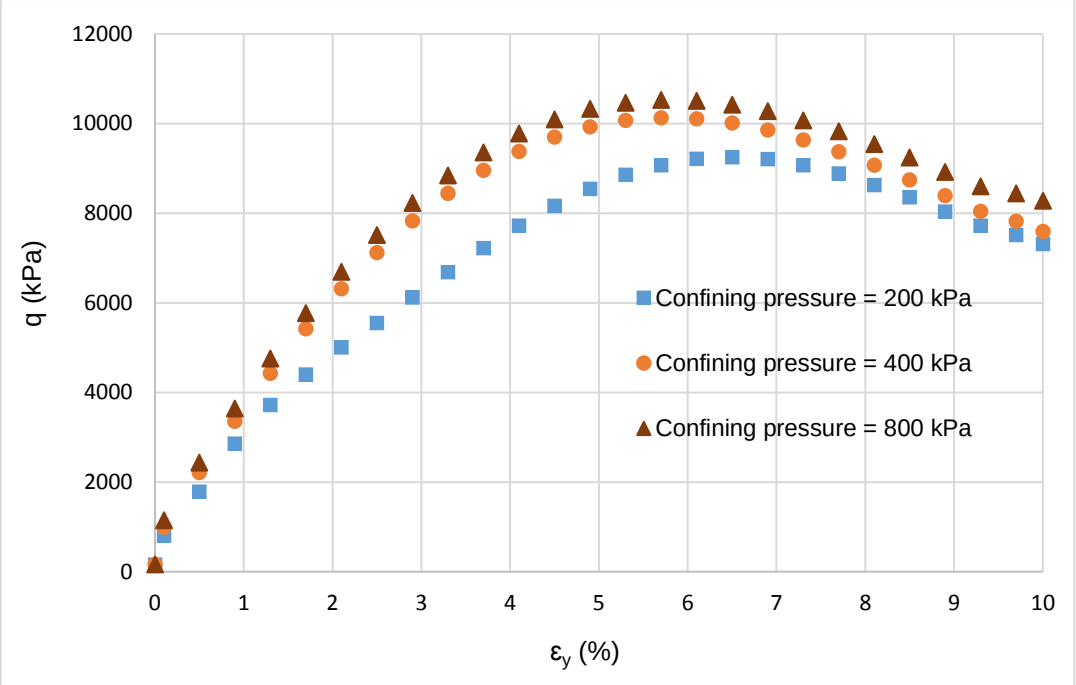

Figure 6-7: Effect of confining pressure on the behaviour of the frozen soil.

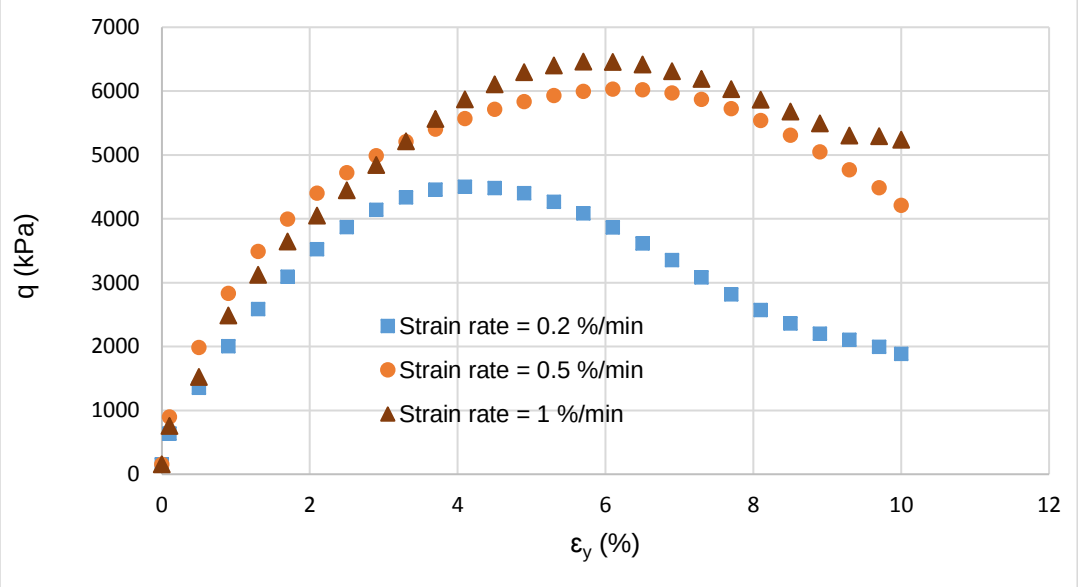

Figure 6-8: Effect of strain rate on the behaviour of the frozen soil.

In this application, a comprehensive set of experimental data from unconsolidated undrained (UU) triaxial tests on a frozen sandy soil are used to develop a model, using evolutionary polynomial regression (EPR), to predict the shear behaviour of a frozen soil.

The model considers the effects of temperature, confining pressure and strain rate on the soil behaviour. The results show the ability of the proposed model in capturing and representing the complex behaviour of frozen soils. Furthermore, predicting the entire stress-strain curve (point by point) is another verification of the capabilities of the developed model. The results of the parametric study show the EPR model is able to extract and predict the effect of each parameter on the entire shear-stress curve of frozen soil.

6.3 Simulation of triaxial experiments using EPR-based self-learning approach

The main target of the EPR based self-learning algorithm is to develop a constitutive model that is trained directly from experimental or field data and is used to predict the behaviour of other structures with the same material under different loading conditions. In this application the behaviour of a clay (kaolin) in triaxial experiments is analysed under consolidated drained (CD) conditions. The experimental data reported in (Cekerevac and Laloui, 2004) are used as the measurement data for the EPR based self-learning algorithm. Figure (6-9) illustrates the two-dimensional axisymmetric finite element simulation of triaxial test in ABAQUS.

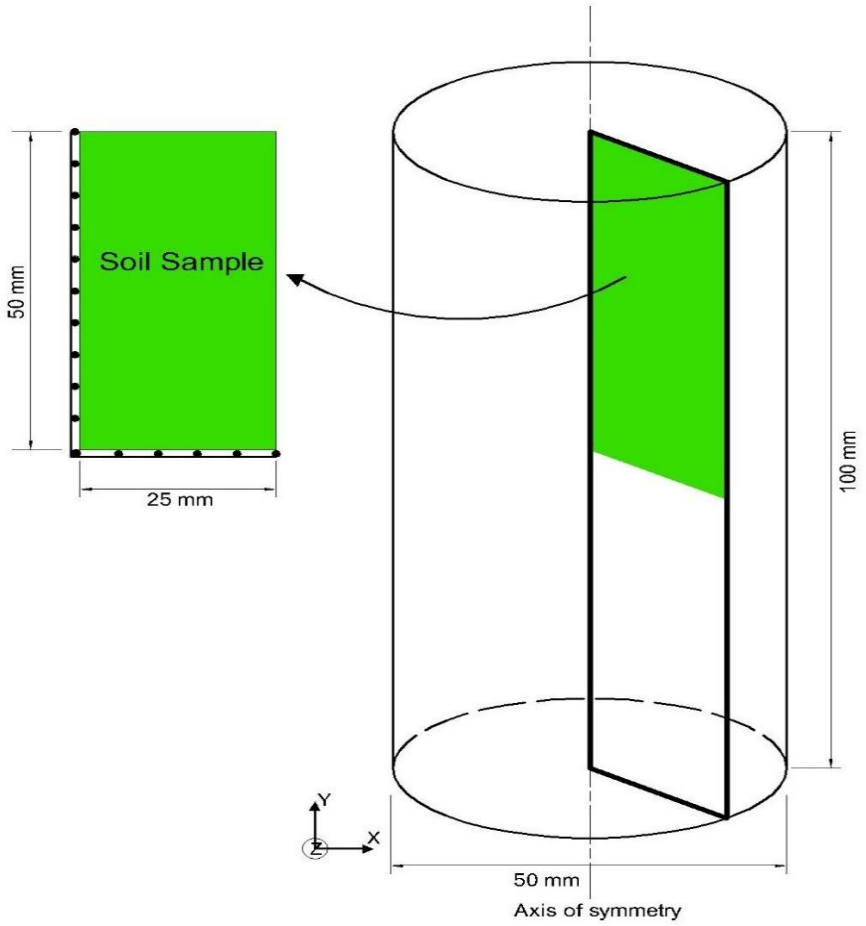

Figure 6-9: Axisymmetric finite element simulation of triaxial test.

The incremental stress-strain strategy is employed in this application in the same way that was presented in the previous application, however, in this case the invariants of stresses and strains are used for training. The general expression of the volumetric and distortional stresses and strains is defined as (Muir Wood, 1990):

$$p' = \frac{\sigma_x' + \sigma_y' + \sigma_z'}{3} \tag{6-2}$$

$$q = \left[\frac{(\sigma_y' - \sigma_z')^2 + (\sigma_z' - \sigma_x')^2 + (\sigma_x' - \sigma_y')^2}{2} + 3(\tau_{yz}^2 + \tau_{zx}^2 + \tau_{xy}^2)\right]^{0.5} \tag{6-3}$$

$$\varepsilon_v = \varepsilon_x + \varepsilon_y + \varepsilon_z \tag{6-4}$$

$$\varepsilon_q = \frac{1}{3}\left\{\left[(\varepsilon_y - \varepsilon_z)^2 + (\varepsilon_z - \varepsilon_x)^2 + (\varepsilon_y - \varepsilon_z)^2 + 3\,(\gamma_{yz}{}^2 - \gamma_{zx}{}^2 + \gamma_{xy}{}^2)^2\right]\right\}^{0.5} \tag{6-5}$$

Generally, the constitutive relationship is given in the form of δσ = Dδε (Owen and Hinton, 1980), where (D) is material stiffness (or Jacobian) matrix. This matrix can be expressed in terms of modulus of elasticity (*E*) and Poisson's ratio (*μ*). For the triaxial tests, the parameters of mean effective stress p'^i, deviator stress q^i, volumetric strain ε_v^i, axial strain ε_y^i and increment of axial strain $\Delta\varepsilon_y^i$ are chosen as input parameters corresponding to the current state of stresses and strains in a load increment i, while deviator stress q^{i+1} corresponding to the input increment of the axial strain $\Delta\varepsilon_y^i$ is used as the output parameter. The triaxial test results on the clay (Cekerevac and Laloui, 2004) presented the shear and volumetric behaviour of the soil samples. For triaxial test conditions, due to the axisymmetric nature of the problem, these stresses and strains can be written as:

$$p' = (\sigma_1' + 2\sigma_3')/3 \tag{6-6}$$

$$q = \sigma_1' - \sigma_3' \tag{6-7}$$

$$\varepsilon_v = \varepsilon_y + 2\varepsilon_r \tag{6-8}$$

$$\varepsilon_y = (\varepsilon_q + \varepsilon_v)/2 \tag{6-9}$$

$$\varepsilon_q = 2(\varepsilon_y + \varepsilon_r)/3 \tag{6-10}$$

where σ_1' and σ_3' are the major and minor principle stresses, and ε_q and ε_r are the deviator and radial strains respectively. In order to build the Jacobian matrix, at each run an EPR-based model with highest *CoD* is chosen and the value of *E* is calculated as:

$$E = \frac{q^{i+1} - q^{i}}{\Delta\varepsilon_y^i} \tag{6-11}$$

while the value of μ is assumed to be 0.3 for simplicity. Six monitoring points are specified on the top of the sample, monitoring the vertical deformations. The EPR based self-learning methodology is applied in which the FE-A and FE-B models were simulated in ABAQUS in parallel.

The soil sample is meshed with 50 eight-node pore fluid/stress axisymmetric quadrilateral elements with biquadratic displacement and bilinear pore pressure. Figure (6-10) shows the FE models with mesh, applied load and boundary conditions for both analyses.

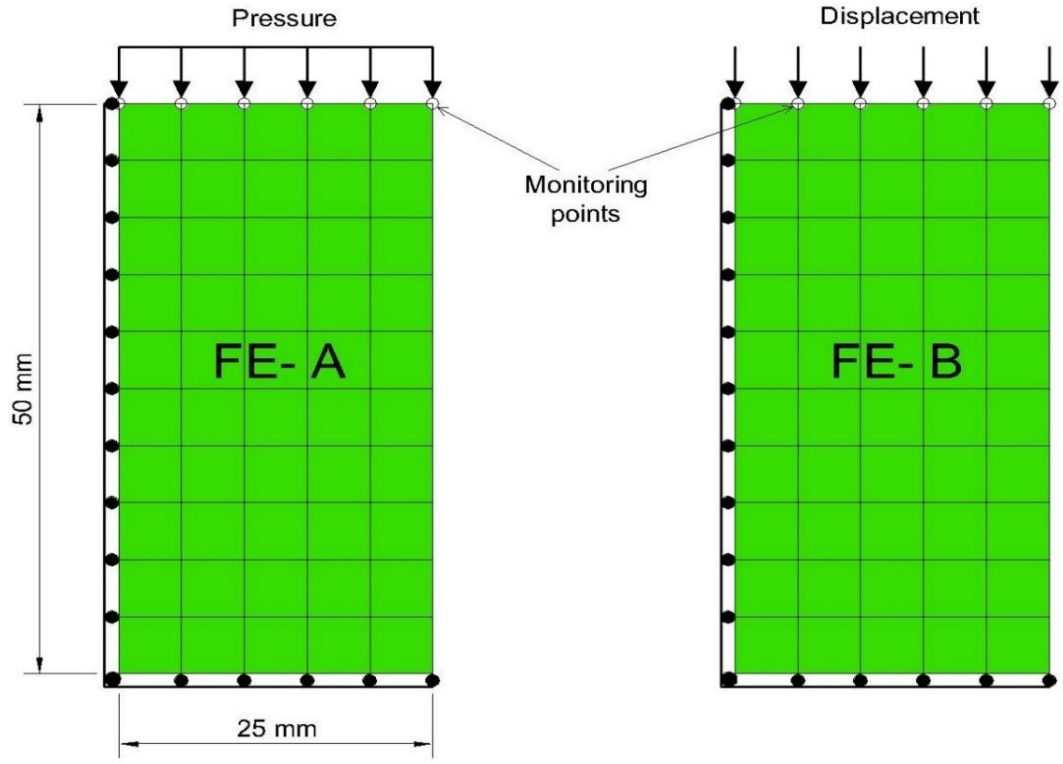

Figure 6-10: Finite element models of triaxial test showing FE-A and FE-B with their mesh, loading and boundary conditions.

Experimental data from 6 triaxial tests conducted at different confining pressures ranging from 100 to 600 kPa are used for training of EPR within the self-learning algorithm. Each confining pressure is applied individually and one EPR based model is developed to represent the soil behaviour for each confining pressure.

The procedure is started by assuming an initial value for Young's modulus *E* for the first run only, which is in the linear portion of the global stress-strain curve. The initial value of *E* is set for all confining pressures to 20 x10^3 kPa and μ is set to 0.3. Once the Jacobian matrix was constructed, it is implemented in ABAQUS via its UMAT. The same procedure as described in the previous chapter is applied for running the EPR based self-learning model. The EPR settings for each confining pressure are specified by a trial and error procedure. For all confining pressures, the exponents are limited to the range [-1 0 1 2 3] and the maximum number of terms is set to 8. The input and output parameters are set as follows:

$$q^{i+1} = F(\varepsilon_v^i, \varepsilon_y^i, \Delta\varepsilon_y^i, q^i, p'^i)$$

Figure (6-11) shows the actual data that are used to extract the pressure-displacement data as the measurement data (applied pressure and corresponding displacement in FE-A and FE-B respectively). In the dataset, for the soils that exhibited softening behaviour, the data after the failure points are removed. Modelling of the softening behaviour introduces additional challenges in training of the EPR (or ANN) models which is outside the scope of the present work. Six EPR models are developed with various *CoD* values and taking different number of cycles of self-learning as summarized in Table (6-3).

Table 6-3: *CoD* values of EPR models with their training process.

Confining pressure (kPa)	*CoD* value of the selected EPR model	No. of cycles of EPR-Self-learning
100	99.92%	One cycle of self-learning
200	99.63%	One cycle of self-learning
300	99.78%	One cycle of self-learning
400	99.86%	Two cycles of self-learning
500	99.27%	Three cycles of self-learning
600	99.86%	Two cycles of self-learning

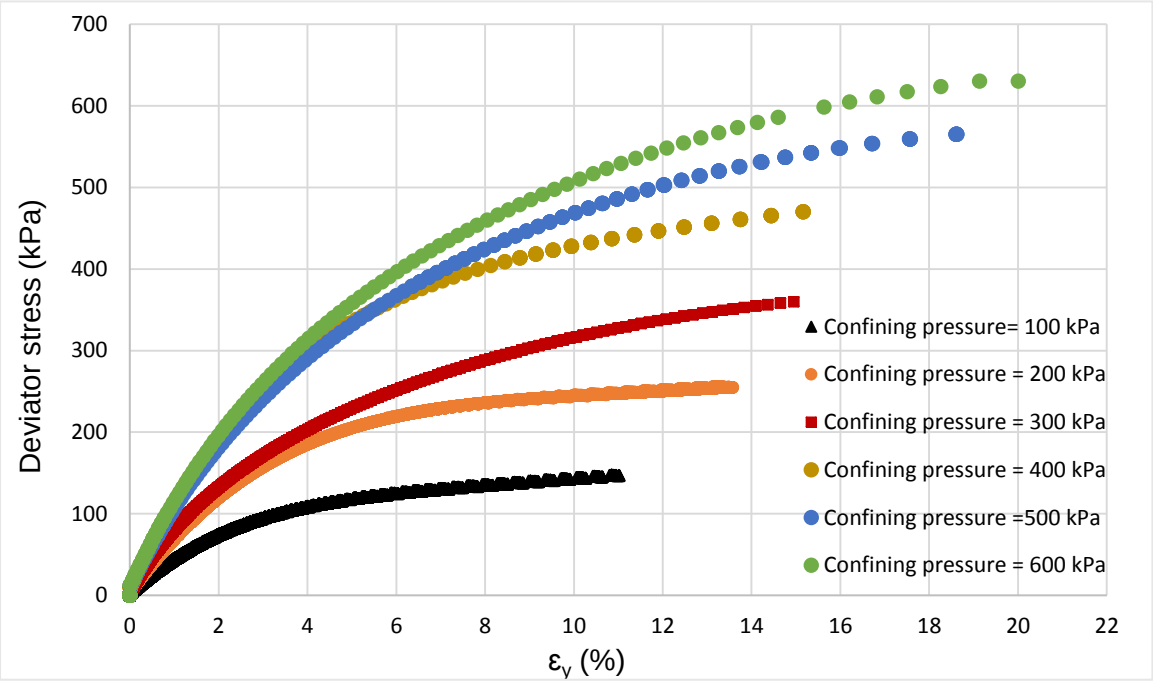

Figure 6-11: Experimental data of triaxial tests on kaolin (after Cekerevac and Laloui, 2004).

The best EPR models (six models) after a single pass of self-learning with different number of cycles for 100 to 600 kPa confinig pressures are as follows:

*

$$q_{100}^{i+1} = 0.96\,q - 72.2\,\varepsilon_y\,(0.24\varepsilon_v + 1)^2 - 0.068\,\,(0.02\,p - 2)^3\,\, + 50\,\Delta\varepsilon_y(0.24\varepsilon_v + 1)^3 + 9.4\,\times 10^{-4}\left(\frac{q\,\varepsilon_y{\varepsilon_v}^3}{6.8 + \Delta\varepsilon_y}\right) + 13.5 \quad (6\text{-}12)$$

$$q_{200}^{i+1} = 1.06\,q - 0.39\,\varepsilon_y\,(0.2\,\varepsilon_v + 1)^2 + 70.5\,\Delta\varepsilon_y\,(0.2\,\varepsilon_v + 1)^3 + 77.4 \times 10^{-11}\,p\varepsilon_v q^3 + 3.9\,\times\,10^{-10}\,p\,q^3 - 15\,\times 10^{-9}\,\varepsilon_v\,q^3 + 0.25\,\times 10^{-6}\,\frac{\varepsilon_y\,(0.2\,\varepsilon_v + 1)^3}{(\Delta\varepsilon_y - 0.28)} \quad (6\text{-}13)$$

$$q_{300}^{i+1} = 102\,\Delta\varepsilon_y + 1.03\,q + 91.11\,(0.18\,\varepsilon_v + 1)^3 - 8\,\times 10^{-3}\,\varepsilon_y\,\Delta\varepsilon_y - \frac{6.5\,\times 10^{-2}\,\Delta\varepsilon_y q^2}{\varepsilon_y} + \frac{(3.4\,\times\,10^{-9}\,q^3 + 0.01\,q(0.18\,\varepsilon_v + 1)^3)}{\Delta\varepsilon_y} - 9.6 \quad (6\text{-}14)$$

$$q_{400}^{i+1} = 1.99\,\varepsilon_v + 5.1q + 175\,\,\Delta\varepsilon_y(0.16\,\varepsilon_v + 1\,)^2 - 0.64\,q\,\varepsilon_v + \frac{1.2 \times 10^{-2}\varepsilon_y}{q\Delta\varepsilon_y} - 345.5\,\Delta\varepsilon_y q\,(0.16\,\varepsilon_v + 1\,)^2 - \frac{1.2 \times 10^{-2}\varepsilon_y\,(6.14 \times 10^{-3}p - 2.58)^2}{q} - 2.9 \times 10^{-2}\Delta\varepsilon_y(6.14 \times 10^{-3}p - 2.58)^2\,(0.16\,\varepsilon_v + 1\,)^3 \quad (6\text{-}15)$$

$$q_{500}^{i+1} = q + 0.38\,\varepsilon_y(5.36\,\times 10^{-3}p - 2.68)^2 + \frac{3.2 \times 10^{-9}q}{\Delta\varepsilon_y} + \,\Delta\varepsilon_y(5.36\,\times 10^{-3}p - 2.68)^2(4.9\varepsilon_v + 364) + 180\Delta\varepsilon_y(0.135\varepsilon_v + 1)^3 - 1.3 \times 10^{-2}\varepsilon_y\frac{(5.36\,\times 10^{-3}p - 2.68)^2}{\Delta\varepsilon_y} - 2.6 \quad (6\text{-}16)$$

*Units: q, p in KN/m^2

*

$$q_{600}^{i+1} = 180\,\Delta\varepsilon_y\,(0.13\varepsilon_v + 1)^3 - 153\,(0.13\varepsilon_v + 1)^3 - 1190\,\Delta\varepsilon_y\,(0.13\varepsilon_v + 1)^3(4.8\,10^{-3}\,p - 2.88)^2 - 6.4\,\times 10^{-9}\varepsilon_y^2\,q^3 + \left(\frac{0.142\,p - 8.22}{\Delta\varepsilon_y}\right) + 0.233\,q^2 + 1.002\,q - 86.21\,\varepsilon_v + 3862.44 \quad (6\text{-}17)$$

The analysis results are presented in terms of the convergence criterion in which FE-A and FE-B are approximatly matched after different cycles of self-learning (see Figure 6 -12). For confining pressures 100, 200 and 300 kPa, convergence was achived only after the first cycle of one pass of the EPR based self-learning algorithm and there is a good match between the model predictions in both analyses. For the confining pressures 400, 500 and 600 kPa, convergence was achived after two, three and two cycles of one pass of EPR based self-learning respectively (Figure 6-13).The difference between the different confining pressures could be related to the training data, especially within the plastic region.

Figures (6-14 to 6-16) show comparison between the stress-strain relationships predicted using the EPR-based self-learning models and the actual data for the all confining pressures.

It can be noted that during the self-learning cycles, the performance of the EPR based models improved significantly. This is because during cycles much more data were generated which improved the accuracy of training and predictions of the EPR models.The results show that EPR has been able to learn and predict the material behaviour under different conditions with very good accuracy. Figure (6-17) shows the results of stress paths (relationship between mean effective stress and deviator stress) of the developed EPR based models and the actual data, showing excellent agreeement.

*Units: q, p in KN/m^2

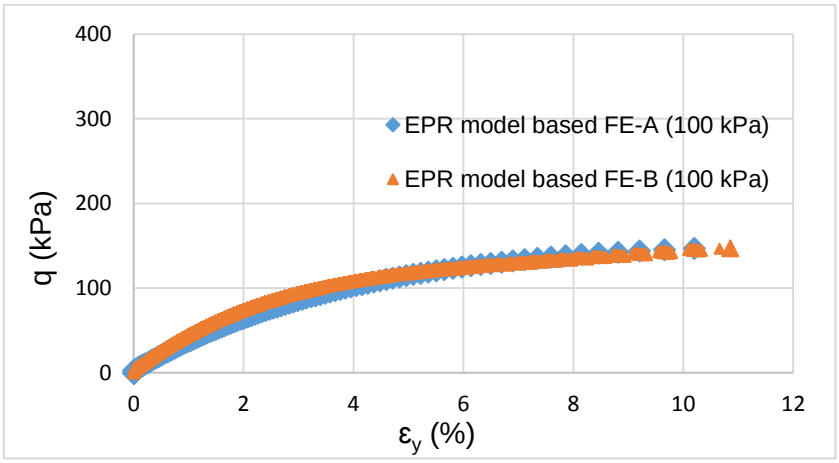

(a)

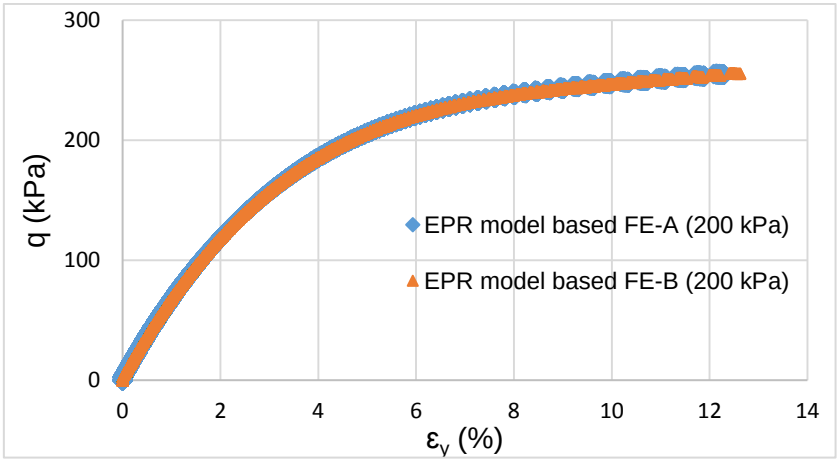

(b)

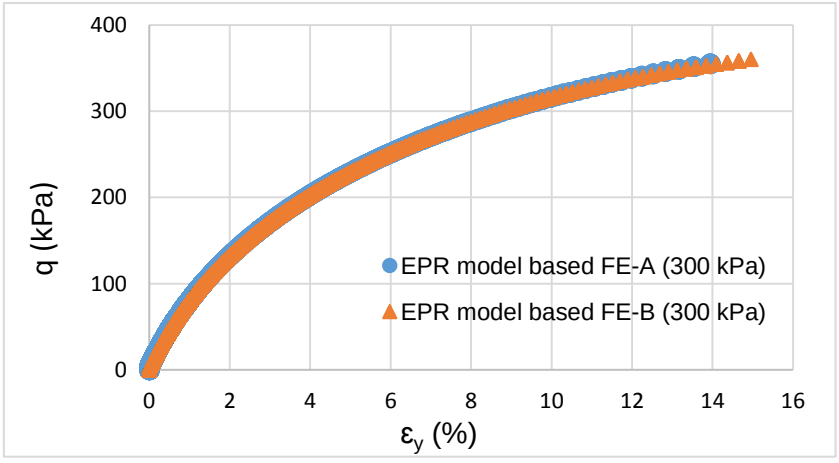

(c)

Figure 6-12: Convergence of FE-A and FE-B models using the developed EPR models for the confining pressures (a) 100 kPa, (b) 200 kPa and (c) 300 kPa.

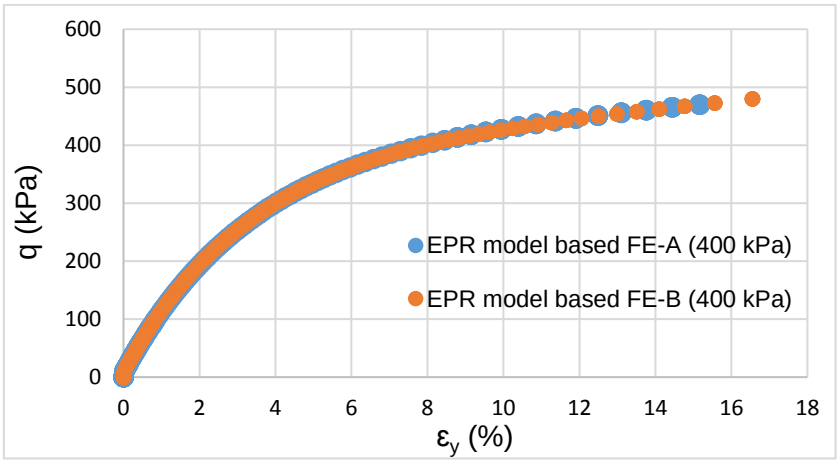

(a)

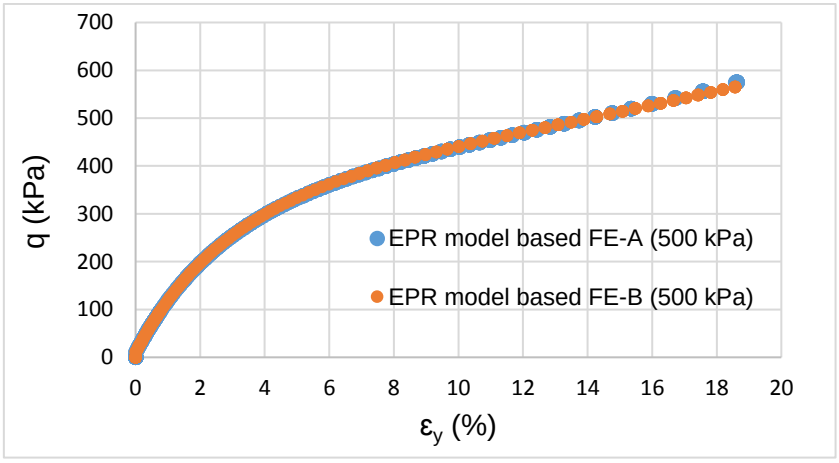

(b)

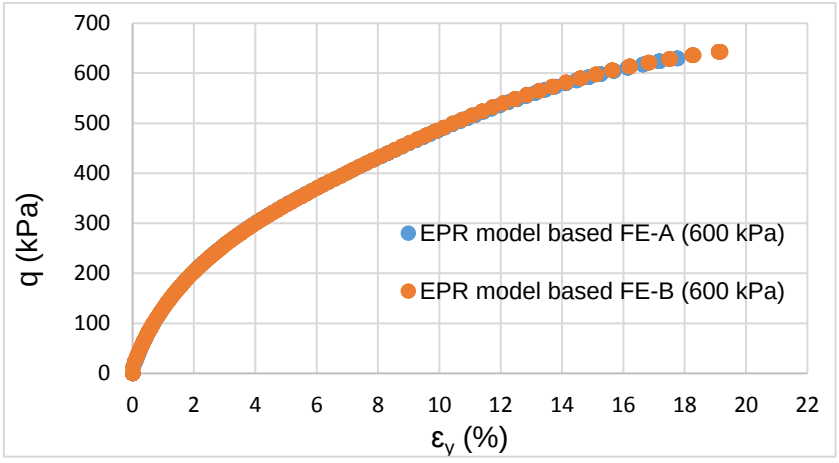

(c)

Figure 6-13: Convergence of FE-A and FE-B models using the developed EPR models for the confining pressures (a) 400 kPa, (b) 500 kPa and (c) 600 kPa.

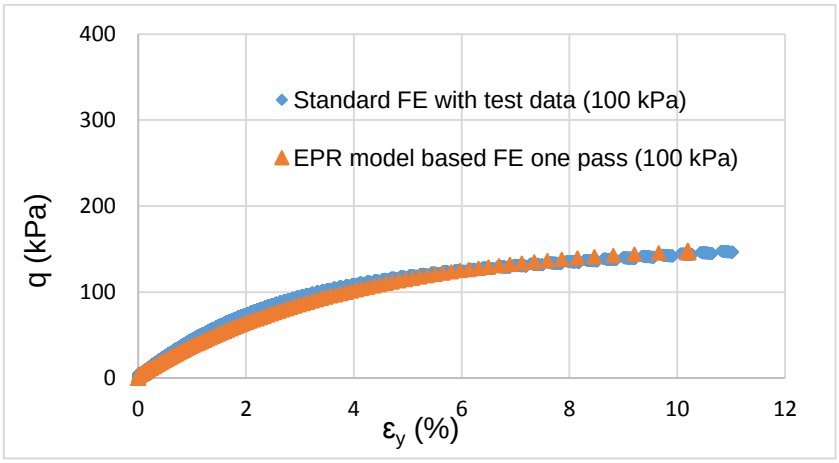

(a)

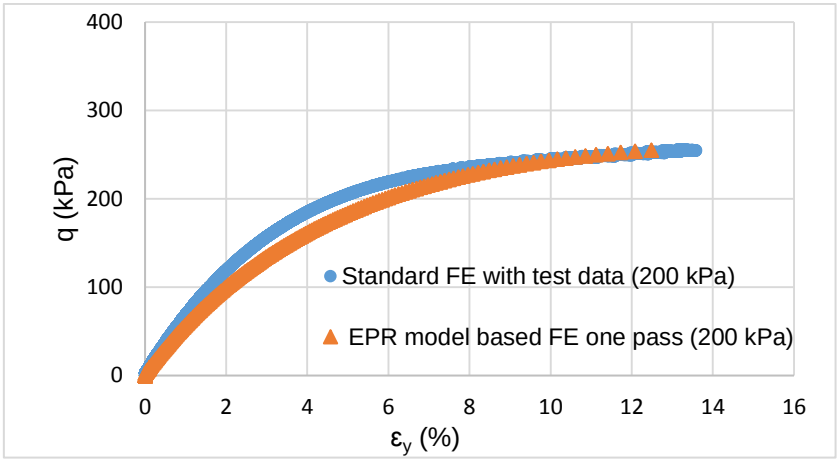

(b)

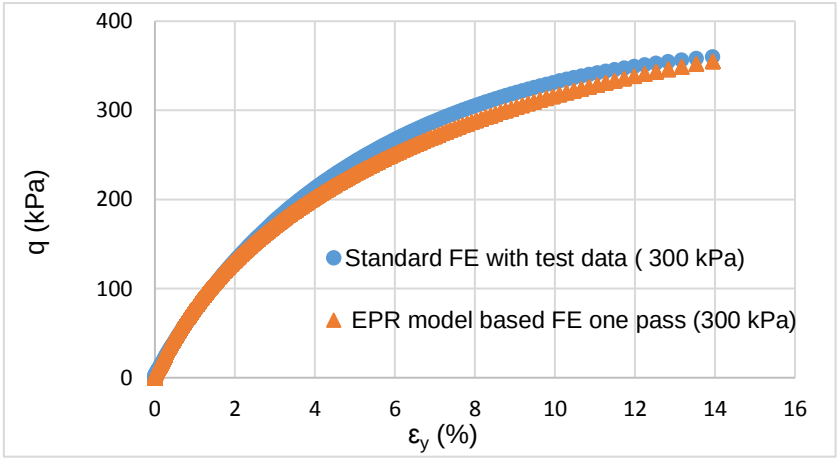

(c)

Figure 6-14: Comparison of stress-strain curves predicted by the developed EPR models and the actual data based FE for confining pressures (a) 100 kPa, (b) 200 kPa and (c) 300 kPa.

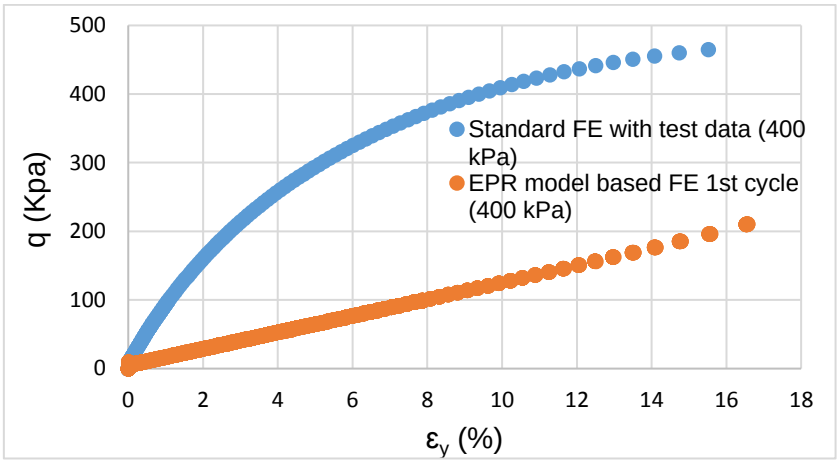

(a)

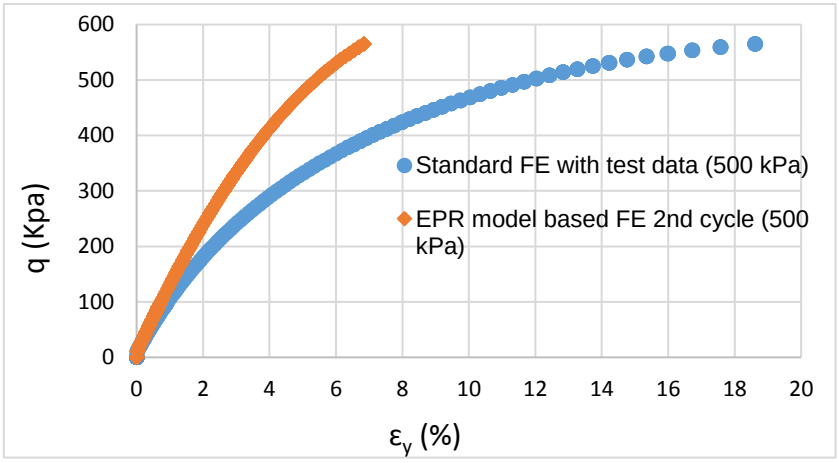

(b)

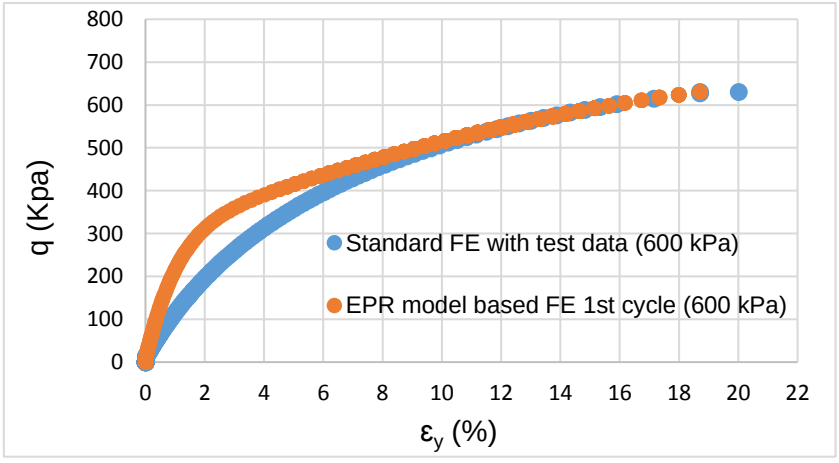

(c)

Figure 6-15: Comparison of stress-strain curves predicted by the developed EPR models and the actual data based FE for confining pressures (a) 400 kPa, (b) 500 kPa and (c) 600 kPa.

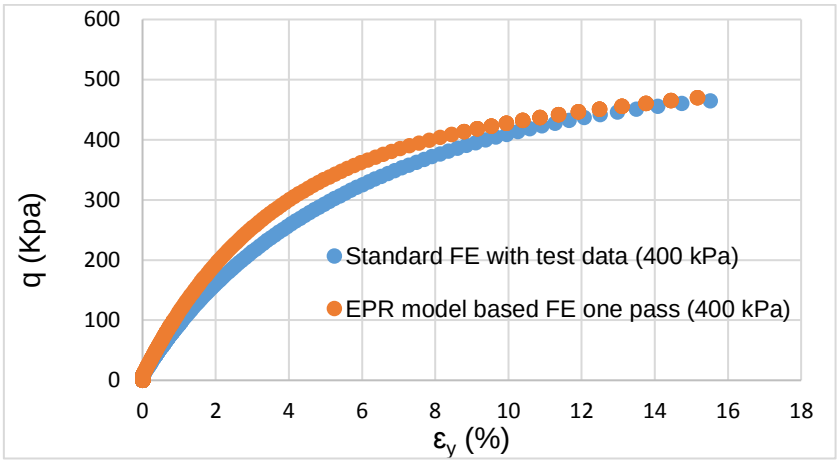

(a)

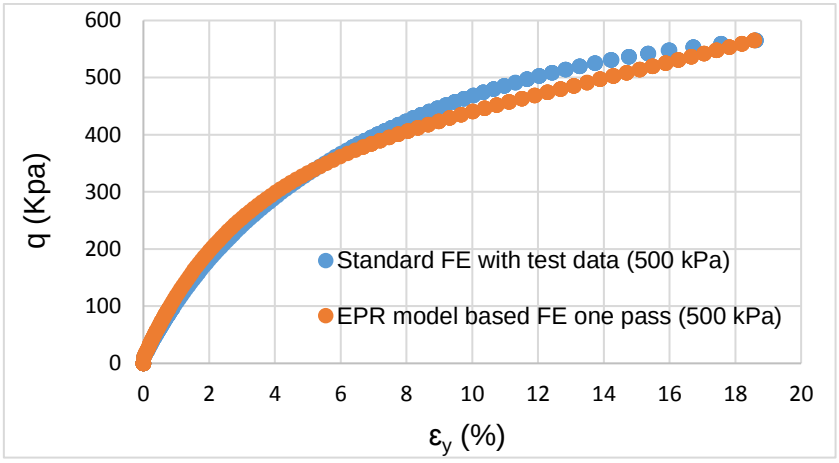

(b)

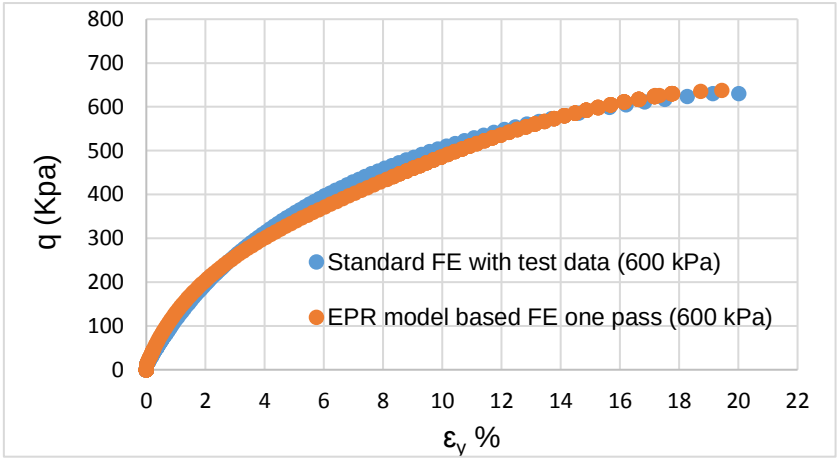

(c)

Figure 6-16: Comparison of stress-strain curves predicted by the developed EPR models based FE after completion of learning and the actual data based FE for confining pressures (a) 400 kPa, (b) 500 kPa and (c) 600 kPa.

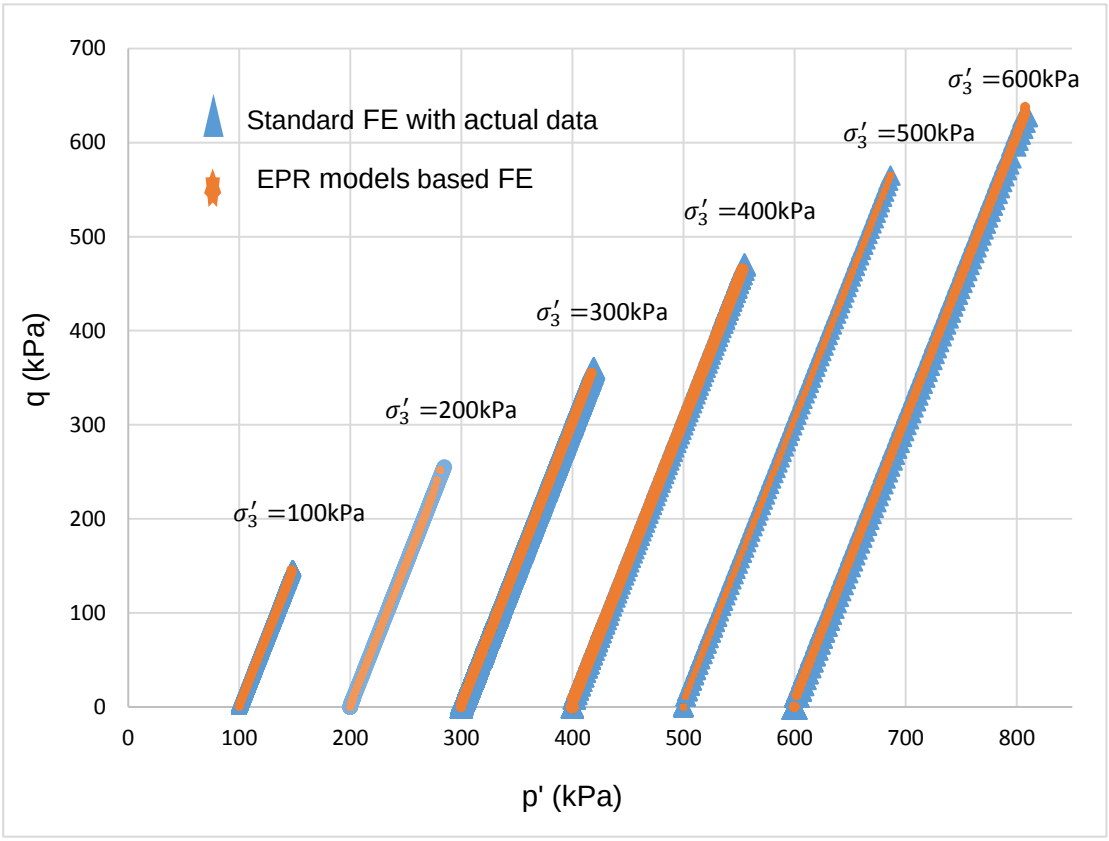

Figure 6-17: Comparison of (p'-q) curves of the developed EPR based self-learning FE models and the actual data.

6.4 Summary

In this chapter modelling of complex geomaterials was introduced using EPR-based material modelling. The conventional approach to represent the mechanical behaviour of frozen soils requires special equipment and environment which could be expensive, time consuming and not available in all scenarios. In addition, the behaviour of such soils is very complex because of the multi-phase nature of the mixture. In the first application, a comprehensive set of experimental data from unconsolidated undrained (UU) triaxial tests on a frozen sandy soil was used to develop a model, using EPR, to predict the shear behaviour of a frozen soil. The model considers the effects of temperature, confining pressure and strain rate on the soil behaviour.

The results showed the ability of the proposed model in capturing and representing the complex behaviour of frozen soils. Furthermore, predicting the entire stress-strain curve (point by point) was presented successfully as another verification of the capabilities of the developed model. A parametric analysis was introduced to assess the sensitivity of the developed EPR model to variations of the individual variables including temperature, confining pressure and strain rate. The results showed the EPR model is able to extract and predict the effect of each parameter on the entire shear-stress curve of frozen soil.

In the second application, the EPR based self-learning methodology was used for the analysis of triaxial tests using a series of triaxial drained test data as experimental measurements. In this application the behaviour of a clay soil was modelled under different confining pressures. This application was presented to validate the ability of the EPR-based self-learning approach in capturing the complex soil behaviour. The developed EPR models gave accurate predications compared with the actual data with one or several cycles of a single pass of the self-learning algorithm. The results revealed that the EPR-based self-learning method can be a robust tool for linking laboratory (or field) testing and constitutive modelling. The main advantage of using EPR in material modelling is that it provides a unified approach to material modelling. It can also provide an explicit and well-structured model representing the behaviour of the material. EPR has several advantages over other types of data mining tools such as neural network. It is able to extract the complex nonlinear behaviour of different materials such as soils by feeding it with large amount of data.

It should be noted that, like any other data mining technique, the trained EPR models in both applications are good in interpolation but could be not so good at extrapolation. Therefore, any attempts to use the developed EPR models outside the range of the training or measurement data may not provide reliable results.

CHAPTER 7

Conclusions and Recommendations for Future Research

7.1 Introduction

Material modelling is one of the most vital scientific research areas which significantly contributes in solving very complex engineering problems and providing deep understanding of material behaviour. A lot of research has been done to investigate the modelling of different engineering materials employing various constitutive models and mathematical procedures.

The numerical analysis techniques such as FEM, are widely used to analyse a range of engineering applications in different fields including civil, geotechnical, mechanical, hydrological, chemical and many more. The accuracy of such numerical techniques relies heavily on the constitutive material model used in the FE code. Significant amount of research has been done looking for developing constitutive models that can adequately represent the real material behaviour under different conditions. In recent years, with the rapid developments in computational techniques, postprocessing, automation processes etc., the use of data mining technique has been introduced as an effective alternative approach to constitutive modelling. Data mining techniques such as artificial neural network (ANN) have been used in modelling the response of different materials. However, as mentioned in chapter 3, ANN has a number of shortcomings. An alternative approach named evolutionary polynomial regression (EPR) has been introduced to overcome some of the ANN drawbacks.

Training of such data mining techniques (ANN or EPR) requires large quantities of data which could be costly and may not be available under certain conditions. The self-learning methodology is a realistic approach for training of data mining techniques. The self-learning algorithm is an inverse analysis technique which creates a constitute model that represents a material response using global load-displacement boundary measurements.

In this thesis, by utilising the benefits of EPR in material modelling, EPR was adapted as a machine learning technique in the self-learning framework. Three software packages were used in this study including EPR as the data mining engine, ABAQUS finite element tool and MATLAB environment. The EPR based self-learning framework was coded in MATLAB using its functionality and comprehensive library. The developed self-learning finite element model was applied to analyse a number of structural and geotechnical problems using synthetic and experimental data. EPR offers great advantages especially when it is incorporated in finite element analysis. It creates explicit formula that can be readily incorporated in FEM.

A separate application was presented in this thesis involving the development of a constitutive model for a very challenging soil behaviour (frozen soil) to show the ability of EPR in material modelling in general and encourage the investigation of multiphase material behaviour for future studies.

7.2 Limitations of the proposed methodology

Although the EPR based self-learning algorithm has been successfully applied to modelling different material behaviour, there are a couple of limitations that need to be carefully considered.

- In the EPR based self-learning process, moving to another pass of self-learning could cause overfitting problem in the EPR model. Therefore, once an appropriate convergence is achieved the training process should be terminated.

- As any data mining technique, EPR model performs well in interpolation, however, it is not good at extrapolation. A trained EPR model may be unable to accurately predict the material behaviour outside the range of the training data.

7.3 Conclusions

The following conclusions are the main outcomes from this research:

- The new approach of using EPR based self-learning methodology is introduced in this work. EPR is a new hybrid data mining algorithm, based on an evolutionary computational procedure. When applied to material modelling, its target is to find the best polynomial equation representing the behaviour of the material in a unified framework.

- The multi-objective function was utilised in the EPR algorithm and two strategies were used to train EPR within the self-learning procedure (i.e. total stress-strain and incremental stress-strain strategies).

- The whole framework of self-learning simulation was coded in MATLAB environment which considerably simplifies the way that EPR is trained and implemented in FE code. EPR has been shown to be an effective tool in the heart of the self-learning algorithm. It provides the user with explicit and symbolic equations that can be implemented in FE code.

- The feasibility of the developed methodology was validated through a number of structural applications using hypothetical data to simulate various material behaviour.

- A triaxial compression test was simulated and analysed using the developed EPR based Self-learning approach. A series of experimental data were utilised as boundary measurements and a set of EPR based constitutive models were developed for different confining pressures.

- The EPR based self-learning approach is a direct link between the laboratory tests and material modelling. The results from the above applications reveal that using such comprehensive approach in training of EPR is very promising in capturing the material behaviour.

- It should be noted that this methodology is generic and can be applied to analysis of different engineering problems.

- The capability of EPR in material modelling was also examined by modelling the behaviour of frozen soils using experimental data. Although this application does not involve the self-learning approach, it illustrates the capability of EPR in modelling of a complex coupled soil behaviour and opens the possibility to model such complex behaviour within the self-learning approach in future. The results of the developed EPR model predictions were compared with the actual data of the frozen soil and it was shown that the proposed model can extract and reproduce the behaviour of the frozen soil with a very high accuracy.

7.4 Recommendations for future research work

The EPR based self-learning methodology is a comprehensive approach to link between experimental or field tests and numerical modelling. This methodology is generic and can be applied for any material. EPR offers valuable advantages in material modelling and using EPR in the developed framework is very promising. The work presented in this thesis can be extended to analyse different engineering problems. There are a number of recommendations for further research using the developed algorithm:

- The developed methodology can be applied to simulate triaxial compression tests with end friction which leads to a non-uniform stress-strain state and the developed EPR model can be used to solve boundary value problems.

- The geotechnical applications of EPR based self-learning method presented in this thesis have not included the effect of Poisson's ratio. Developing another EPR model for this parameter using the self-learning framework should be investigated.

- Modelling a complex behaviour of frozen soils using the EPR-based model opens the opportunity to implement the EPR model in FEM and also the EPR based self-learning simulation. This would be very challenging and interesting application because of the implementation of coupled thermo-mechanical analysis.

- The developed methodology was applied to extract the linear and non-linear behaviour without softening state. Considering the softening behaviour requires further investigation.

- The developed algorithm was applied to model soil under saturated state. More complex behaviour of unsaturated soil using triaxial experimental data can be the subject of future work.

- All applications presented in this thesis were under only static condition. Extending the algorithm to include dynamic conditions such as earthquake events need to be investigated.

- The methodology can be applied on a case study application, especially for analysis of geotechnical boundary value problem using field measurements.

References

ABAQUS, 2016. User Subrotine Reference Manual.

Ahangar-Asr, A., Faramarzi, A., Javadi, A.A., 2011. Modelling Mechanical Behaviour of Rubber Concrete Using Evolutionary Polynomial Regression. Int. J. Comput. Eng. 28(4), 492–507.

Ahangar-Asr, A., 2012. Application of an evolutionary data mining technique for constitutive modelling of geomaterials. PhD thesis, University of Exeter.

Ahangar-Asr, A., Faramarzi, A., Mottaghifard, N., Javadi, A.A., 2011. Modeling of permeability and compaction characteristics of soils using evolutionary polynomial regression. Comput. Geosci. 37, 1860–1869. doi:10.1016/j.cageo.2011.04.015

Ahangar-Asr, A., Javadi, A.A., Khalili, N., 2015. An evolutionary approach to modelling the thermomechanical behaviour of unsaturated soils. Int. J. Numer. Anal. Methods Geomech. 39, 539–557.

Ahangar-Asr, A., Johari, A., Javadi, A.A., 2012. An evolutionary approach to modelling the soil–water characteristic curve in unsaturated soils. Comput. Geosci. 43, 25–33. doi:10.1016/j.cageo.2012.02.021.

Alangar-Asr;, Javadi, A.A., 2011. Modeling soil-water characteristic curve using EPR Modeling characteristic curve using EPR. Unsaturated Soils Theory Pract. 2011 379–383.

Aquino, W., Brigham, J.C., 2006. Self-learning finite elements for inverse estimation of thermal constitutive models. Int. J. Heat Mass Transf. 49, 2466–2478. doi:10.1016/j.ijheatmasstransfer.2006.01.031.

Banimahd, M., Yasrobi, S.S., Woodward, P.K., 2005. Artificial neural network for stress-strain behaviour of sandy soils: Knowledge based verification. Comput. Geotech. 32, 377–386. doi:10.1016/j.compgeo.2005.06.002.

Basan, R., 2016. Constitutive modelling and material behaviour.

Berardi, L., Giustolisi, O., Kapelan, Z., Savic, D. a., 2008. Development of pipe deterioration models for water distribution systems using EPR. J. Hydroinformatics 10, 113. doi:10.2166/hydro.2008.012.

Bower, A.F., 2010. Applied Mechanics of Solids. CRC Press, USA.

Cekerevac, C., Laloui, L., 2004. Experimental study of thermal effects on the mechanical behaviour of a clay. J . Numer . Anal . Meth . Geomech 28, 209–228. doi:10.1002/nag.332.

Chamberlain, E.J., 1981. Overconsolidation effects of ground freezing. Eng. Geol. 18, 97–110.

Chen, C., 1985. Mechanics of Geomaterials, In: Z. Bazant; John Wiley & Sons Ltd (Ed.),. pp. 65–86.

Correia, A.G., Cortez, P., Tinoco, J., Marques, R., 2013. Artificial Intelligence Applications in Transportation Geotechnics 861–879. doi:10.1007/s10706-012-9585-3.

Czurda, K. A., & Hohmann, M., 1997. Freezing effect on shear strength of clayey soils. Appl. Clay Sci. 12(1), 165–187.

Doglioni A., 2004. A Novel Hybrid Evolutionary Technique for Environmental Hydraulic Modelling, PhD Thesis. Technical University of Bari, Italy.

Doglioni, A., Giustolisi, O., Savic, D.A., Webb, B.W., 2008. An investigation on stream temperature analysis based on evolutionary computing. Hydrol. Process. 22(3), 315–326.

Doglioni, A., Mancarella, D., Simeone, V., Giustolisi, O., 2010. Inferring groundwater system dynamics from hydrological time-series data. Hydrol. Sci. J. Hydrol. Sci. J. – J. des Sci. Hydrol. 55, 593–608. doi:10.1080/02626661003747556.

Doglioni, A., Simeone, V., 2014. Data-driven modeling of the dynamic response of a large deep karst aquifer. Procedia Eng. 89, 1254–1259. doi:10.1016/j.proeng.2014.11.430.

Duncan, J.M.; Chang, C.Y., 1970. Non-linear analysis of stress and strain in soils. ASCE J. Soil Mech. Found. Div. 96(SM5), 1629–1653.

Ellis, G., Yao, C.., Zhao, R.., Penumadu, D., 1995. Stress-Strain Modeling of Sands using Artificial Neural Netwoks. ASCE J. Geotech. Eng. Div. 121(5), 429–435.

Ellis, G., Yao, C.., Zhao, R., 1992. Neural network modelling of mechanical behaviour of sand. Proc. 9th ASCE Conf. Eng. Mech. Texas 421–424.

Esmaeili-falak, M., Katebi, H., Javadi, A., 2017. Experimental Study of the Mechanical Behaviour of Frozen Soils - A Case Study of Tabriz Subway. Period. Polytech. Civ. Eng. 1–9.

Faramarzi, A., Mehravar, M.., Veladi, H.., Javadi, A.., Ahangar-Asr, A.., 2011. A Hysteretic Model for Steel Plate Shear Walls, in: Proceedings of the 19th ACME Conference, 5-6 April. Edinburgh, Heriot-Watt University, pp. 69–72.

Faramarzi, A., 2011. Intelligent computational solutions for constitutive modelling of materials in finite element analysis. PhD thesis, University of Exeter.

Faramarzi, A., Javadi, A.A., Alani, A.M., 2012. EPR-based material modelling of soils considering volume changes. Comput. Geosci. 48, 73–85. doi:10.1016/j.cageo.2012.05.015.

Faraway, J., Chatfield, C., 1998. Time Series Forecasting with Neural Networks: A Comparative Study Using Airline Data. J. R. Stat. Soc. Ser. C (Applied Stat. 47, 231–250.

Fatehnia, M., Amirinia, G., 2018. A review of Genetic Programming and Artificial Neural Network applications in pile foundations. Int. J. Geo-Engineering 9, 2. doi:10.1186/s40703-017-0067-6.

Fu, Q., Hashash, Y.M.A., Jung, S., Ghaboussi, J., 2007. Integration of laboratory testing and constitutive modeling of soils. Comput. Geotech. 34, 330–345. doi:10.1016/j.compgeo.2007.05.008.

Furukawa, T., Hoffman, M., 2004. Accurate cyclic plastic analysis using a neural network material model. Eng. Anal. Bound. Elem. 28 (3), 195–204.

Gandomi, A.H., Yun, G.J., 2015. Coupled SelfSim and genetic programming for non-linear material constitutive modelling. Inverse Probl. Sci. Eng. 23, 1101–1119. doi:10.1080/17415977.2014.968149.

Ghaboussi, J., Pecknold, D.A.., M, Z., R.M., H.-A., 1998. Autoprogressive Training of neural network constitutive models. Int. J. Numer. Methods Eng. 42(1), 105–26.

Ghaboussi J., Garret J.H., X., W., 1991. Knowledge-based modelling of material behaviour with neural networks. J. Eng. Mech. Div. 117(1), 153–164.

Ghaboussi, J., Pecknold, D.A.., Zhang, M., Haj-Ali, R.M., 1998. Autoprogressive training of neural network constitutive models. Int. J. Numer. Methods Eng. 42, 105–126. doi:10.1002/(SICI)1097-0207(19980515)42:1<105::AID-NME356>3.0.CO;2-V.

Ghaboussi, J., Sidarta, D.E., 1998. New nested adaptive neural networks (NANN) for constitutive modelling. ”Computers Geotech. 22(1), 29–52.

Giustolisi, O., Doglioni, A., Savic, D.A., Webb, B.W., 2007. A multi-model approach to analysis of environmental phenomena. Environ. Model. Softw. 22, 674–682. doi:10.1016/j.envsoft.2005.12.026.

Giustolisi, O., Savic, D.A., 2009. Advances in data-driven analyses and modelling using EPR-MOGA. J. Hydroinformatics 11, 225–236. doi:10.2166/hydro.2009.017.

Giustolisi, O., Savic, D.A., 2006. A symbolic data-driven technique based on evolutionary polynomial regression. J. Hydroinformatics 8, 207–222. doi:10.2166/hydro.2006.020.

Groholski;, D.R., Hashash, Y.M.A., 2013. Development of an inverse analysis framework for extracting dynamic soil behaviour and pore pressure response from downhole array measurements. Int. J. Numer. Anal. Methods Geomech. 37, 1867–1890. doi:10.1002/nag.2172.

Groholski, D.R., Hashash, Y.M.A., Matasovic, N., 2014. Learning of pore pressure response and dynamic soil behaviour from downhole array measurements. Soil Dyn. Earthq. Eng. 61–62, 40–56. doi:10.1016/j.soildyn.2014.01.018.

Harris, J.S., 1995. Ground Freezing in Practice. Thomas Telford, London.

Hashash, Y.M. a., Fu, Q., Ghaboussi, J., Lade, P. V., Saucier, C., 2009. Inverse analysis–based interpretation of sand behaviour from triaxial compression tests subjected to full end restraint. Can. Geotech. J. 46, 768–791. doi:10.1139/T09-015.

Hashash, Y.M., Fu, Q., Butkovich, J.N., 2004a. Generalized strain probing of constitutive models. Int. J. Numer. Anal. Methods Geomech. 28(15), 1503–1519.

Hashash, Y.M., Jung, S., Ghaboussi, J., 2004b. Numerical implementation of a neural network based material model in finite element analysis. Int. J. Numer. Methods Eng. 59, 989–1005. doi:10.1002/nme.905.

Hashash, Y.M.A., Asce, M., Marulanda, C., Asce, M., Ghaboussi, J., Asce, M., 2006a. Novel Approach to Integration of Numerical Modeling and Field Observations for Deep Excavations 1019–1032.

Hashash, Y.M.A., Ghaboussi, J.J., Fu, Q., Marulanda, C.C., 2006b. Constitutive Soil Behaviour Representation via Artificial Neural Networks: A Shift from Soil Models to Soil Behaviour Data, in: Proceedings of GeoCongress 2006: Geotechnical Engineering in the Information Technology Age. Atlanta, pp. 1–6.

Hashash, Y.M.A., Ghaboussi, J.J., Jung, S.S., 2006c. Characterizing Granular Material Constitutive Behaviour Using SelfSim with Boundary Load-Displacement Measurements, in: Proceedings of the Tenth Biennial ASCE Aerospace Division International Conference on Engineering, Construction, and Operations in Challenging Environments, Houston, USA. Houston, USA., pp. 1–8.

Hashash, Y.M.A., Levasseur, S., Osouli, A., Finno, R., Malecot, Y., 2010. Comparison of two inverse analysis techniques for learning deep excavation response. Comput. Geotech. 37, 323–333. doi:10.1016/j.compgeo.2009.11.005.

Hashash, Y.M.A., Marulanda, C.., Ghaboussi, J.., Jung, S., 2003. Systematic update of a deep excavation model using field performance data. Comput. Geotech. 30, 477–488. doi:10.1016/S0266-352X(03)00056-9.

Hashash, Y.M.A., Song, H., 2008. The Integration of Numerical Modeling and Physical Measurements through Inverse Analysis in Geotechnical Engineering 12, 165–176. doi:10.1007/s12205-008-0165-2.

Hashash, Y.M.A., Song, H., Osouli, A., 2011. Three-dimensional inverse analyses of a deep excavation in Chicago clays. Int. J. Numer. Anal. Methods Geomech. 35(9), 1059–1075.

Hooke, R., 1675. A description of helioscopes and some other instruments. London.

Jahed Armaghani, D., Tonnizam Mohamad, E., Momeni, E., Narayanasamy, M.S., Mohd Amin, M.F., 2015. An adaptive neuro-fuzzy inference system for predicting unconfined compressive strength and Young's modulus: a study on Main Range granite. Bull. Eng. Geol. Environ. 74, 1301–1319. doi:10.1007/s10064-014-0687-4.

Javadi, A. A., Rezania, M., 2009a. Applications of artificial intelligence and data mining techniques in soil modelling. Geomech. Eng. An Int. Journal, 1, 53–74.

Javadi, A., Faramarzi, A., Ahangar-Asr, A., 2012. Analysis of behaviour of soils under cyclic loading using EPR-based finite element method. Finite Elem. Anal. Des. 58, 53–65. doi:10.1016/j.finel.2012.04.005.

Javadi, A.A., Rezania, M., Nezhad, M.M., 2006. Evaluation of liquefaction induced lateral displacements using genetic programming. Comput. Geotech. 33(4-5), 222–233.

Javadi, A.A., Rezania, M., 2009b. Intelligent finite element method : An evolutionary approach to constitutive modeling. Adv. Eng. Informatics 23, 442–451. doi:10.1016/j.aei.2009.06.008.

Javadi, A.A.., Rezania, M., 2006. A new genetic programming-based evolutionary approach for constitutive modeling of soils. Proceeding 7th World Congr. Comput. Mech. Los Angeles, California, USA.

Javadi, A.A., Ahangar-Asr, A., Johari, A., Faramarzi, A., Toll, D., 2012. Modelling stress-strain and volume change behaviour of unsaturated soils using an evolutionary based data mining technique, an incremental approach. Eng. Appl. Artif. Intell. 25, 926–933. doi:10.1016/j.engappai.2012.03.006.

Javadi, A.A., Tan, T.P.., Zhang, M., 2003. Neural network for constitutive modelling in finite element analysis. Comput. Assist. Mech. Eng. Sci. 10(4), 375–381.

Johari, A., Javadi, A.A., Habibagahi, G., 2011. Modelling the mechanical behaviour of unsaturated soils using a genetic algorithm-based neural network. Comput. Geotech. 38, 2–13. doi:10.1016/j.compgeo.2010.08.011.

Jung, S., Ghaboussi, J., 2010. Inverse identification of creep of concrete from in situ load-displacement monitoring. Eng. Struct. 32, 1437–1445. doi:10.1016/j.engstruct.2010.01.022.

Jung, S., Ghaboussi, J., 2006. Characterizing rate-dependent material behaviours in self-learning simulation. Comput. Methods Appl. Mech. Eng. 196, 608–619. doi:10.1016/j.cma.2006.06.006.

Jung, S., Ghaboussi, J., Marulanda, C., 2007. Field calibration of time-dependent behaviour in segmental bridges using self-learning simulation. Eng. Struct. 29, 2692–2700. doi:10.1016/j.engstruct.2006.12.017.

Kessler, B.S., El-Gizawy, A.S., Smith, D.E., 2007. Incorporating Neural Network Material Models Within Finite Element Analysis for Rheological Behaviour Prediction. J. Press. Vessel Technol. 129, 58. doi:10.1115/1.2389004.

Khademi, F., Jamal, S.M., Deshpande, N., Londhe, S., 2016. Predicting strength of recycled aggregate concrete using Artificial Neural Network, Adaptive Neuro-Fuzzy Inference System and Multiple Linear Regression. Int. J. Sustain. Built Environ. 5, 355–369. doi:10.1016/j.ijsbe.2016.09.003.

Kim, J.H., Ghaboussi, J., Elnashai, A.S., 2010. Mechanical and informational modeling of steel beam-to-column connections. Eng. Struct. 32, 449–458. doi:10.1016/j.engstruct.2009.10.007.

Koza, J.R., 1992. Genetic Programming: on the Programming of Computers by Natural Selection. Massachusetts Inst. Technol. Press. Cambridge, Massachusetts, USA.

Lackner, R., Amon, A., Lagger, H., 2005. Artificial Ground Freezing of Fully Saturated Soil: Thermal Problem. J. Eng. Mech. 131(2), 211–220.

Lai, Y., Liao, M., Hu, K., 2016. A constitutive model of frozen saline sandy soil based on energy dissipation theory. Int. J. Plast. 78, 84–113. doi:10.1016/j.ijplas.2015.10.008.

Laucelli, D., Giustolisi, O., 2011. Scour depth modelling by a multi-objective evolutionary paradigm. Environ. Model. Softw. 26, 498–509. doi:10.1016/j.envsoft.2010.10.013.

Lemaitre, J.; Chaboche, J.., 2000. Mechanics of Solid Materials. Cambridge University Press, Cambridge, USA, USA.

Li, X., Tian, Y., Gaudin, C., Cassidy, M.J., 2015. Comparative study of the compression and uplift of shallow foundations. Comput. Geotech. 69, 38–45. doi:10.1016/j.compgeo.2015.04.018.

Loukidis, D., Salgado, R., 2009. Bearing capacity of strip and circular footings in sand using finite elements. Comput. Geotech. 36, 871–879. doi:10.1016/j.compgeo.2009.01.012.

Ma, W., Chang, X., 2002. Analyses of strength and deformation of an artificially frozen soil wall in underground engineering. Cold Reg. Sci. Technol. 34(1), 11–17.

Mestat, P., Bourgeois, E., Riou, Y., 2017. Numerical modelling of embankments and underground works To cite this version : HAL Id : hal-01007125.

Muir Wood, D., 1990. Soil Behaviour and Critical State Soil Mechanics. Cambridge University Press.

Millar, D.L., 2008. Parallel Distributed Processing In Rock Engineering Systems. PhD thesis, Imperial College of Science, Technology & Medicine, London.

Momeni, E., Nazir, R., Armaghani, D.J., Maizir, H., 2014. Prediction of pile bearing capacity using a hybrid genetic algorithm-based ANN. Measurment 57, 122–131. doi:10.1016/j.measurement.2014.08.007.

Moon, S., Hashash, Y.M.A., 2015. From Direct Simple Shear Test to Soil Model Development and Supported Excavation Simulation : Integrated Computational-Experimental Soil Behaviour Characterization Framework 141, 1–12. doi:10.1061/(ASCE)GT.1943-5606.0001351.

Munda, J., Pradhan, P.K., Nayak, A.K., 2014. A Review on the performance of Modified Cam Clay Model for fine grained soil 1, 65–71.

Nassr, A., Javadi, A., Faramarzi, A., 2018. Developing constitutive models from EPR-based self-learning finite element analysis. Int. J. Numer. Anal. Methods Geomech. 42, 401–417. doi:10.1002/nag.2747.

Ng, C.W.W., Sun, H.S., Lei, G.H., Shi, J.W., Mašín, D., 2015. Ability of three different soil constitutive models to predict a tunnel's response to basement excavation. Can. Geotech. J. 52, 1685–1698. doi:10.1139/cgj-2014-0361.

Osouli, A., Hashash, Y.M.A., Song, H., 2010. Interplay between Field Measurements and Soil Behaviour for Capturing Supported Excavation Response. J. Geotech. Geoenvironmental Eng. 136, 69–84. doi:10.1061/(ASCE)GT.1943-5606.0000201.

Owen, D.R.J., Hinton, E., 1980. Finite Element in Plasticity: Theory and Practice; Pineridge Press Limited, Swansea.

Penumadu, D.., Zhao, R., 1999. Triaxial compression behaviour of sand and gravel using artificial neural networks. Comput. Geotech. 24(3), 207–230.

Pimentel, E., Papakonstantinou, S., Anagnostou, G., 2012. Numerical interpretation of temperature distributions from three ground freezing applications in urban tunnelling. Tunn. Undergr. Sp. Technol. Inc. Trenchless Technol. Res. 28, 57–69. doi:10.1016/j.tust.2011.09.005.

Ramberg; W, Osgood; WR, 1943. Description of stress-strain curves by three parameters. National advisory committee for aeronutics. (Technical note No. 902).

Rezania;, M., Javadi;, A., Orazio Giustolisi, 2008. An Evolutionary-Based Data Mining Technique for Assessment of Civil Engineering Systems. Eng. Comput. Int. J. Comput. aided Eng. Softw. 25, 500–517.

Rezania, M.., Javadi, A.A., 2007. A new genetic programming model for predicting settlement of shallow foundations. Can. Geotech. J. 44(12), 1462–1473.

Rezania, M., 2008. Evolutionary Polynomial Regression Based Constitutive Modelling and Incorporation in Finite Element Analysis. PhD thesis, University of Exeter.

Rezania, M., Faramarzi, A., Javadi, A.A., 2011. An evolutionary based approach for assessment of earthquake-induced soil liquefaction and lateral displacement. Eng. Appl. Artif. Intell. 24, 142–153. doi:10.1016/j.engappai.2010.09.010.

Roscoe, K.H.., Burland, J.., 1968. On the generalised stress-strain behaviour of “wet” clay". Eng. Plast. (Eds. Heyman J. Leckie F.A.), Cambridge Univ. Press.

Roscoe, K.H.., Schofield, A.N., 1963. Mechanical behaviour of an idealized `wet’ clay. Proceeding 2nd Eur. Conf. Soil Mech. Found. Eng. Wiesbaden, Ger. 47–54.

Rotta Loria, A.F., Frigo, B., Chiaia, B., 2017. A non-linear constitutive model for describing the mechanical behaviour of frozen ground and permafrost. Cold Reg. Sci. Technol. 133, 63–69. doi:10.1016/j.coldregions.2016.10.010.

Shahin, M.A., Jaksa, M.B., Maier, H.R., 2008. State of the Art of Artificial Neural Networks in Geotechnical Engineering. Electron. J. Geotech. Eng. 8, 1–26.

Sharma, L.K., Vishal, V., Singh, T.N., 2017. Developing novel models using neural networks and fuzzy systems for the prediction of strength of rocks from key geomechanical properties. Meas. J. Int. Meas. Confed. 102, 158–169. doi:10.1016/j.measurement.2017.01.043.

Shin, H.., Pande, G., 2001. Intelligent finite elements., in: Proceeding of Asian-Pacific Conference for Computational Mechanics-APCOM 01, (Pp. 1301-1310). Sydney, Australia.

Shin, H.S., 2001. Neural network based constitutive models for finite element analysis. PhD Thesis. University of Wales Swansea, UK.

Shin, H.S., Pande, G.N., 2003. Identification of elastic constants for orthotropic materials from a structural test 30, 571–577. doi:10.1016/S0266-352X(03)00062-4.

Shin, H.S., Pande, G.N., 2000. On self-learning finite element codes based on monitored response of structures. Comput. Geotech. 27, 161–178. doi:10.1016/S0266-352X(00)00016-1.

Sidarta, D.E., Ghaboussi, J., 1998. Constitutive modeling of geomaterials from non-uniform material tests. Comput. Geotech. 22, 53–71. doi:10.1016/S0266-352X(97)00035-9.

Stasa F.L., 1986. Applied Finite Elemenet Analysis for Engineers. CBS College Publishing.

Ti, K.S., Gue See, S., Huat, B.B.., Noorzaei, J., Saleh, M., 2009. A Review of Basic Soil Constitutive Models for Geotechnical Application. Electron. J. Geotech. Eng. 14, 18.

Timoshenko, S.P and Goodier, J.N., 1970. Theory of Elasticity. McGraw-Hill.

Tsai, C., Hashash, Y.M.A., 2009. Learning of Dynamic Soil Behaviour from Downhole Arrays. Geotech. Geoenvironmental Eng. 135, 745–757. doi:10.1061/(ASCE)GT.1943-5606.0000050.

Tsai, C.C., Hashash, Y.M.A., 2008. A novel framework integrating downhole array data and site response analysis to extract dynamic soil behaviour. Soil Dyn. Earthq. Eng. 28, 181–197. doi:10.1016/j.soildyn.2007.06.008.

Wang, Y., Liu, X., Zhang, Z., Yang, P., 2016. Analysis on slope stability considering seepage effect on effective stress. KSCE J. Civ. Eng. 20, 2235–2242. doi:10.1007/s12205-015-0646-z.

Xu, X., Lai, Y., Dong, Y., Qi, J., 2011. Laboratory investigation on strength and deformation characteristics of ice-saturated frozen sandy soil. Cold Reg. Sci. Technol. 69, 98–104. doi:10.1016/j.coldregions.2011.07.005.

Xu, X., Wang, Y., Yin, Z., Zhang, H., 2017. Effect of temperature and strain rate on mechanical characteristics and constitutive model of frozen Helin loess. Cold Reg. Sci. Technol. 136, 44–51. doi:10.1016/j.coldregions.2017.01.010.

Xue-lei, C., Shun-qun, L., Shi-juan, S., 2013. Application of Principal Component Analysis in the Microstructure of Frozen Soil. Electron. J. Geotech. Eng. 1801–1811.

Yan, F., Lin, Z., Wang, X., Azarmi, F., Sobolev, K., 2017. Evaluation and prediction of bond strength of GFRP-bar reinforced concrete using artificial neural network optimized with genetic algorithm. Compos. Struct. 161, 441–452. doi:10.1016/j.compstruct.2016.11.068.

Yang, Y., Lai, Y., Dong, Y., Li, S., 2010. The strength criterion and elastoplastic constitutive model of frozen soil under high con fi ning pressures. Cold Reg. Sci. Technol. 60, 154–160. doi:10.1016/j.coldregions.2009.09.001.

Yu, H.S., 1998. CASM: A unified state parameter model for clay and sand. Int. J. Numer. Anal. Methods Geomech. 22, 621–653.

Yun, G., Ghaboussi, J., Elnashai, A.S., 2006. Self-learning simulation for modeling of beam-column connections in steel frams, in: 4th International Conference on Earthquake Enginnering, October 12-13 . Taipei, Taiwan.

Yun, G.J., Asce, A.M., Saleeb, A., Asce, M., Shang, S., Binienda, W., Asce, F., Menzemer, C., Asce, M., 2012. Improved SelfSim for Inverse Extraction of Nonuniform , Nonlinear , and Inelastic Material Behaviour under Cyclic Loadings 25, 256–272. doi:10.1061/(ASCE)AS.1943-5525.

Yun, G.J., Ghaboussi, J., Elnashai, A.S., 2008a. A new neural network-based model for hysteretic behaviour of material. Int. J. Numer. Methods Eng. 73(4), 447–469.

Yun, G.J., Ghaboussi, J., Elnashai, A.S., 2008b. A design-variable-based inelastic hysteretic model for beam–column connections. Earthq. Eng. Struct. Dyn. 37(4), 535–555.

Yun, G.J., Ghaboussi, J., Elnashai, A.S., 2008c. Self-learning simulation method for inverse nonlinear modeling of cyclic behaviour of connections. Comput. Methods Appl. Mech. Eng. 197, 2836–2857. doi:10.1016/j.cma.2008.01.021.

Ziegler, M., Schüller, R., Mottaghy, D., 2013. Numerical simulation of energy consumption of artificial ground freezing applications subject to water seepage. In Proceedings of the 18th International Conference on Soil Mechanics and Geotechnical Engineering: The academia and practice of geotechnical engineering, Paris, France., pp. 2985–2988.